# CHAPTER 1

# AN INTRODUCTION TO CLEFT LIP AND PALATE

## 1.1 Background to the Present Investigation

Oral-facial clefts, particularly non-syndromic cleft lip with or without cleft palate (CLP) and isolated cleft palate (ICP), are the most common craniofacial deformities affecting one in every 700 to 1000 newborns worldwide (Murray, 2000). Due to their disturbing appearance in many cases, these deformities have attracted much attention in terms of treatment and research. The large impact of the defects on facial growth, function and social integration renders them a major public health problem worldwide.

There are significant ethnic differences in the incidence of cleft lip and palate, with the highest rates in Asian populations and Native Americans, intermediate rates in Caucasians, and lowest rates in African American (Marazita *et al.,* 1986; Melnick *et al.,* 1986; Murray 2002). Even though environmental influences on facial development have been described, a strong genetic component has been demonstrated (Murray 1995, 2002). The nature of the genetic contribution to the aetiology of CLP is still being studied. Although earlier investigations suggested a multifactorial threshold model (Fraser, 1970), more recently complex segregation analysis of several populations has supported mixed models with major gene influences (Marazita *et al.,* 1992; Chung *et al.,* 1986; Hecht *et al.,* 1991). Many researchers worldwide are currently studying the location and nature of mutations in genes

associated with cleft lip and palate.

## 1.2 History of Cleft Lip and Palate

Descriptions of cleft lip and palate date back many centuries. There are examples of oil paintings, sculptures and drawings created by artists as early as the 15th and 16th centuries that depict people who had apparently had operations for cleft lip (Poswillo, 1989; Pirsig *et al.,* 2001).

The first medical illustration of cleft lip surgery was published in 1564 by Ambroise Pare (Pirsig *et al.,* 2001). He introduced a pin and the 'figure of eight' suture in a patient with cleft lip.

## 1.3 Aetiology of Cleft Lip and Palate

Cleft lip and palate can appear as an isolated birth defect or associated with other congenital malformations. If cleft lip and palate appear together with a number of other malformations the cleft condition is referred to as 'syndromic', whereas cleft lip and palate alone is referred as a 'non-syndromic' condition. The present thesis will focus on 'non-syndromic' clefts. Most studies suggest that about 70% of cases of CLP and 50% of ICP are non-syndromic (Murray, 2002).

The attainment of adequate contact for merging of facial prominences depends on many developmental events, each of which may be influenced by genetic or environmental factors or both**.**

A study conducted in Sweden indicates that cigarette smoking during pregnancy is

associated with increased risk of CLP (Kallen, 1997). Despite the controversy aroused by this article, this finding cannot be ignored.

From the above list of possible causes of developmental failures it is reasonable to assume that the pathogenesis of human cleft lip and palate is heterogeneous.

However, data from human and animal studies continue to strengthen the view that the aetiology of cleft lip and palate results from gene-environment interaction (Murray, 2002). The details of these genetic and environmental factors are discussed in Section A, Chapter 2.

## 1.4 Overview of Normal Embryonic Craniofacial Development

### 1.4.1 Formation of the Primary Palate

The first, second and third branchial arches play a critical role in the development of the face, mouth and tongue. The development of the face is well described and illustrated (Fig. 1.1) in terms of its formation and merging of various processes or prominences (Moore, 1982). About embryonic day 24 (E24) the frontonasal process can be clearly identified, bounded on each side by maxillary processes that are derived from the first branchial arch. By E28 (end of fourth week), bilateral oval-shaped thickenings of the surface ectoderm (nasal placodes) develop on each side of the lower part of frontal prominence. The next step is the migration of neural crest cells into the frontonasal region and the region from which the maxillary prominences will develop. This subsequently causes the mesenchyme to proliferate at the margins of these placodes, producing horseshoe-shape medial and lateral nasal processes.

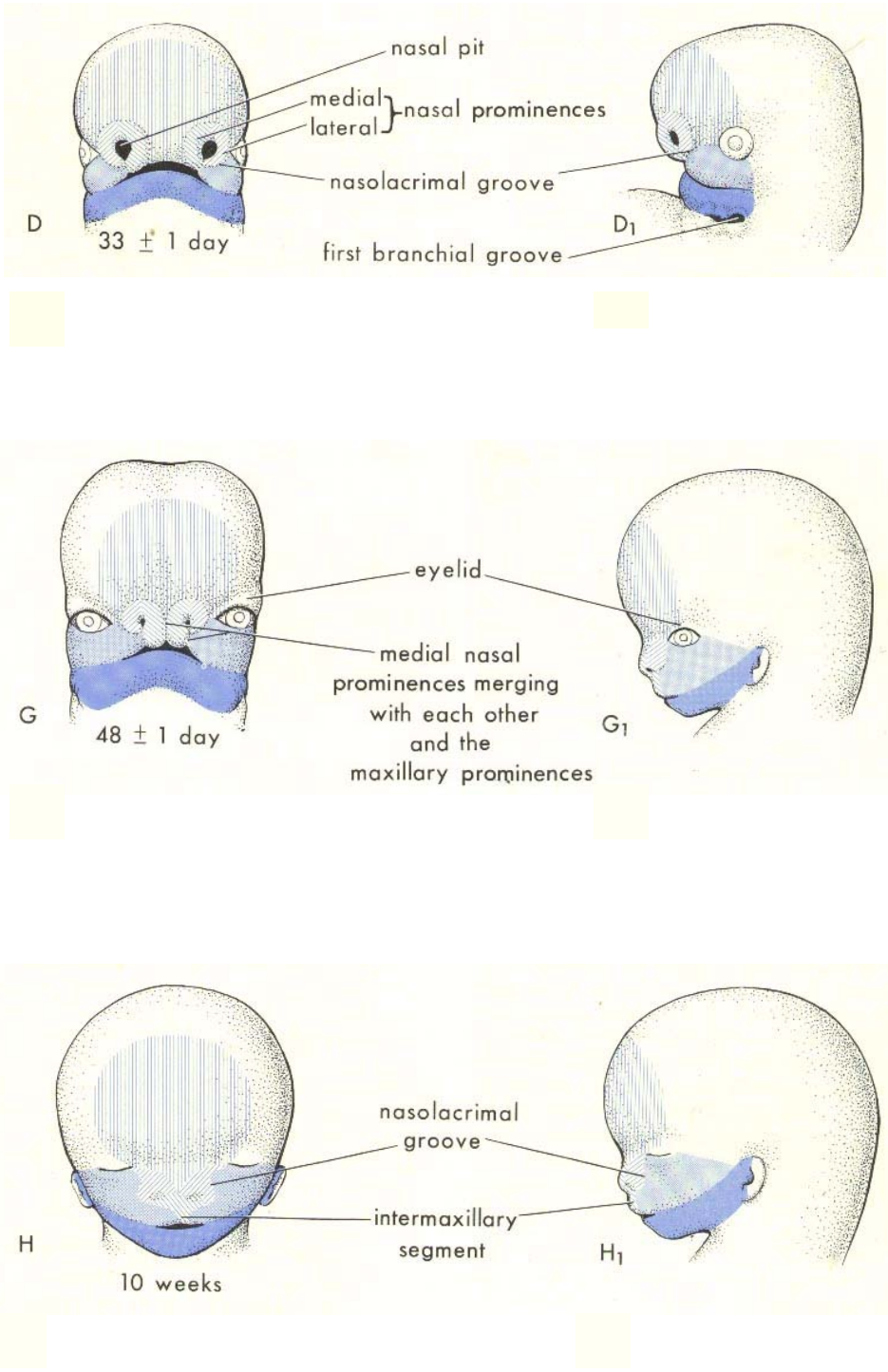


**Figure 1.1** The formation of the face (Moore, 1982)

The maxillary process at this time grows medially and soon approaches both the medial and lateral nasal processes**.** All the three processes grow downward and forward but the mechanism of the interaction and coordination is unclear (Johnston and Bronsky, 1995). The medial growth of the maxillary prominences pushes the medial nasal process toward the midline, where it merges with its anatomic counterpart from the opposite side, eliminating the frontonasal process. This occurs between E40 and E48 (around sixth week of human development). At the same time, the medial nasal prominences merge with each other to form the inter-maxillary segment. This segment gives rise to the middle portion or philtrum of upper lip, and the primary palate, an area of the palate bounded by two lines from the incisive foramen to the alveolar bone between the lateral incisor and canine on each side.

Johnston and Bronsky (1995) highlighted the important of the positioning of the olfactory (nasal) placode. Positioning of the placodes abnormally close to the midline could possibly cause facial clefting. Young *et al.* (2000) in their review mentioned that a failure in the growth of the median and lateral nasal processes prevents the subsequent merging of these structures. As a consequence, clefts develop between their derivatives. In the mildest cases, the clefts may be limited to the vermillion border of the lip (Fig. 1.2). In progressively more severe cases, the cleft develops through the tissue of the lip (unilateral or bilateral cleft lip), and can also involve the side of the nose (typically referred to as oblique clefts).

### 1.4.2 Development of the Palate

The secondary palate is a structure that separates the nasal passage from the oral cavity. The palate proper develops from both primary and secondary components. The formation of the primary palate has already been described. The secondary

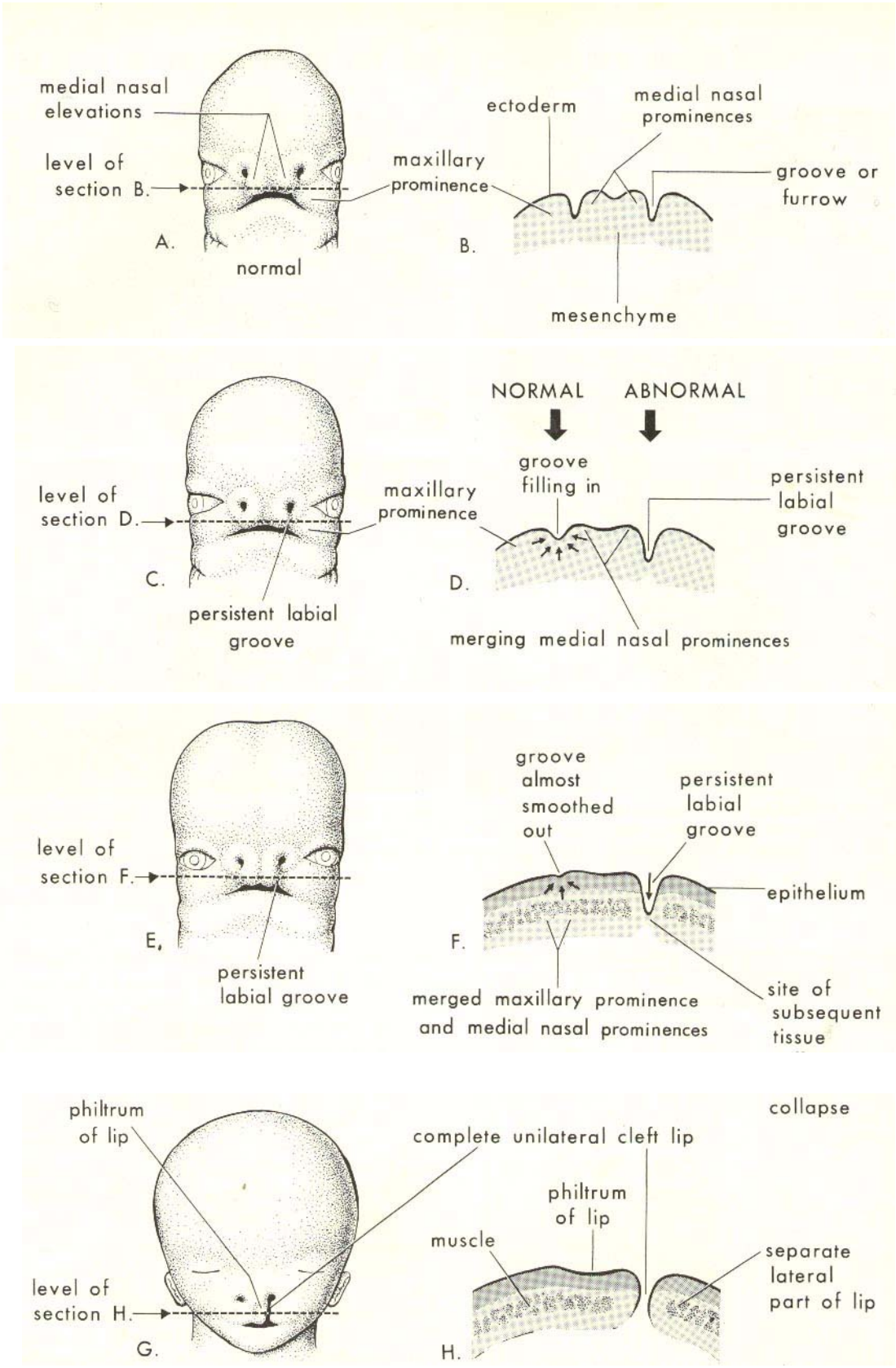


**Figure 1.2** The formation of cleft lip (Moore, 1982)

palate begins development in the sixth week from projections of the paired maxillary processes of the first branchial arches, termed palatal shelves or lateral palatine processes (Fig. 1.3). Initially these shelves are in a vertical position on each side of the developing tongue, but as the mandible grows the tongue moves downward and the shelves become more horizontal and grow medially toward each other. They also merge with the primary palate. An intrinsic shelf-elevating force, generated by the hydration of hyaluronan (Ferguson, 1988) primarily causes elevation of the palatal shelves. This osmotic shelf-elevating force is directed by the collagen fibers, mesenchymal cell orientation, and contraction within the palate.

Merging begins anteriorly during the ninth week and is completed posteriorly by twelfth week of embryonic life. During merging, the apposed epithelia form an epithelial seam that undergoes apoptosis, migration or transformation and results in mesenchymal continuity (Ferguson, 1988). Before merging of the palatal shelves, the outer epidermal layer is sloughed off, leaving the basal epithelial layer. The basal epithelial layer constitutes the medial edge epithelium (MEE) of each shelf. The shelves grow toward the midline, and the MEE of each shelf approximates and forms the midline epithelial seam. This seam is subsequently disrupted, leading to mesenchymal confluence between the two shelves.

Pertubations caused by genetic, mechanical, or teratogenic factors can occur at any of these steps, and may result in a cleft palate (Young *et al.*, 2000) (Fig. 1.4). Probably the event most subject to error in human palate development is removal of the tongue from between the palatal shelves (Young *et al.,* 2000). This event appears to involve active movements including jaw opening and tongue protrusion, as well as differential growth of the lower jaw (Johnston and Millicovsky, 1985)**.**

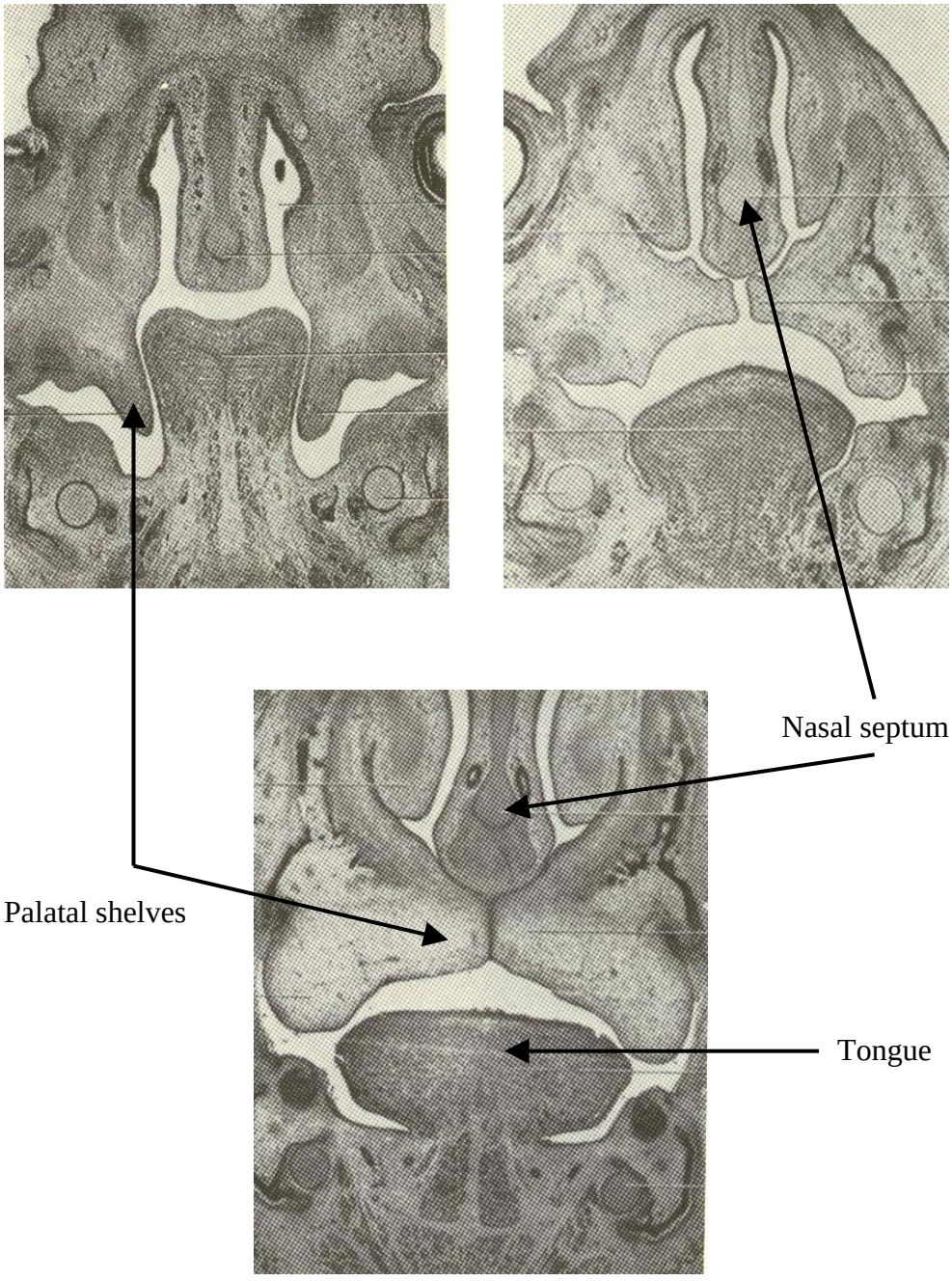


**Figure 1.3** Coronal section of a 52-day to 57-day human embryo, showing the fusion of the palatal shelves with each other and the nasal septum (Sperber, 2001)

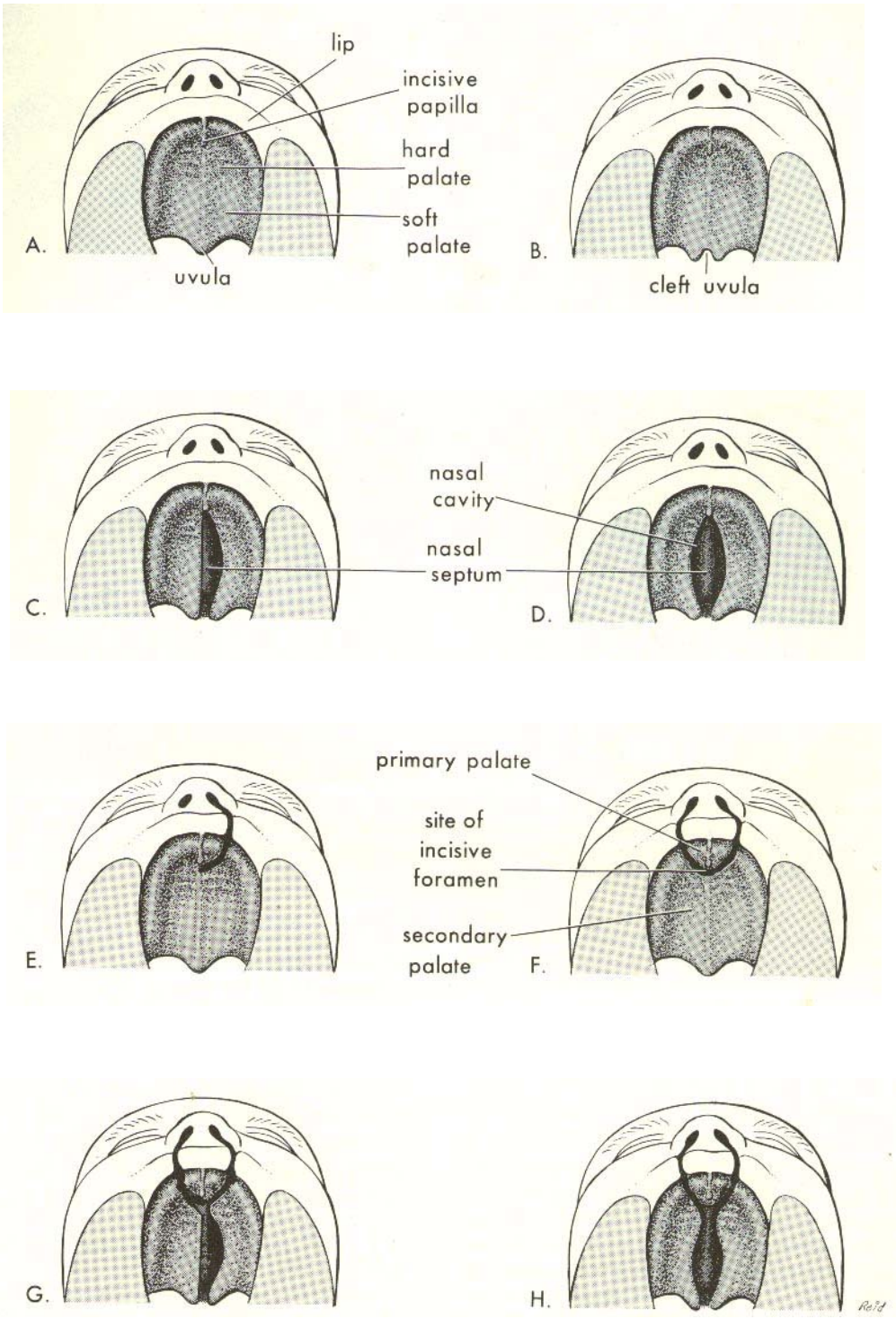


**Figure 1.4** Formation of cleft lip and palate (Moore, 1982)

The posterior portions of the palatal shelves are not ossified but extend beyond the nasal septum and merge to form the soft palate and uvula. The palatal raphe permanently indicates the line of merging of the palatal shelves (Moore, 1982).

Furthermore, disruptions to the patterning, migration, proliferation, and differentiation of cells can result in the clefting (Young *et al.,* 2000).

It is important to realise that the critical aspect of development is the convergence of facial processes to permit apposition and merging. This requires that the processes appear in the right place, achieve the correct shape and size, and have no obstruction to merging. Given the complex nature of these processes, a number of opportunities occur for disruption to normal development of the lip and palate.

## 1.5 Classification of Cleft Lip and Palate

Clefts of the lip and palate are classified according to the embryonic development described by Kernahan (1990) (Fig. 1.5). This thesis deals with Cleft Lip with or without primary palate (CL), Complete Cleft Lip Palate – Unilateral (UCLP), Complete Cleft Lip Palate – Bilateral (BCLP) and Isolated Cleft Palate (ICP). The four groups combined are referred to, for the purposes of this thesis, as the cleft lip and palate group (CLP).

### 1.5.1 Cleft Lip, with or without Clefting of the Alveolar Process (Cleft of the Primary Palate) (CL)

The alveolar ridge is intact. The cleft involves the height of the lip to some degree. The cleft lip (CL) may be unilateral or bilateral. Cleft lip can occur with clefts of the

alveolar process. In the characteristic forms without cleft palate, the cleft extends only as far as the anterior palatine foramen.

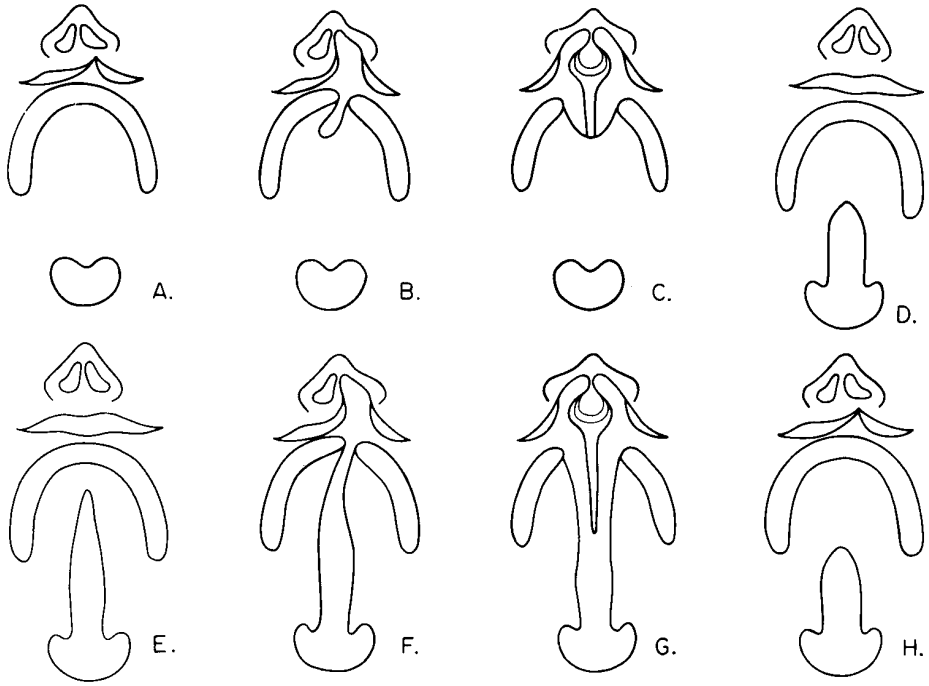


**Figure 1.5** The classification of Kernahan (1990). This divides the deformity into three groups: clefts of the primary palate alone, clefts of the secondary palate alone, and clefts of the primary and secondary palates.

### 1.5.2 Isolated Cleft Palate (ICP)

Both the soft palate and the hard palate are divided. A complete palatal cleft is classified as unilateral if the vomer is attached to one of the palatal shelves. When the vomer is totally separated from the palatal shelves, its lower free border can be detected between them. The cleft is then classified as bilateral, although it remains median.

### 1.5.3 Combined Cleft Lip and Palate (UCLP and BCLP)

Subjects with combined cleft lip and palate have clefts in both the primary and secondary palate. The cleft malformation may be complete or incomplete; unilateral

or bilateral. Although the palatal cleft is always median, rotation of the vomer may cause it to be appear lateral.

## 1.6 Care for Cleft Children in Kota Bharu, Malaysia

The Multidisciplinary Combined Cleft Lip and Palate Clinic is held on a monthly basis at the Orthodontic Clinic, Main Dental Clinic, Kota Bharu. The clinic gives the opportunity for the parents and specialists to interact and discuss their child's progress and treatment during the clinical session.

The key members of the multidisciplinary cleft lip and palate team are as follows: Plastic Surgeon, Orthodontist, Paediatrician, Oral-Maxillofacial Surgeon, Paedodontist, ENT Surgeon and Speech Pathologist. This also involves a Cleft Coordinator to coordinate the activities of the multidisciplinary team, including the maintenance of a cleft register and liaison with other relevant parties.

The non-government organization, Kelantan Cleft Lip and Palate Association (CLAPAK) plays an important role in providing patients, families and members of the multidisciplinary team the opportunity to interact and exchange personal experiences, ideas and information. This helps to give moral support and encouragement to the patients, as well as to foster a closer relationship between patients and the multidisciplinary team.

## 1.7 Pre-operative Craniofacial Morphology in Infants with Cleft Lip and Palate

Numerous studies have shown that craniofacial morphology in children, adolescents

and adults with cleft lip and palate departs from the norm (Dahl *et al.*, 1982). Hermann *et al.* (1999a) suggested that those with complete cleft lip and palate deviate more severely than those with incomplete clefts.

Hermann *et al.* (2000) analysed and compared the craniofacial morphology of 22-month-old lip operated children after the cleft lip and anterior part of the palate had been surgically closed at 2 months of age with cleft lip controls. Comparison of the post-operative craniofacial morphology with the control group indicated that the posterior height of the maxilla was still reduced. The mandible was still short and retrognathic with bimaxillary retrognathia. The lateral segment on the cleft moved toward the mid-sagittal plane resulting in a narrow dental arch at the level of deciduous canine and first molar.

Post-operative craniofacial growth in unilateral complete cleft lip and palate was similar to the controls (unilateral incomplete cleft lip), with normal growth potential observed in all craniofacial regions except where the growth had been influenced by surgical intervention. However, the mandible and maxilla showed a more vertical growth pattern than that observed in the control group (Hermann *et al.*, 1999b).

Dado and Kernahan (1986) have reported that, before pre-surgical intervention, considerable variations in craniofacial morphology were seen in newborn children with clefting. Variation in the dimensions and shape of the cranial base has been described (Horswell and Gallup, 1992). Most studies have concentrated on the cranial base viewed from the lateral aspect. Jensen and Kreiborg (1993), using lateral cephalometric radiographs, reported an increased width of the spheno-occipital synchondrosis in newborns with cleidocranial dysplasia. Moreover, the spheno-occipital synchondrosis has been found to be wider in 3-month-old children with

complete clefts of the lip, alveolus and palate compared with 3-month-old children with minor incomplete clefts of the lip (Molsted *et al.,* 1993). Richtsmeier *et al.* (1994) have shown that pups (Brittany spaniels) with cleft palate have wider posterior palates and cranial bases than pups with no clefts, which is in agreement with the results in humans presented by Molsted *et al.* (1995).

Maue-Dickson and Dickson (1980) described an increased distance between right and left pterygoid plates in human clefts. Furthermore, they noticed an increased pharyngeal width and an increased area of the eustachian tube cartilage. These findings suggest that many ear problems that afflict cleft children, particularly in early infancy, are related not only to cleft palate and associated functional conditions in the pharynx, but also to the anatomic conditions in the sphenoid and temporal bones.

The above findings indicate that combined cleft lip and palate deformities are not localised to the areas of the lower and middle-third of the craniofacial skeleton, but may also be associated with morphological alterations in the developing cranial base.

Previous studies of cleft lip and palate have generally applied two-dimensional lateral cephalometric methods but these have significant limitations, such as superimposition of structures, difficulty in identifying landmarks and poor visualization of 3D structures (Maue-Dickson 1979; Moyers and Bookstein, 1979; Cohen, 1984; Richtsmeier and Cheverud, 1986; Fisher *et al.,* 1999; Singh *et al.,* 2004). Furthermore, the subjects of these studies were older children and adults, and were limited to specific ethnic groups.

Dickson and Maue-Dickson (1983) did a qualitative study on cleft lip and palate using a CT scan on a full-term human foetus to reveal soft and hard tissue

morphologic details. Schendel and Delaire (1986) used CT scans of seven infants with unoperated cleft lip and palate, which were compared with five age matched control infants. Selected axial scans were then traced and the cranio-orbital polygons were created. The findings showed asymmetric cranial bases with plagiocephalic features in the cleft infants.

It is believed that only one study of three-dimensional computerized tomography (3D CT) in cleft lip and palate exists in the recent literature. Fisher *et al*. (1999) conducted a geometric analysis on three-dimensional CT scan data from twelve 3-month-old infants with complete unilateral cleft lip and palate prior to surgery. The above study also highlighted the asymmetry of both bony and soft tissue landmarks at the nasal base which is evident in three-dimensions.

Researchers investigating CLP have recognized the potential advantages of applying 3D CT in order to further the knowledge of the biology of cleft lip and palate and to clarify whether CLP is associated with other craniofacial malformations or is a localized anomaly (Maue-Dickson and Dickson, 1980).

An awareness of this need has led to the research reported in this thesis.

## 1.8 Aims of this Study

The aims of this study were to use CT imaging and computer technology:

i. To compare pre-operative craniofacial morphology in four groups of infants with clefts: unilateral cleft lip palate (UCLP); bilateral cleft lip and palate (BCLP); isolated cleft palate (ICP); and cleft lip primary palate/alveolus (CL)

with a NC (non-cleft) group and to develop a quantitative description based on the determination of the position of anatomical landmarks in 3D, derived from CT scan data.

ii. To compare the morphology of ICP with other affected groups as embryological studies suggest that they are etiologically different (Johnston and Bronsky, 1995; Hart *et al.,* 2000).

iii. To see if differences in craniofacial morphology exist between males and females with cleft lip and palate.

iv. To apply this information to increase our understanding of the underlying basis of cleft lip and palate in order to focus on improving the strategies required to deal with the management of these patients.

It was hypothesized that the CLP infants would have a significantly different pattern of craniofacial morphology than the NC infants.

In particular it was hypothesized that:

i. The morphology of the hyoid bone in unoperated infants with cleft lip and palate (CLP) would differ from non-cleft infants (NC). It was aimed to quantify any anatomical variation and to relate the findings to any clinical problems, such as aspiration pneumonia.

ii. The height of individual cervical vertebral bodies, intervertebral spaces and overall cervical length in CLP infants would differ from non-cleft (NC) infants. It was also aimed to quantify anatomical variations of the cervical spine.

iii. The morphology of the skeletal components of the naso-pharyngeal area in infants with CLP would differ from NC infants. It was also aimed to quantify anatomical variations.

iv. The width and dimension of the cranial base in CLP infants would differ from NC infants.

v. The width and dimension of the spheno-occipital synchondrosis in CLP infants would differ from NC infants.

Statistical testing, using a linear modelling approach, was used to make comparisons between groups relating to the above hypotheses.

## 1.9 Significance of this Study

### 1.9.1 Longitudinal Studies

By publishing these chapters it is hoped to advance knowledge in this field in such a way that the long-term aspects of this disorder can be evaluated. Knowledge derived from research in this area has potential value to many disciplines. By advancing the knowledge of craniofacial biology, particularly in the morphogenesis of CLP, this project may attract the attention of many persons across disciplines with a variety of backgrounds and skills. With respect to the patients in the current cross-sectional study it is intended that there be long-term follow-up. Prospective longitudinal investigations are important in clinical management of cleft lip and palate children since the data can provide answers to problems such as when is the best time to treat, what are the best techniques of treatment and what are the effects of treatments. There is a need to establish cleft and craniofacial centres devoted to longitudinal studies of children with clefts over the years from birth to adulthood.

### 1.9.2 Centre for Craniofacial Sciences at Universiti Sains Malaysia (USM)

The data obtained will be pooled in a data bank and thus be made accessible for future comparison. Furthermore, there is an opportunity to enrich the training of paediatricians, orthodontists, oral-maxillofacial surgeons, and other clinicians by using these data to demonstrate the continuity of morphologic variations that may be expected. This study will have major significance for the management of patients in Malaysia at the Centre for Craniofacial Sciences, Hospital Universiti Sains Malaysia, Kota Bharu, Kelantan. The motto of Universiti Sains Malaysia is '*We Lead'* and it is hoped that this will provide leadership and a focus for further work in the region.

## 1.10 Structure of the Thesis

This is one of the first 3D CT studies of unoperated infants with CLP. This thesis contains a general literature review, the general methodology used and chapters discussing the hyoid bone, the cervical spine, the naso-pharynx, the cranial base and the spheno-occipital synchondrosis. The references for each chapter have been listed at the end of each to facilitate publication of chapters four to eight separately in international peer reviewed journals.

## References

Cohen AM (1984). Uncertainty in cephalometrics. *Br J Orthod* 11:44-48.

Chung CS, Bixler D, Watanabe T, Koguchi S, Fogh-Anderson P (1986). Segregation analysis of cleft lip with or without cleft palate: a comparison of Danish and Japanese data. *Am J Hum Genet* 39: 603-611.

Dado DV, Kernahan DA (1986). Radiographic analysis of the midface of a stillborn children with unilateral cleft lip and palate. *Plast Reconstr Surg* 78: 238-241.

Dahl E, Kreiborg S, Jensen BL, Anderson PF (1982). Comparison of craniofacial morphology in infants with incomplete cleft lip and infants with isolated cleft palate. *Cleft Palate J* 19:258-266.

Dickson DR, Maue-Dickson W (1983). Tomographic assessment of craniofacial structures: Cleft lip and palate. *Cleft Palate J* 20:23-34.

Ferguson MW (1988). Palate development. *Development* 103(Suppl):41-60.

Fisher DM, Lo LJ, Chen YR, Noordhoff MS (1999). Three-dimensional computed tomographic analysis of the primary nasal deformity in 3 month old infants with complete unilateral cleft lip and palate. *Plast Reconstr Surg* 103. 1826-1834.

Fraser FC (1970). Research revisited. The genetics of cleft lip and cleft palate. *Am J Hum Genet* 22:336-352.

Hart TC, Marazita MC, Wright JT (2000). The impacts of molecular genetics on oral health paradigms. *Crit Rev Oral Biol Med* 11: 25-56.

Hecht JT, Wang YP, Blanton SH, Michels VV, Daiger SP (1991). Cleft lip and palate: no evidence of linkage to transforming growth factor alpha. *Am J Hum Genet* 49:682-686.

Hermann NV, Jensen BL, Dahl E, Bolund S, Kreiborg S (1999a). A comparison of the craniofacial morphology in 2 month-old unoperated infants with complete unilateral cleft lip and palate, and incomplete unilateral cleft lip. *J Craniofac Genet Dev Biol* 19:80-93.

Hermann NV, Jensen BL, Dahl E, Bolund S, Darvann TA, Kreiborg S (1999b). Craniofacial growth in subjects with unilateral complete cleft lip and palate, and unilateral incomplete cleft lip, from 2 to 22 months of age. *J Craniofac Genet Dev Biol* 19:135-147.

Hermann NV, Jensen BL, Dahl E, Bolund S, Kreiborg S (2000). Craniofacial comparisons in 22-month-old lip operated children with unilateral complete cleft lip and palate and unilateral incomplete cleft lip. *Cleft Palate Craniofac J* 37:303-317

Horswell BB, Gallup BV (1992). Cranial base morphology in cleft lip and palate: a cephalometric analysis from 7-18 years of age. *J OralMaxfac Surg* 5: 681-685.

Jensen BL, Kreiborg S (1993). Development of skull in infants with cleido-cranial dysplasia. *J Craniofac Genet Dev Biol* 13:89-97.

Johnston MC, Bronsky PT (1995). Prenatal craniofacial development: New insights on normal and abnormal mechanism. *Crit Rev Oral Biol Med* 6:368-422.

Johnston MC, Millcovsky G (1985). Normal and abnormal development of the lip and palate. *Clin Plast Surg* 12:521-531.

Kallen K (1997). Maternal smoking and orofacial cleft. *Cleft Palate Craniofac J* 34:11-16.

Kernahan DA, Rosenstein SW, Dado DV (1990). Cleft Lip and Palate- A system of Management. Baltimore: William and Wilkins.

Marazita ML, Spence MA, Melnick M (1986). Major gene determination of liability to cleft lip with or without cleft palate: A multiracial view. *J Craniofac Genet Dev Biol* 8:47-51.

Marazita ML, Hu DN, Spence MA, Liu YE, Melnick M (1992). Cleft lip with or without cleft palate in Shanghai, China: evidence for autosomal major locus. *Am J Hum Genet* 51:648-653.

Maue-Dickson W (1979). The craniofacial complex in cleft lip and palate: an update review of anatomy and function. *Cleft Palate J* 16:291-317.

Maue-Dickson W, Dickson DR (1980). Anatomy and physiology related to cleft palate: current research and clinical implications. *Plast Reconstr Surg* 65: 83-90.

Melnick M, Marazita ML, Hu DN (1986). Genetic analysis of cleft lip with or without cleft palate in Chinese kindreds. *Am J Med Genet* 21:183-190.

Molsted K, Kjaer I, Dahl E (1993). Spheno-occipital synchondrosis in three month children with clefts of the lip and palate: a radiographic study. *Cleft Palate-Craniofacial J* 30: 569-573.

Molsted K, Kjaer I, Dahl E (1995). Cranial base in newborn with complete cleft lip and palate: a radiographic study. *Cleft Palate-Craniofacial Journal* 32: 199-205.

Moore KL (1982). The branchial apparatus. In: The Developing Human, Clinical Oriented Embryology. Philadelphia: W.B Saunders Co., pp156-187.

Moyers RE, Bookstein FL (1979). The inappropriateness of conventional cephalometrics. *Am J Orthod* 75:599-617.

Murray JC (1995). Face Facts: genes, environment and clefts (invited editorial). *Am J Hum Genet* 57:227-332.

Murray JC (2002). Gene/environment causes of cleft lip and/or palate. *Clin Genet* 61: 248-256.

Pirsig W, Haase S, Palm F (2001). Surgically repaired cleft lips depicted in paintings of the late Gothic period and the Renaissance. *Br J Oral Maxfac Surg* 39:127-133.

Poswillo DE (1989). Myths, masks and mechanism of facial deformity. *Eur J Orthod* 11:1-9.

Richtsmeier JT and Cheverud JM (1986). Finite element scaling analysis of normal growth of the human craniofacial complex. *J Craniofac Genet Dev Biol* 6: 289-323

Richtsmeier JT, Sack GH Jr, Grausz HM, Cork LC. (1994). Cleft palate with autosomal recessive transmission in Brittany Spaniels. *Cleft Palate Craniofac J* 31:364-371.

Schendel SA and Delaire J (1986). Computed axial tomographic assessment of cranioorbital anatomy in unilateral clefts. *Ann Plast Surg* 120-124.

Singh GD, Rivera-Robles J, Jesus-Vinas J (2004). Longitudinal craniofacial growth patterns in patients with orofacial clefts: geometric morphometrics. *Cleft Palate Craniofac J* 41:136-143.

Sperber GH (2001). Craniofacial development. Hamilton: BC Decker Inc.

Young DL, Schneider RA, Hu D, Helms JA (2000). Genetic and teratogenic approaches to craniofacial development. *Crit Rev Oral Biol Med* 11:304-317.

# CHAPTER 2

# GENERAL LITERATURE REVIEW

The purpose of this review is to:

(a) present current concepts on the etiology of non-syndromic cleft lip and palate and isolated cleft palate, in particular the genetic and environmental factors that have been identified in the scientific literature.

(b) review the importance of morphometric analysis of the human craniofacial region for clinical and research purposes. The author will start with background on the history of anthropometric techniques and follow with an introduction to radiographic cephalometrics and its limitations, then consider advances in craniofacial imaging.

## Section A

## 2.1 Genetic and Molecular Basis of Cleft Lip and Palate

Embryological studies suggest that cleft lip with or without clefting of the alveolus (CL) and complete cleft lip and palate (UCLP and BCLP) are etiologically distinct from isolated cleft palate (ICP) (Johnston and Bronsky, 1995; Hart *et al*., 2000). Cox (2004) has recently provided a detailed review of current understanding of the

molecular and cellular processes involved in morphogenesis of the midface.

### 2.1.1 Transforming Growth Factor

Transforming growth factors (TGFα) are an extensively studied set of growth factors. They have been shown to be present and to regulate palate development (Fitzpatrick *et al.,* 1990) and to be present at high levels in the medial edge epithelium of palatal shelves. Ardinger *et al.* (1989) performed an association study comparing genetic variation at candidate gene loci in a group of unrelated cleft individuals with a group of controls. The study demonstrated a significant association between two out of three restriction fragment length polymorphisms (RFLPs) around the transforming growth factor-α (TGFα) gene and non-syndromic cleft lip with or without cleft palate (CLP). However no association was found in the CLP group without a positive family history. This association suggests that the abnormality in this gene may underlie a predisposition for clefting in some individuals or that an as yet unidentified clefting gene may be tightly linked to the TGFα locus (e.g., the TGFα allele and the CLP "allele" are in linkage disequilibrium).

A similar study in an Australian population of Anglo-Celtic descent showed a significant association with one of the RFLPs at the TGFα locus (Chenevix-Trench *et al.,* 1992). In a further study, Holder *et al.* (1992) studied 60 unrelated British Caucasian subjects with non-syndromic cleft lip with or without cleft palate. Their research further supports the role of TGFα as a gene of major effect in the development of orofacial clefts in humans. Holder's results suggest that a mutation in the same gene underlies a proportion of clefting in all three populations studied

(American, Australian, and British), who are predominantly of northern European origin.

Lidral *et al.* (1998) found a significant association of MSX1 and TGFβ3 with non-syndromic clefting in humans using linkage-disequilibrium (LD) strategy, suggesting that these genes are involved in pathogenesis of clefting. The expression of TGFβ3 has not been described during primary palate formation but may be expressed in the epithelium of the developing nasal and maxillary processes in the area of future merging.

### 2.1.2 Extracellular Matrix

For the normal development of the palate, balance is required in the components of the extracellular matrix (ECM) including hyaluronan and glycosaminoglycans (GAG). Furthermore, during the normal merging process, the disappearance of the midline epithelial seam is accompanied by an increase in both proteoglycans (PG) and collagen expression (Ferguson, 1988). Control of ECM metabolism in the embryonic oral facial region, therefore, appears to be essential for normal palatal development. ECM molecules in turn promote the activities of growth factors and cytokines present in the epithelial cell and palatal mesenchyme (Bodo *et al.*, 1995).

Failure of any of the cellular activities mentioned above or perturbation of the ECM composition in the oral facial region can lead to production of cleft palate. For this reason Bodo *et al.* (1999) were prompted to investigate further the transforming growth factors (TGFα and TGFβ isoforms) particularly TGFα, TGFβ1, and TGFβ3 isoform expressions, and their effects on ECM macromolecule production of normal and cleft palatal fibroblasts in vitro. The results indicated that TGFα was not

evidenced in CLP and normal fibroblasts, but the CLP fibroblasts produced less active TGFβ1 with a parallel decrease in TGFβ1 transcription. However CLP fibroblasts secreted more TGFβ3, had high PG decorin expression, and produced greater quantities of collagen and GAG compared with normal cells. These data represent the first report from a human model in vitro that TGFβ1 and TGFβ3 are differently expressed and correlated to the CLP phenotypes. These findings confirm the existence of a dynamic interaction between growth factors and ECM during palatal development. Furthermore, they lead to the conclusion that the typical features in CLP fibroblasts relate to the concerted action of TGFα and TGFβ isoforms. Bodo *et al.* (1999) believed that their study could introduce the possibility of using TGF isoforms in future therapy in the correction of cleft palate. Furthermore, since this orofacial abnormality is genetically determined, hereditary control of the growth factor production could be the key factor in its etiology and pathogenesis.

### 2.1.3 Proto-oncogene BCL3

Although, the role of B-cell leukemia/lymphoma 3 (BCL3) in the etiology of CLP is unknown, BCL3 is related to genes involved in cell lineage determination and cell cycle regulation. Epithelial cell disruption at the edges of the developing maxillary process and growth of underlying mesenchyme leading to mesenchymal continuity and seam formation are critical in palate development (Ferguson, 1988). A dominant mutation in BCL 3, resulting in increased binding to the transcription factor, could lead to inhibition of the expression of genes important to growth in the developing mesenchyme. Growth failure in these cells could result in CLP.

Stein *et al.* (1995), have demonstrated linkage of non-syndromic CLP to BCL 3, a growth factor in 17 multigenerational CLP families. Their analyses showed evidence for involvement of chromosome 19 in the etiology of clefting. These results suggest that a major gene does play an etiologic role in the development of CLP and that these loci can be detected in linkage studies with sufficient numbers of families. Martinelli *et al.,* (1998) supported these findings using different methods. In addition the data reported by Stein *et al.* (1995) for the chromosome region 19q13.2 provided "suggestive" linkage, i.e., statistical evidence expected to occur one time at random in a genome scan. Although suggestive linkage is only indicative, by definition, so far three different groups have found suggestive linkage for this locus. This is an encouraging sign that the locus is "real" and that it is relevant for different populations. Martinelli *et al.* (1998) believed that BCL 3 or a nearby gene seems to be implicated in some way in this congenital facial malformation. However, the difficulties in demonstrating significant linkage indicate the 19q13.2 gene is not a major clefting gene.

In conclusion, it appears that BCL3 plays a role in the etiology of CLP. However, it is not known at present whether it acts as a modifier or as additive gene for this malformation.

### 2.1.4 Retinoic Acid Receptors (RARα)

Retinoic acid receptor alpha (RARα) showed a significant association with CLP in an Australia population (Chenevix-Trench *et al.,* 1992), but no association in a British population (Vintiner *et al.,* 1993).

Juriloff and Mah (1995) in their study found the chromosomal location of the mouse gene in which mutation occurs that can cause non-syndromic CLP. The region on chromosome 11 associated with CLP in this animal model is homologous to 17q21-q24 in humans. This region, marked by retinoic acid receptor-α (RARα) has shown association with CLP in some populations (Chenevix-Trench *et al.,* 1992). This study has strengthened the case for CLP locus linked to RARα in humans.

### 2.1.5 Chromosome 6

Chromosome 6 has been of interest to investigators because of the association of alleles at the H2 locus with corticosteroid-induced clefting in the mouse. HLA (on chromosome 6p) is the human homologue of H2. Eiberg *et al.* (1987) performed a linkage study in CLP, suggesting a significant linkage with F13A (blood clotting factor XIIIA) on chromosomes 6, as F13A is known to be located distally on chromosome 6. Three other studies rejected linkage with F13A (Hecht *et al.,* 1993; Vintiner *et al.,* 1993), while one other study found linkage with an anonymous marker closely linked to F13A (Carrinci *et al.,* 1995).

## 2.2 Environmental Factors

Naturally occurring folates are found widely in foodstuffs, especially in liver, legumes and fresh vegetables. Folic acid (pteroylmonoglutamic acid) is a commercially available compound used for supplementation. It does not occur naturally in living tissues, but is readily converted in vivo into the biologically active folates. Folates are essential in the synthesis of purines and pyrimidines, which are components of

DNA and RNA required in the regulation of gene expression and cell differentiation. In humans, drugs that interfere with folate metabolism, for example phenytoin, are known to have teratogenic effects. Low blood folate levels were associated with spontaneous abortion and developmental abnormalities of the foetus (Hartridge *et al.,* 1999). However, studies have found significant protective effects of the role of folic acid in orofacial clefting. There also appears to be an association between maternal smoking and oral clefting (Kallen, 1997).

## 2.3 Isolated Cleft Palate (ICP)

The incidence of ICP is generally about half the incidence of CLP i.e. 1: 2000 livebirths (Johnston and Bronsky, 1995). The percentage of ICP that is syndromic is about 20-30% and is higher than CLP.

Recurrence rates of non-syndromic isolated cleft palate (ICP) are lower than CLP indicating a somewhat lesser role for genetic factors (Johnston and Bronsky, 1995). Recently, homeobox genes of the MSX class have been shown to be expressed in the epithelial or mesenchymal components of disparate tissues undergoing morphogenesis (Satokata and Maas 1994). Mice lacking MSX1 gene function display reduced shelf growth, failure or delay shelf elevation, a failure of epithelial adhesion, and post-merging rupture leading to clefting of the secondary palate. The features observed in non-syndromic cleft palate in humans are consistent with the phenotypes of MSX1 deficient mice. This similarity establishes the human homologue of MSX1 as a strong candidate gene for involvement in cleft palate in humans.

The results of the study by Satokota and Maas were supported by Ferguson (1994) who suggested that MSX1 is a candidate gene for mutation in human craniofacial disorders, particularly non-syndromic cases of cleft palate, with associated dental and skull abnormalities.

Taya *et al.* (1999) developed an animal model to describe the pathogenesis of cleft palate in TGFβ3 knockout mice. They investigated the molecular mechanisms by which TGFβ3 regulates normal and cleft palate formation using wild-type and TGFβ3 null mice. These experimental studies found that all homozygous null (-/-) mice embryos had cleft palate, whereas heterozygous (+/-) and homozygous (+/+) normal embryos had normal intact palate in vivo. These results confirm that the pathogenetic mechanism underlying cleft palate in the TGFβ3 null mouse is a failure of palatal shelf merging. This study suggests that TGFβ3 induces normal palatal medial edge epithelial (MEE) cell fusion, whereas its absence leads to cleft palate.

## 2.4 Summary

To summarise genetic linkage and association studies to date, no one locus has clearly emerged as 'necessary' for the development of CLP. On the contrary, the genetic etiology of CLP appears to be more complex, with several loci showing significant effects in at least some studies. In addition to genetic factors, environmental factors clearly play a role in non-syndromic CLP, such as maternal nutrition deficiencies, alcohol, or cigarette use (Wyszynski *et al.,* 1996). These can increase the risk of an individual developing oral facial clefts, as can rare exposure to certain teratogens (such as phenytoin and Valproic acid). There are also studies on gene-environment

interaction such as the role of vitamins or smoking with TGFα acting as a covariate (Shaw *et al.*, 1996). Studies of other animal models may prove useful in the understanding further these interactions. As embryological studies suggest that CLP is etiologically distinct from ICP, one of the aims of this study is to compare the morphology of the cleft lip and palate groups with isolated cleft palate.

## Section B

## 2.5 Anthropometric Evaluation of Craniofacial Abnormalities

Measurements of the human face have been performed since ancient times and many measurements defined then can still be found in modern clinical anthropometry. The popularity of anthropometry stems in part from its relatively simple methodology and requirement for inexpensive equipment (Vegter and Hage, 2000).

Farkas *et al.* (1993) applied anthropometric methods in assessing the effects of surgery on 81 Caucasian children with unilateral cleft lip and palate (UCLP) and bilateral cleft lip and palate (BCLP). They found that there was a high frequency of disproportionately wide noses in relation to height in both cleft types before primary lip repair. Repair of the lip also resulted in a more aesthetic nasal appearance. The authors concluded that the quantitative determination of this nasal stigma in cleft lip and palate patients who had undergone primary lip repair provides valuable information for surgical correction of the cleft soft tissue deformities.

Previous studies have applied anthropometric methods to individuals with craniofacial deformities and their findings have provided results that have

complemented and augmented the accepted clinical description of the condition (Ward and Bixler, 1987; Kolar *et al.,* 1987). The above- mentioned studies indicate the importance of anthropometric measurements or analysis as a valuable tool in the understanding of craniofacial anomalies. These techniques can identify defective areas not immediately apparent from qualitative observation. Anthropometric norms of the measurements and indices are useful guides but they do not impose strict rules. The final judgement is the hand and eye of the experienced surgeon. Proportion indices can define the gross shape of areas but the surgeon must be aware of the total morphologic pattern of this complex.

## *2.6* Introduction to Cephalometric Radiology

To be able to 'see' into the body has always been, and remains, a primary capability desired and necessary to study and elucidate the basic processes of life, and to diagnose and treat the disease conditions that perturb and endanger the normal function of biological processes (Robb, 1995).

### 2.6.1 Cephalometric Analysis

In 1931, Broadbent introduced the basic techniques of radiographic cephalometrics using an X-ray machine and a head holder called a cephalostat (McNamara, 1984**).** Cephalometric radiology is a technique that uses standardised radiographs to obtain facial measurements, and its principles follow closely those of craniometry, which has long been used in the quantitative study of dried skulls.

### 2.6.2 Limitation of Cephalometrics

Despite recent advances in diagnostic tools, clinical use of the cephalometric radiograph remains important as an aid in the diagnosis of craniofacial deformities. Previous studies of cleft lip and palate and craniofacial deformities have applied two-dimensional lateral cephalometric (e.g. Kreiborg *et al.*, 1977) methods but these have significant limitations, such as superimposition of structures, difficulty identifying landmarks and poor visualization of 3D structures (Moyers and Bookstein, 1979; Cohen, 1994; Richtsmeier and Cheverud, 1986; Fisher *et al.*, 1999; Singh *et al.*, 2004).

Maue-Dickson (1979) in his review article highlighted the fallacies which may result from the selection of any particular landmark in making judgements about the direction of facial growth. The placement of metallic markers in the growing jaws has permitted superimposition on some presumably stable structures (Bjork, 1969). However, the gonial angle measured using lateral head films demonstrates a difference of about 5 to 7 degrees compared to craniometric methods. The difference is statistically significant and may be attributed to a systemic error in the roentgenocephalometric method involving a magnification of gonial angle. This serves as a reminder of the need for caution using the above techniques.

## 2.7 Computed Tomography

### 2.7.1 History of CT

CT has its roots in the early part of this century. In 1917, the Austrian mathematician, Johann Radon (1887-1956) described a mathematically rigorous inversion formula for reconstruction of an object from its projections. Although Radon's work fell into

obscurity after the First World War, the problems of image reconstruction were tackled by Ronald N. Bracewell (1956) in the field of astronomy, and William H. Oldendorf (1961) an American neurologist frustrated by the inadequacy of X-ray images, devised an electronic apparatus designed to overcome existing technical and computational difficulties (Robb, 1995). In the late 1950s, Allen McLeod Cormack (physicist) proposed that if sufficient X-ray views were taken at different angles, a cross-sectional matrix of mathematical coefficients could be calculated. These coefficients could then each in turn be given a value of intensity on a grey scale from which an image of the internal structure or anatomy of the object or body being studied could be constructed. His early studies led to a mathematically accurate way of quantitatively reconstructing cross-sectional images from x-ray projections (Romm, 1984).

In the late 1960s, the British scientist Godfrey Hounsfield was independently developing his ideas that mathematical techniques could be used to reconstruct the internal structure of the body from a number of x-ray measurements. He concluded that quantitative tomographic techniques could produce up to 100 times more accurate measurements than conventional radiographic methods. This realization motivated the construction and testing of several prototype scanners in the Central Research Laboratories of Elector-Musical Instruments Ltd. (EMI).

These efforts eventually resulted in the construction of the first clinical X-ray CT scanner of the head, called the EMI brain scanner, which was installed at Atkinson Morleys Hospital, Wimbledon, England, in 1971. With the successful introduction of the EMI brain scanner into the clinical arena, an explosive development and marketing of CT scanners started with an increasing accumulation of published data

in the early 1980s. The potential utilization of 3D imaging in biomedical in biomedical research is beginning to be explored. The realisation that this tool may be useful in basic biological investigations has been precipitated by continually improving the capability of 3D imaging for quantitative tissue characterisation and by the promise of dynamic scanning for measurement of functional parameters.

### 2.7.2 Application of 3D Imaging to the Study of Craniofacial Dysmorphology

#### *2.7.2.1 Assessment of craniofacial deformities*

Medical imaging of the craniofacial area was limited to the mid-sagittal plane, primarily using cephalometric methodology, until the introduction of 3D surface reconstructions from CT scans. The ability to remove the cranial vault made the endocranial base visible; the ability to disarticulate the mandible exposed the entire exocranial base. The resultant 3D images are useful for longitudinal measurement of cranial length, width, and height, as well as assessment of symmetry of the calvaria about the midsagittal plane and the paired components of the three endocranial fossae. (Marsh *et al.*, 1986; Marsh and Vannier., 1987). Reformatted CT data, displayed both as 2-D slice and 3D images, provide the simulator with the information necessary for comprehension of the relevant anatomy (Lo *et al.*, 1994).

Ono *et al.* (1992) studied deformities in patients with congenital facial anomalies, such as cleft lip and palate and hemifacial microsomia using 3D CT images. Using this system, they prepared a wire frame model called a ‘skeletogram’, for detailed morphological analysis. This study allowed detection of severe and complex

deformities (e.g. cranial deformation and mandibular displacement) and severe facial asymmetry.

Sakurai *et al.* (1998) developed an hypothesis about the mechanisms by which the craniofacial bones are deformed in plagiocephaly (unilateral premature synostosis of the coronal suture). Three-dimensional CT data were obtained from two patients with plagiocephaly and three-dimensional skeletal replicas were made to analyse the deformities of the cranium, facial bones, and mandible. From this analysis it was concluded that the asymmetric deformation of the facial bones in these patients was caused by a combination rotation of the calvaria and facial bones, and the displacement of the temporo-mandibular joint on the affected side.

#### *2.7.2.2 3D CT morphometric analysis of craniofacial deformity*

The most recent approaches to the study of growth in three dimensions have come from the field of morphometrics, a field that joins biology and geometry (Ohman and Richtsmeier, 1994; Richtsmeier *et al.,* 2002). Morphometric techniques use the location of particular biological loci called 'landmarks' (for example, foramina, sutural intersection, or bony prominences) to define form. Forms are quantitatively compared on the basis on these data.

For example, a CT examination of a patient usually consists of a set of parallel images, and 3D coordinates of landmarks located within this set of CT images can be used as input for morphometric analysis. Because a CT image is actually a matrix of pixels (picture elements) organised in rows and columns, the coordinates of landmarks within an image can be expressed by row, or x coordinates, and column, or y coordinate, and the direction perpendicular to the parallel image planes is the z

direction. If landmark coordinate data such as these are collected from a form at one point in time (from CT examination) and then collected from the same form later in time (a subsequent CT examination), the changes in the relative location of these landmarks provide a 3D description of growth based on landmark data.

As an example of this approach, Richtsmeier *et al.* (1991) used longitudinal data to study growth of the cranial base in patients with various types of craniosynostosis. The 3D coordinate set of landmarks located on the cranial base was identified on the preoperative, perioperative, and postoperative CT scans for a set of patients. Quantitative comparison of the relative location of the set of landmarks on the preoperative scans compared with the perioperative scans was interpreted as preoperative growth, whereas the comparison on the landmark location in the perioperative scans versus the postoperative scans was interpreted as postoperative growth.

Comparisons were made using two different morphometric methods: Euclidean Distance Matrix Analysis (EDMA) (Lele and Richtsmeier, 1991) and finite element scaling analysis (FESA) (Richtsmeier and Cheverud, 1986). EDMA uses landmark coordinate data to calculate all possible linear distances between landmarks. A FESA can be used to display developmental transformations in terms of allometry (size-related shape-change) and anisotropy (directionality of shape-change) (Singh *et al.*, 2004). It compares forms in order to determine the amount of change required to produce a target (older) morphology from an original (younger) morphology. Both of these methods enable the localization of form difference between two objects or two samples of objects. This particular study concluded that growth patterns of the cranial base in children with craniosynostosis differ according to which sutures are affected.

Kreiborg *et al.* (1993) did a study to describe and analyze Apert and Crouzon syndromes skulls from 3D reconstructions of CT scans. Their results showed that Apert and Crouzon syndromes are very different in cranial development and their dysmorphology is highly age dependent. They suggested that cartilage abnormalities, especially in the cranial base, play a primary role in cranial development in the Apert syndrome from very early intrauterine life. Thus adult craniofacial morphology in Apert syndrome is a combined result of the primary malformation together with subsequent dysmorphic and compensatory growth changes, probably compounded by early cranial deformation.

The primary abnormality in Crouzon syndrome appears to be early fusion of the sutures and synchondroses. Based on the findings at birth and early infancy, it would appear that sutural fusions occur relatively late in fetal life. The adult cranial form is explainable by the resultant dysmorphic and compensatory growth changes.

Zumpano *et al.* (1999) did a study to quantify the morphological differences in three dimensions among individuals with untreated isolated metopic synostosis (trigonocephaly). Comparisons between the metopic age groups found that trigonocephalic phenotype worsens with time.

#### *2.7.2.3 Intra-cranial volume*

Another promising application using CT or magnetic resonance (MR) examinations, or both, is the evaluation of cranial volume. One of the objectives of surgery in patients afflicted with craniosynostosis is to relieve intra-cranial pressure due to the diminished volume or the altered shape of the intra-cranial cavity, or both.

Previous studies have indicated the important of the relationship between intracranial

volume (ICV) and intracranial pressure in patients with craniosynostosis. A few studies suggested that the constricted effect of untreated craniosynostosis on an otherwise normal brain would cause elevation of intracranial pressure during periods of rapid brain growth. This could consequently produce brain damage. Therefore, surgical decompression was advocated to release the prematurely fused metopic or sagittal suture in the hope that spontaneous brain reshaping would occur and prevent brain damage.

As the 3D software has become more advanced, intracranial volume measurements can be calculated non-invasively from standard CT scans.

In 1995 Posnick et al. measured ICV in craniosynostosis patients before and after surgery. Using a 3D software package – CT Pak – all the holes in the skulls (i.e., foramina and fontanelles) could be blocked off using the mouse. The computer then counted the number of voxels within the cranial cavity and calculated its volume. Their findings suggested that premature closure of either the sagittal or metopic suture did not result in diminished intracranial volume.

In 2000 Abbott *et al.* measured ICV for normal populations of children using *Persona* 3D software package. *Persona* automatically contours the bone in each slice and saves into separate files that are processed by a procedure called contour triangulator to produce a triangular mesh. The ICV is calculated by summing the cross-sectional areas that intersect the region of interest and multiplying by slice separation (referred as the Cavalieri estimator).

#### *2.7.2.4 Stereolithography (STL)*

The fabrication of models of the craniofacial complex depends on adequate

information about the size and shape of the object to be constructed. CT data have been used to provide a triangular surface description of the craniofacial bones for this purpose. STL is a computer-mediated method to create anatomically correct three-dimensional models based on CT. A variety of methods such as STL and laser sintering are used to accurately reproduce both the internal and external anatomy of craniofacial structures for pre-operative planning of craniofacial, orthognathic and maxillofacial surgery (Lambrecht and Brix, 1990; Abbott *et al.*, 1997; Sailer *et al.*, 1998; Onishi and Maruyama 2001). Dolz *et al.* (2000) have indicated the potential application of STL in the field medicine. The authors suggest that the production of 3D models could be useful in court to demonstrate injuries and convey information to jurors that would be more useful than standard photographs and diagrams.

## 2.8 Summary

Computer assisted medical imaging technologies provide new tools for the study of congenital craniofacial deformities. The post-processing of CT scan data to produce 3D surface reconstructions has facilitated the comprehension and quantitation of such data by nonradiologists. While 3D reconstructions were applied initially to assist clinical management of patients with craniofacial deformities, these images are now finding utility in the study of unique anomalies, the definition of group characteristics for dysmorphic heads, the differentiation of similar phenotypes, and the documentation of the effects of craniofacial surgery on craniofacial growth. These findings should assist the formation and evaluation of hypotheses regarding mechanisms of congenital malformation and deformation.

## References

Abbott AH, Netherway DJ, Niemann D, Cole J, Moore M, David D (2000). CT-determined intracranial volume for normal population. *J Craniofac Surg* 11:211-233.

Abbott JR, Netherway DJ, Wingate PG (1997). Role of computer generated models in reconstruction of oral and craniofacial defects using alloplastic and autogeneous materials. *Asian J Surg* 20:35-41

Ardinger HH, Buetow KH, Bell GI, Bardach J, VanDemark DR, Murray JC (1989). Association of genetic variation of the transforming growth factor alpha gene with cleft lip and palate. *Am J Hum Genet* 45:348-353.

Bjork A (1969). Prediction of mandibular growth rotation. *Am J Orthod* 55: 585-599

Bodo M, Baroni T, Carrinci F, Becchetti E, Belluci C, Pezzeti F, *et al*. (1999). TGFβ Isoforms and decorin gene expression are modified in fibroblast obtained from non-syndromic cleft lip and palate subjects. *J Dent Res* 78:1783-1790.

Carrinci F, Pezetti F, Scapoli L, Padula E, Bacillero U, Curioni C, *et al.* (1995). Non-syndromic cleft lip and palate: evidence of linkage to the a microsatellite marker on 6p23. *Am J Hum Genet* 56:337-339.

Chenevix-Trench G, Jones J, Green A, Duffy DL, Martin N (1992). Cleft lip with or without cleft palate: association with transforming growth factor-alpha and retinoic acid receptor loci. *Am J Hum Genet* 51: 1377-1385.

Cohen AM (1984). Uncertainty in cephalometrics. *Br J Orthod* 11:44-48

Cox TC (2004). Taking it to the max: the genetic and developmental mechanisms coordinating midfacial morphogenesis and dysmorphology. Clin Genet 65:163-176.

Dolz MS, Cina SJ, Smith RS (2000). Stereolithography: A potential new tool in forensic medicine. *Am J Forensic Med Pathol* 21:119-123.

Eiberg H, Bixler D, Forg Anderson P, Conneally PM, Mohr J (1987). Suggestion of linkage of a major locus for non-syndromic orofacial cleft with F13A and tentative assignment to chromosome 6. *Clin Genet* 32:129-132.

Farkas LG, Hajnis K, Posnick JC (1993). Anthropometric and anthroposcopic findings of the nasal and facial region in cleft patients before and after primary lip and palate repair. *Cleft Palate Craniofac J* 30:1-12.

Ferguson MW (1988). Palate development. *Development* (Suppl) 103:41-60.

Ferguson MW (1994). Craniofacial malformation: towards a molecular understanding. *Nat Genet* 6:329-330.

Fisher DM, Lo JL, Chen YR, Noordhoff MS (1999). Three-dimensional computed tomography analysis of the primary nasal deformity in 3-month-old-infants with complete unilateral cleft lip and palate. *Plast Reconstr Surg* 103:1826-1834.

Fitzpatrick DR, Denhez F, Kondaiah P, Athurst RJ (1990). Differential expression of TGFβ isoforms in murine palatogenesis. *Development* 109:585-595.

Hartridge T, Illing HM, Sandy JR (1999). The role of folic acid in orofacial clefting. *Br J Orthod* 26:115-120.

Hart TC, Marazita ML, Wright JT (2000). The impacts of molecular genetics on oral health paradigms. *Crit Rev Oral Biol Med* 11:26-56.

Hecht JT, Wang Y, Connor P, Blanton SH, Daiger SP (1993). Non-syndromic cleft lip and palate: no evidence of linkage to HLA or factor 13A. *Am J Hum Genet* 52:1230-1233.

Holder SE, Vintiner GM, Farren B, Malcolm S, Winter RM (1992). Confirmation of an association between RFLPs at the transforming growth factor-alpha locus and non-syndromic cleft lip and palate. *J Med Genet* 29:390-392.

Johnston MC, Bronsky PT (1995). Prenatal craniofacial development: New insights on normal and abnormal mechanisms. *Crit Rev Oral Biol Med* 6:368-422.

Juriloff DM, Mah DG (1995). The major locus for multifactorial nonsyndromic cleft lip maps to mouse chromosome 11. *Mamm Genome* 6:63-69.

Kallen K (1997). Maternal smoking and orofacial cleft. *Cleft Palate Craniofac J* 34:11-16.

Kolar JC, Munro IR and Farkas LG (1987). Anthropometric evaluation of dysmorphology in craniofacial anomalies: Treacher Collins syndrome. *Am J Phys Anthropol* 74: 441-451

Kreiborg S, Marsh JL, Cohen MM Jr., Liversage M, Pedersen H, Skorby F, Borgosen SE, Vannier MW (1993). Comparative three-dimensional analysis of CT scans of the calvaria and cranial base in Apert and Crouzon Syndrome. *J Craniomaxfac Surg* 21: 181-188

Kreiborg S, Dahl E, Prydsoe U (1977). A unit of infant roentgencephalometry.

*Dentomaxillofac Radiol* 6:107-111

Lambrecht JT, Brix F (1990). Individual skull model fabrication for craniofacial surgery. *Cleft Palate Craniofac J* 27:382-386.

Lele S and Richtsmeier JT (1991). Euclidean distance matrix analysis. *Am J Phys Anthropol* 86: 415-428

Lidral AC, Romitti PA, Basart AM, Doetschman T, Leysens NJ *et al.* (1998). Association of MSX1 and TGFβ3 with nonsyndromic clefting in human. *Am J Hum Genet* 63:557-568.

Lo LJ, Marsh JL, Vannier MW and Patel VV (1994). Craniofacial computed assisted surgical planning and evaluation. *Clin Plast Surg* 23: 87-100.

Marsh JL and Vannier MV (1987). The anatomy of cranio-orbital deformities of craniosynostosis: Insight from 3D images of CT scans. *Clin Plast Surg* 14: 49-60

Marsh JL and Vannier MW (1986). Cranial base changes following surgical treatment of craniosynostosis. *Cleft Palate J* 23 (Suppl): 9-18

Martinelli M, Scapoli L, Pezzetti F, Carrinci F, Carrinci P, Baciliero U, Padula E and Tognon M (1998). Suggestive linkage between markers on chromosomes 19q13.2 and nonsyndromic orofacial cleft malformation. *Genomics* 51:177-181.

Maue-Dickson W (1979). The craniofacial complex in cleft lip and palate: an update review of anatomy and function. *Cleft Palate J* 16:291-317.

McNamara (1984). A method of cephalometric evaluation. *Am J Orthod* 86:449-469.

Moyers RE, Bookstein FL (1979). The inappropriateness of conventional cephalometrics. *Am J Orthod* 75:599-617.

Ohman JC and Richtsmeier JT (1994). Perspective on craniofacial growth. *Clin Plast Surg* 21: 489-499

Onishi K and Murayama Y (2001). Three-dimensional solid model integrated with dental model for maxillofacial surgery. *Plast Reconstr Surg* 108:1696-1699.

Ono I, Ohura T, Narumi E, Kawashima K, Matsuno I, Nakamura S, *et al.* (1992). Three-dimensional analysis of craniofacial bones using three-dimensional computer tomography. *J Craniomaxfac Surg* 20: 49-60.

Posnick JC, Armstrong D, Bite U (1995). Metopic and sagittal synostosis: intracranial volume measurements prior to and after cranio-orbital reshaping in childhood. *Plast Reconstr Surg* 96:299-309.

Richtsmeier JT, Deleon VB, Lele RS (2002). The promise of geometric morphometrics. *Yearbook of Physical Anthropology* 45: 63-91.

Richtsmeier JT and Cheverud JM (1986). Finite element scaling analysis of normal growth of the human craniofacial complex. *J Craniofac Genet Dev Biol* 6: 289-323.

Richtsmeier JT, Grausz HM, Marsh JL (1991). Three-dimensional analysis of cranial base in craniosynostosis using tomographic data. *Cleft Palate Craniofac J* 28: 55-67

Robb RA (1995). Three-Dimensional Imaging. VCH, New York.

Romm S, Goldstein S, Gottlieb S, Luce E (1984). Computed Tomography: A new horizon for the plastic surgeon. *Plast Reconstr Surg* 73:476-489.

Sailer HF, Haers PE, Zollikofer CPE, Warnke T, Carls FR, Stucki P (1998). The value of stereolithography models for preoperative diagnosis of craniofacial deformities and planning of surgical corrections. *Int J Oral Maxfac* 27:327-333

Sakurai A, Hirabayashi S, Sugawara Y and Harri K (1998). Skeletal analysis of craniofacial asymmetries in plagiocephaly (unilateral coronal synostosis). *Scand J Plast Reconstr Hand Surg* 32 : 81-89.

Satokata I and Maas R (1994). MSX1 deficient mice exhibit cleft palate and abnormalities of craniofacial and tooth development. *Nat Genet* 6: 348-356

Shaw GM, Wasserman CR, Lammer EJ, O'Malley CD, Murray JC, Basart AM, *et al.* (1996). Orofacial clefts, parental cigarette smoking, and transforming growth factor alpha gene variants. *Am J Hum Genet* 58 : 551-556.

Singh GD, Rivera-Robles J, Jesus-Vinas J (2004). Longitudinal craniofacial growth patterns in patients with orofacial clefts: geometric morphometrics. *Cleft Palate Craniofac J* 41:136-143

Stein J, Mulliken JB, Stal S, Gasser DL, Malcolm S, Winter R, *et al.* (1995). Nonsyndromic cleft lip with or without cleft palate: evidence of linkage to BCL3 in 17 multi-generational families. *Am J Hum Genet* 57 : 257-272.

Taya Y, O'Kane S, Ferguson MJ (1999). Pathogenesis of cleft palate in TGFβ3 knockout mice. *Development* 126: 3869-3879.

Vegter F and Hage JJ (2000). Clinical anthropometry and canons of the face in historical perspective. *Plast. Reconstr. Surg* 106: 1090-1096.

Vintiner GM, Lo KK, Holder SE, Winter RM, Malcolm S (1993). Exclusion of candidate genes from a role in cleft lip with or without cleft palate: linkage and association studies. *J Med Genet* 30:773-778.

Ward RE and Bixter D (1987). Anthropometry analysis of the face in hypohidrotic ectodermal dysplasia: a family study. *Am J Phys Anthropol* 74: 453-458.

Wyszynski DF, Beaty TH, Maestri NE (1996). Genetics of nonsyndromic oral clefts re-visited. *Cleft Palate Craniofac J* 33:406-417.

Zumpano MP, Carson BS, Marsh JL, Vanderkolk CA, Richtsmeier JT (1999). Three dimensional morphological analysis of isolated metopic synostosis. *Anat Rec* 256:177-188.

# CHAPTER 3

# GENERAL METHODOLOGY AND STUDY SAMPLE

## 3.1 Ethical Approval

Ethical approval was given by the Ethics and Research Committee USM dated 30/8/01, Number: USM/PPSG/Ethics Com./2001[61.3(1)] (Appendix 1). Data collection took place in Malaysia from September 2001 to August 2002. The Ethics Committee of the Women's and Children's Hospital was also notified about the study who approved the procedures adopted for handling the CT records.

## 3.2 Patient Selection

The study subjects were non-syndromic babies born with cleft lip with or without cleft palate and isolated cleft palate. Any syndromic babies were excluded.

## 3.3 Participating Clinical Units

A number of specialist clinical units cooperated in this study by identifying and referring subjects who met the selection criteria: the Combined Cleft Palate and Multidisciplinary Clinic at Kota Bharu Dental Clinic, which is the main craniofacial referral center in Kelantan; the Plastic and Reconstructive Surgery Units at Hospital

Universiti Sains Malaysia (HUSM) and Hospital Kota Bharu; the main Plastic Surgery facilities in Kelantan; and the Oral Maxillofacial Unit (HUSM), which is the principal Maxillofacial referral center in Kelantan.

## 3.4 Preparatory Work - September 2001

The author arrived safely at Kota Bharu on 12th September 2001 from Adelaide. Letters were sent to all Directors of Hospital in the States of Kelantan and Terengganu seeking their cooperation in identifying potential patients born with cleft lip and palate for this study. Letters were also sent directly to clinicians including Plastic Surgeons, Orthodontists, Paediatricians, Oral Maxillofacial Surgeons, Medical and Dental Officers. The approved consent form was explained to potential participants who were then free to sign or decline.

Presentations were given to academic and medical staff regarding the background of this study and the importance of the participation of other staff members such as nurses and radiographers.

## 3.5 Data Collection

The author attended as many Outpatients Clinics as possible at the Kota Bharu Dental Clinic, Hospital Kota Bharu and Hospital Universiti Sains Malaysia. Appointment books were also searched for possible patients to include in the study. Parents were contacted by telephone or letter where possible or were approached on admission to the hospital one day before lip or palate repair. If they agreed to participate, consent was obtained and the CT scan done on the same day.

Some 50 potential subject families were approached with around 25% declining to be involved. An initial subject pool of 38 babies with cleft lip and palate participated in this investigation. Data were collected for 35 patients as three patients failed sedation. Subsequently a further six patients were excluded as they had already undergone lip repair (Table 3.1).

**Table 3.1.** Age and sex distribution of the cleft and NC groups.

| **Group** | **Sex** | **N** | **Mean Age (Days)** | **SD** | **Range min-max** |
|---|---|---|---|---|---|
| CLP | F 12<br>M 17 | 29 | 115 | 76 | 14-340 |
| NC | F 3<br>M 9 | 12 | 145 | 86 | 19-297 |

CT scans were obtained from 29 patients with unoperated non-syndromic cleft lip and palate. They were aged between 0-12 months and compared with 12 NC patients in the same age group (Table 3.1). The NC patients had normal craniofacial morphology but had medical indications for scanning, including meningitis and hydrocephalus (Yusof, 2003). Table 3.1 shows that the age range was greater in the CLP group. A few older children were included in this group because their primary operation had been postponed due to other health problems, such as upper respiratory tract infection and aspiration pneumonia. The distribution of clefts was as follows:

cleft lip and/or alveolus (CL), n=7; unilateral cleft lip and palate (UCLP), n=10; bilateral cleft lip and palate (BCLP), n=4; isolated cleft palate (ICP), n=8; unaffected non-cleft (NC), n=12.

The data collection process is summarised in the following flow chart.

**Flow Chart**

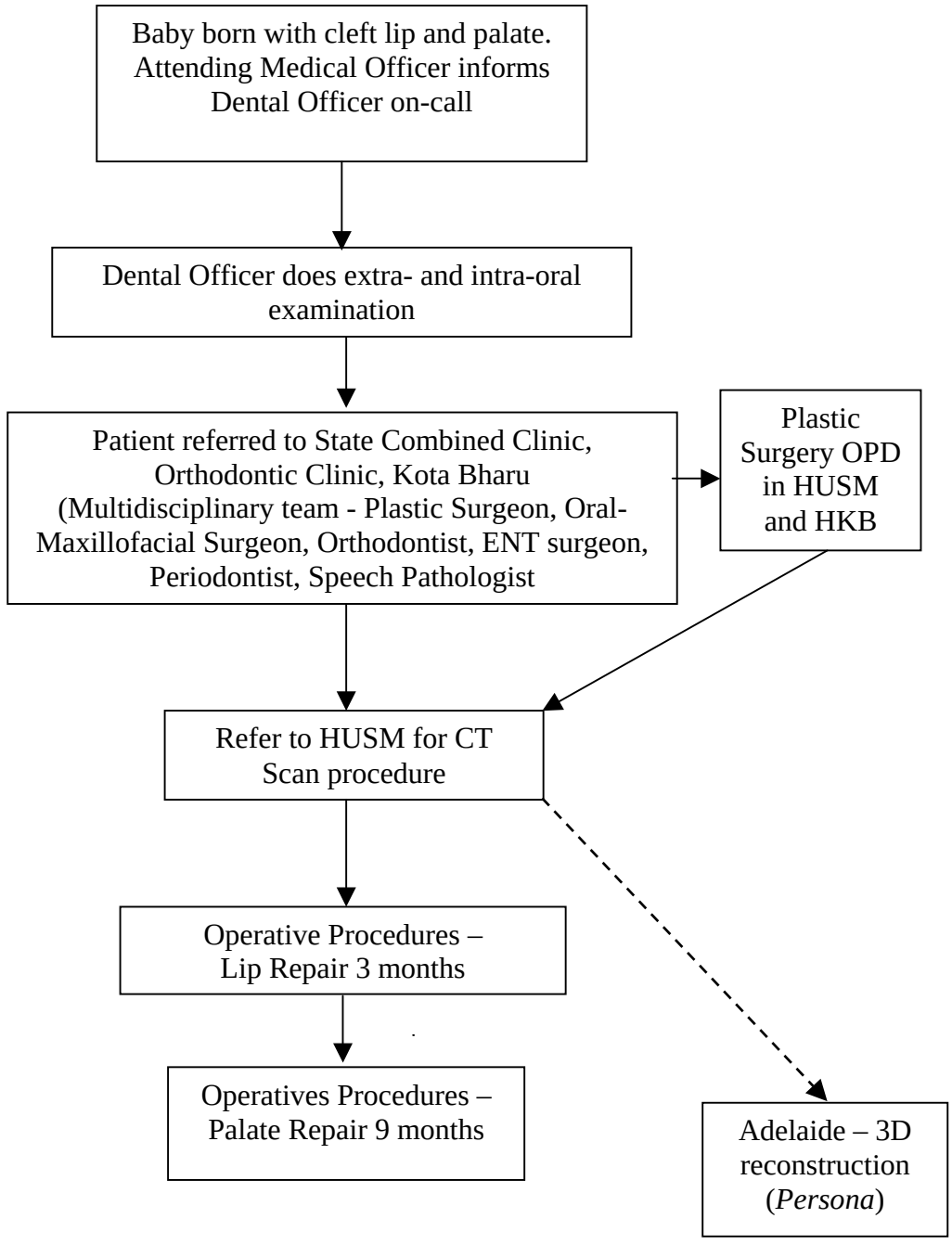

### 3.5.1 Difficulties Encountered

i. Number of cases

The optimal number of cases for the study was based on power studies, originally set at 50, but this proved to be difficult to obtain. Letters were sent to and meetings had to be arranged with Hospital Directors in order to get patients with clefts to be referred to the outpatient clinic or Combined Clinic. In spite of requests to the hospital directors some patients were not referred to either clinic and, of those seen, over 25% of parents refused to allow their child to be part of the study. Although the final sample sizes were smaller than originally planned, preliminary analyses confirmed that they would still provide sufficient power for subsequent statistical analysis.

ii. Duration of Data Collection

The first patients were seen in October 2001 and nearly all were newborns. As this was a prospective study and the age of the baby at scanning had to be close to three months of age, very few records were collected between October and December 2001.

iii. Logistics

In order to gain consent from parents for this study it was necessary for the author to be personally present to explain the objective and procedures. Therefore it was not possible to concurrently collect records from each of the three clinics involved (Hospital Kota Bharu, Kota Bharu Dental Main Clinic and Hospital Universiti Sains Malaysia (HUSM)).

iv. Timing of CT Scan

The patients were scanned when they were admitted to the ward for lip repair; one day prior to surgery. On that day the patients needed to be examined by the anaesthetic team; a procedure that started in the afternoon. Therefore the CT scan had to be obtained after office hours or in the late evening. The radiographer had to be available to perform the scan. Quite often the scan had to be done on the weekend as the operation fell on the first day of the week.

v. Sedation

Prior to scanning, patients were given Syrup Chloral Hydrate (50mg/kg) or IV Sedation (Dormicum 0.15mg/kg) according to body weight. In spite of this sedation three patients moved during the scanning procedure and were not able to be scanned.

## 3.6 CT Scanner, Hospital University Sains Malaysia, Kota Bharu

The GE LightSpeed Computed Tomography (CT) scanner has set the benchmark for multi-slice CT technology. First introduced in 1998, the LightSpeed QX/ I was the world's first four-slice CT scanner. The LightSpeed Plus, which is the one of the 2000 IDSA silver award winners, continues this legacy of the multi-slice benchmark in image quality, anatomic coverage, and system performance with even greater results. In axial mode, LightSpeed axial is 4x faster than single slice axial (Source: Internet, GE Medical System , LightSpeed Plus CT). The selection of the Lightspeed Plus brand was critical in terms of data being compatible with the computer software package at the Australian Craniofacial Unit, Women's and Children's Hospital, Adelaide.

The Universiti Sains Malaysia purchased this machine in 2001 to support this area of research in the newly established Dental School in Kota Bharu. At the moment a number of projects are being undertaken that use data acquired from this source.

### 3.6.1 The CT Scanning Protocol

The infants were first sedated with oral chloral hydrate (25 mg/kg dose) half an-hour before the procedure (Fig 3.1). Intravenous sedation was given to a few patients whose cooperation could be obtained with I.V Dormicum 0.1 mg/kg dose (maximum 0.5 mg/kg dose). The antidote for Benzodiazipine (such as Dormicum or Valium), Flumazenil was put on standby with an ambobag, facemask, endotrachael tube (ETT), pulse oxymeter and oxygen if any emergency arose.

Flumazenil was given (5 mg/kg stat) and repeated every 60 seconds till 40 mg/kg (maximum 2 mg). During scanning a Surgical Registrar was on standby to deal with any emergency. Fortunately no complications arose from the scanning procedure.


**Figure 3.1** Showing the sedated infant prior to CT scanning.

Axial scans were obtained with a GE Lightspeed Plus CT Scanner System at the Department of Radiology, Hospital Universiti Sains Malaysia. The protocol used at the Australian Craniofacial Unit (ACFU), Women's and Children's Hospital, Adelaide (Australia) was followed as the basis for the scanning procedure and is detailed below.

#### *3.6.1.1 Head alignment*

Patients were placed in the supine position during the scanning procedure with the head symmetrically positioned within the head holder, such that the Frankfort plane was perpendicular to the floor (The Frankfort plane is the line joining superior margin of external auditory meatus and infraorbital margin). The field of view extended from the top of the head (vertex) to below the chin (menton) so as to include the cervical spine (Fig. 3.2).


**Figure 3.2** The author and radiographer positioning the infant prior to CT scanning.

### *3.6.1.2 Head immobilisation*

The patient's head was positioned within the head holder using laser-light guiding. Radiolucent tape was placed across the forehead and chin to ensure the head was immobilised (Fig. 3.3).


**Figure 3.3** The author and radiographer immobilising the patient's head.

### *3.6.1.3 Scanning procedure and data transfer*

For patients from birth to 1 year the tube voltage and current were typically 100KV, 120 mA respectively, but minor adjustments to these parameters were made according to the patient's size. Slices of 1.25 mm thickness with a spacing of 1.25 mm were constructed before being transferred to the console operating system or workstation (Fig. 3.4). Once the scans were acquired, data were saved on CDROM (compatible disk) for transfer to the Women's and Children' Hospital using Digital Imaging and Communication in Medicine (DICOM 3) format. To ensure that the decoded orientation was correct, images of axial slices were clearly marked to indicate each

patient's left and right. The names, ID Numbers, Scan Numbers and age were recorded and the CDROM was posted via courier service from Hospital Universiti Sains Malaysia to the Australian Craniofacial Unit, Adelaide.


**Figure 3.4** The CT scanner workstation at the Radiology Department, HUSM.

## 3.7 Steps of 3D CT Reconstruction

### 3.7.1 The Data Processing and Visualization Workstation

Advances in the microelectronics industry have facilitated concomitant advances in image processing, display, and analysis (understanding), particularly in biomedical imaging and scientific visualization (Robb, 1995). As the electronics and hardware for computers have developed, software for computers has also evolved to provide the tools that make the computers much more powerful.

The Silicon Graphics Computer workstations with *Persona* software package at the ACFU (Abbott *et al.,* 2000; Netherway *et al.,* 1997, 1999) provide examples of interactive image processing and visualization imaging systems**.** The workstation consists of :

- 300 MHZ IP30 Processors
- Central Processing Unit: MIPS R12000Processor Chip Revision
- Main Memory Size: 1024 Mbytes
- Disk drive: Unit 1,2,3 on SCSI controller 0
- Tape Drive: unit 3 on SCSI controller 1: DAT
- Optical disk: unit 4 on SCSI controller 1
- Integral Fast Ethernet: efO, version 1, pci 2

### 3.7.2 Transferring Digital Images to the Computer

The two basic methods of transfer are:

1. Compatible intermediate media, such as tape or removable disk, and
2. Computers networks with compatible protocols.

Data, traditionally presented as multiple film slices, is captured in digital form direct from the scanner and loaded into the computer.

The editing facility eliminates unnecessary information and minimizes disk storage.

### 3.7.3 Image Generation and Display

Visualization of 3D biomedical volume images can be divided into two different techniques**:** surface rendering and volume rendering.

Surface rendering techniques characteristically require the extraction of contours that define the surface of the structure to be visualized. Volume rendering techniques are based on ray-casting algorithms through the volume image. The ray-casting technique provides the important advantage that the visualization is created directly from the volume image, with the selection of structures that will be rendered completed during the ray-casting process. It can also display data directly from the grey scale volume. The selection of the data that will appear on the screen is done during the projection of the voxels. This is done using a camera model that consists of a source point (called the Eye), a focus point (where the eye is looking), and a matrix of pixels (the screen). The visible object to display (called the scene) is in front of the camera within a truncated volume called the viewing pyramid. The purpose of the ray-casting model is to define the geometry of the rays cast through the scene. To connect the source point to the scene, for each pixel on the screen, a ray is defined as a straight line from the source point passing through the pixel. To generate the picture, the pixel values are assigned appropriate intensities by the rays passing everywhere through the scene.

Rendering assembles the slice data into 3D volume reconstructions, providing the basis for interrogation, analysis and manipulation.

### 3.7.4 Image Measurement

The *Persona* software package developed by the Research Unit at the ACFU, Women's and Children's Hospital, Adelaide (Abbott *et al.,* 2000; Netherway *et al.,* 1997, 1999) was utilized for three-dimensional reconstruction of the images that were clear and detailed and to determine the 3D coordinates of osseous landmarks on the Silicon Graphics Computer workstation. This package allows the display of the CT scan data simultaneously around a 3D marker in windows containing axial, sagittal and coronal cuts, and 3D reconstruction of the external craniofacial bones and the cranial base. Measurements of distances, angles and shapes of selected bones constituting various regions of the cranium and face were performed using the software package. The measurements were chosen so that they were relatively easy to identify, were reproducible and of clinical relevance.

### 3.7.5 Method for 3D Landmark Determination

The clarity of the 3D CT reconstructions readily allows the well-established landmarks of craniometry to be determined and 2D cephalometry to be extended. Three hundred and fifty craniofacial landmarks have been defined to describe the craniofacial skeleton. Most of these landmarks have been determined with a measurement error in the range 1-2mm, or approximately twice the CT scan pixel size. From previous replicability studies (Abbott *et al.,* 1990) based on 10 skulls using 215 landmarks, the findings of relocation accuracy vary from a minimum of 0.3mm (crista galli) to a maximum of 2.8mm (pterion left) with median 0.9mm. These results are excellent and comparable to 2D cephalometric determination, although for nearly 10 times the number of landmarks. The greater number of useable landmarks is a direct result of the superior discrimination possible using CT data rather than plain film radiography.

The landmark determination module in *Persona* displays a list of landmarks for each craniofacial bone. After shifting the 3D cursor (visible simultaneously on 3D CT reconstructions and on axial, sagittal and coronal images) onto the landmark position, and using “save” to store the position, the landmark can be returned for refinement simply by selecting its name from the list.

### 3.7.6 Morphometric Analyses

In addition to the visualization and measurement software, computer programs in C and C++ were written that execute on the Silicon Graphics computer running a version of the Unix operating system. These programs automatically process 3D landmarks. There is a major look-up table of all landmarks that have been defined with full-name, abbreviated name and a code number. All programs reference this table to ensure landmark names are correct. There are also “measurement files” that list all of the distance, angle and ratio measurements that may be determined from the 3D coordinates. Scripts (in “csh” and “perl”) have been written to utilise all 3D landmark files in each patient/normal group (specified by tables of participants to each group) to determine all the required measurements with one command. In this way, if one wishes to add a new measure, the programs can be re-run to easily update any derived measurements or statistic.

## 3.8 *Persona* 3D Medical Imaging and Analysis

*Persona* is a graphics application designed to handle the assembly and manipulation of image data generated by scanning equipment. A vast amount of information is

generated by modern scanning equipment (CT, MRI, and other modalities). Images have been traditionally presented as multiple film slices. It can also be captured in digital form direct from the scanner and loaded into the computer. *Persona* has been developed to rationalise, display and interpret the image data efficiently, enabling the precise location of markers and the determination of critical measurements.

*Persona* enables:

(i) Editing of the scan data to eliminate unnecessary information and minimise disk storage

(ii) Rendering of the slice data into 3D volume reconstruction

(iii) Interrogation of the 3D reconstruction allowing variable viewing options, measurement facilities and precise location of marker points and boundaries

(iv) Manipulation of the output providing models and construct, laser printer hard copy and information for further analysis.

*Persona* exploits the intuitive 3D graphics environment uniquely available on the advanced technology Silicon Graphics workstations.

The three modules in *Persona* are:

Clip, Wire and Interrogate.

### 3.8.1 Clip

Clip uses the original data from the scanner and prepares the data for used by Interrogate. The main function of this program is to exclude unwanted data, and erase unnecessary features such as head holders and head straps.

### 3.8.2 Wire

Wire is used to examine landmark data determined using Interrogate. Wire is initiated by dragging a folder containing the determined landmarks data ("det_landmarks.dat") into the *Wire* icon to serve as the default starting point for data searches. Individual bones can be selected and wire frames and points can be turned on and off.

### 3.8.3 Interrogate

Interrogate is utilized to display CT data (or other slice formatted data) in a multi-windowed environment in several formats:

(i) Axial, sagittal, coronal slices and any oblique slice through the CT data

(ii) 3D CT reconstructions (stacked slices for producing clear images using the CT data)

(iii) A magnified area around either the screen cursor position or the 'active marker' position that indicates the current position of the selected landmark;

(iv) Stereo mode for each rotation axis of the 3D CT reconstructions. Stereo mode for each rotation axis of the 3D CT reconstructions. Stereo mode on Silicon Graphics workstations works by alternating the left and right eye views of the image on the screen and appropriately activating liquid crystal shutters on a pair of stereo glasses worn by the viewer.

Interrogate is usually started by dragging a 'loc.dat' file to the interrogate icon. The main *Interrogate* menu is then displayed (Fig. 3.5).


Two different types of option are represented. The buttons with lighted squares toggle views on and off. The other buttons give access to new option menus, apart from the Quit button which is used to leave the program.

**Figure 3.5** The main Interrogate menu.

### 3.8.4 Defaults

The default button displays six (6) views on the screen (Fig. 3.5):

**Z Cut** – the Axial Cut view

**Y Cut** – the Coronal Cut view

**X Cut** – the Sagittal cut view

**Images 1 –** defaults to Z-axis 3-D reconstruction

**Images 2 –** defaults to X-axis 3-D reconstruction

**Magnify –** defaults to magnified view of the Axial cut

#### *3.8.4.1 Z, Y, X Cuts*

A sliding bar menu is displayed beneath the Z, Y and X Cut views (Fig. 3.6). The position of the cuts can be altered using the sliding bar scales. The **R** buttons can be toggled to display the view from the opposite direction to the default. The Units button can be toggled to display the view from the opposite direction to the default. The Units button can be toggled to display the scales in either pixels or millimeters.

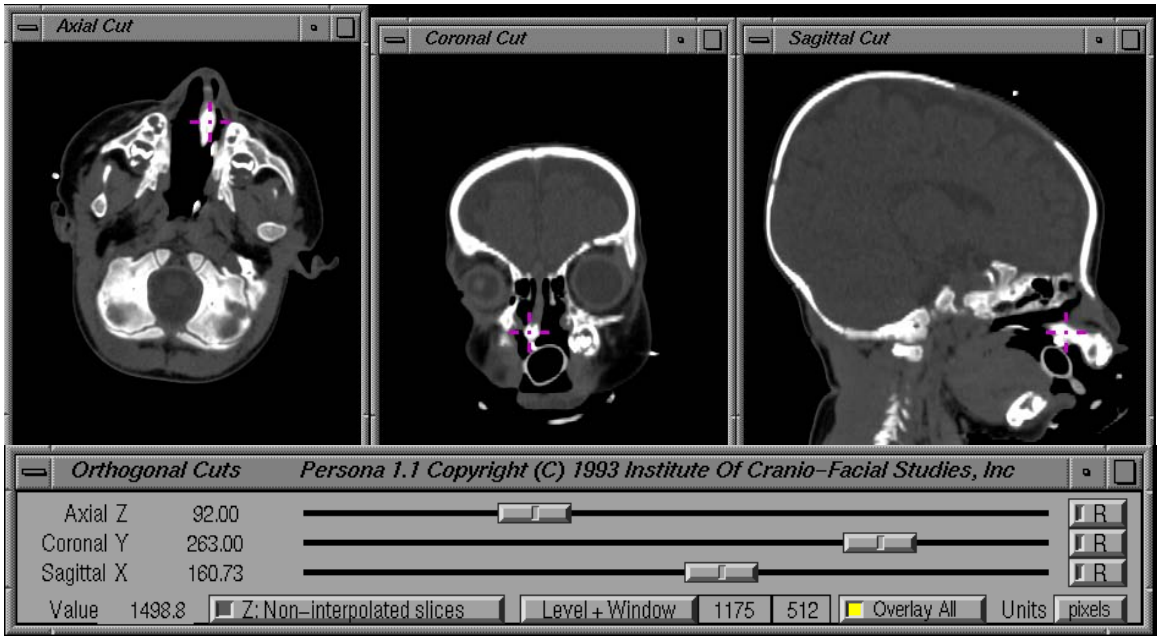


**Figure 3.6** The Z, Y, X axial cuts with the sliding menu display.

**Z Cuts**

The Axial Cut view is displayed looking down on the top of the head (Fig. 3.6). The R button can be toggled on and off to display the view from the underneath rather than on top. The views are perpendicular to the Z-axis. Non-interpolated slices can be displayed, corresponding to the original scanned slices. Interpolated slices can also be displayed.

**Y Cuts**

The Coronal Cut view defaults looking from the back of the head forwards (Fig. 3.6). The R button toggles the view looking from the front towards the back. The views are perpendicular to the Y-axis.

**X Cuts**

The Sagittal Cut view defaults to looking from the right ear to the left (Fig. 3.6). The R button toggles looking from left to right. The views are perpendicular to the X axis.

**Value**

The value displayed is the pixel value of the active marker position (Fig. 3.6).

**Level + Window**

The brightness (level) and contrast (window) of the display can be altered to enhance the view (Fig. 3.6). This can be done using the sliding bar scale to change the settings. The values are displayed beside the bars.

**Units**

The position of the cuts is echoed in the relevant units (i.e. pixels or mm) (Fig. 3.6).

*3.8.4.2 Images 1 and 2 (Fig. 3.7)*

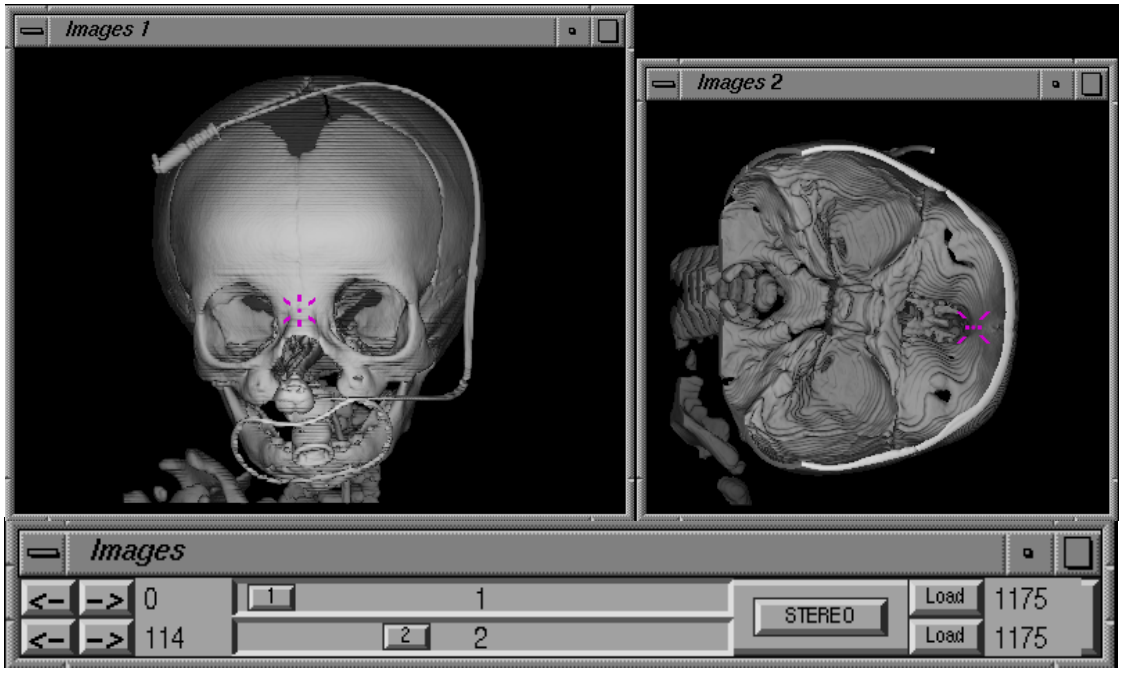


**Figure 3.7** Two reconstructed 3-D images are displayed by default as shown. **Image 1** is the model interpolated from the set of Z-axis views. A 'movie' set of images can be run to show the picture rotating. **Image 2** is the model interpolated from the X-axis views that can also be rotated.

The views are rotated using the sliding bar menu shown below the images. Both views can be rotated at the same time. The back (<-) and forward (->) arrows on the left hand side of the menu can be clicked to go backwards or forwards through the set of images; click the arrow a second time to stop the progress. Alternately, the numbered slides can be positioned to an exact spot using the numbered scales.

### *3.8.4.3 Stereo*

The images can be viewed stereographically by activating the Stereo buttons and using the Stereographic viewing glasses. Within the Stereo option, the views can be rotated as before Fig. 3.8).

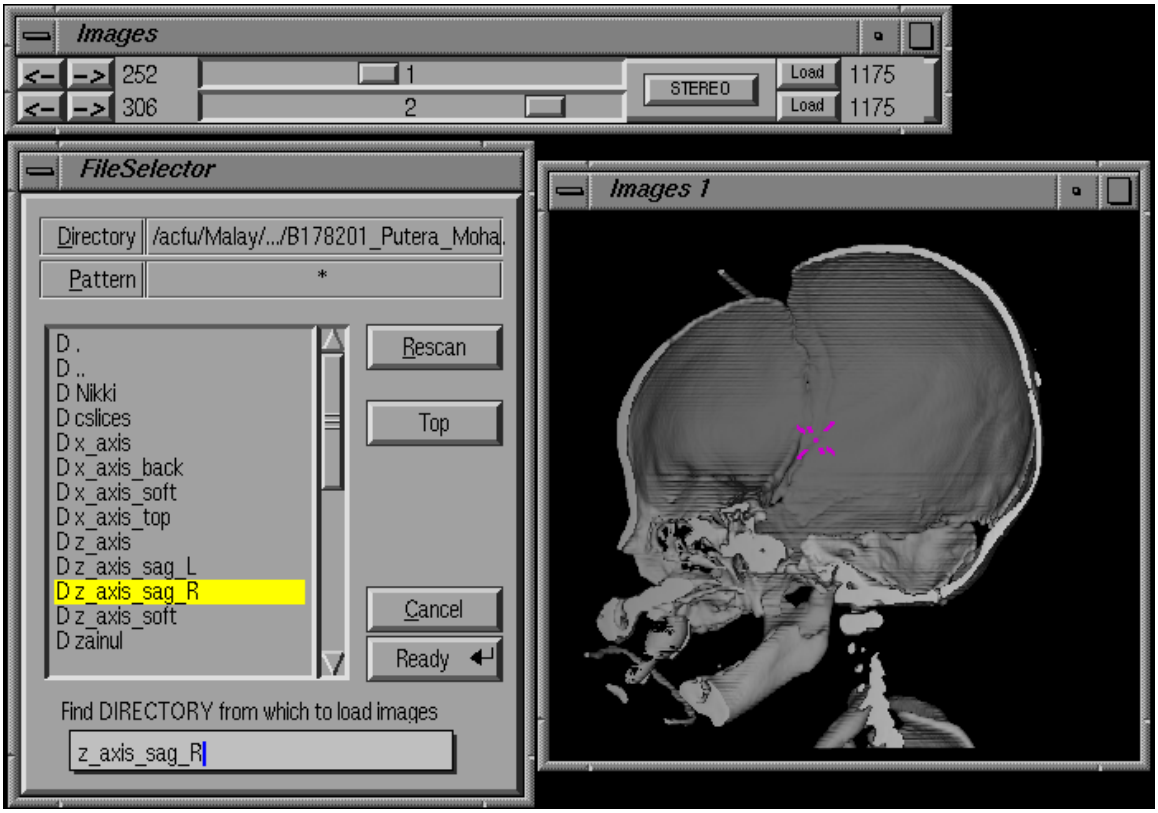


**Figure 3.8** The stereo window. A nominated file is selected using the file selection browser.

### *3.8.4.4 Magnify*

The magnification window (Fig. 3.9) provides an enlarged image for examination of details in the views and to facilitate the positioning of the active markers. The magnified view displays a close up of the area around the active marker which is placed by the cursor in whichever view (Z, Y, X, 1 or 2) is being examined. The active marker is displayed in all views.

The views can also be scaled up by pressing the mouse button in the top right square in the view windows. However, screen resolution does not improve.

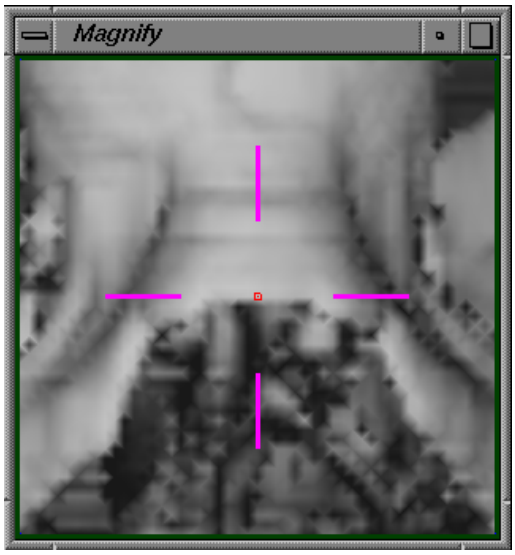


**Figure 3.9** The magnify window.

### *3.8.4.5 Oblique Cutter*

The oblique cutter (Fig. 3.10) is used to display and manipulate views of the data which are not parallel to the X, Y or Z axes. In many cases this will allow a far better interpretation of the data, refining landmark determination and enhancing visualisation. A view can be selected at any orientation through the data volume, and this display can be viewed from any direction. The option is initiated by pressing the Oblique Cut button on the main Interrogate control form.

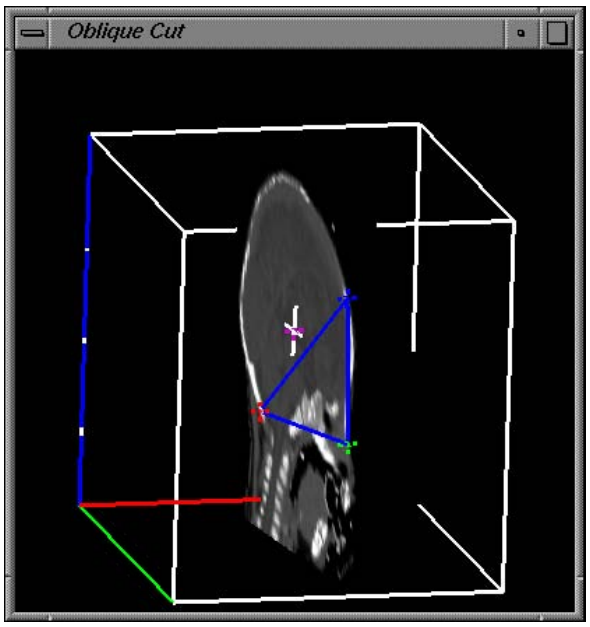


**Figure 3.10** The Oblique Cut view is displayed showing a default slice through the data.

### 3.8.5 Landmark Determination

A landmark is a known position within the data, which can be used for reference and for measurement. Essentially the location of the particular landmark is achieved by positioning the 'active marker' (the cursor is displayed within the view) appropriately in the 3D reconstructions (either in the mono or stereo windows) and in the orthogonal slices. This must be done in more than one view in order to get a correct triangulated position.

The position of the selected landmark in each of the open views is shown by the active marker. As each landmark is determined, its position is saved into the file. If this landmark needs to be modified later it can be reselected.

At any stage a wire-frame model can be viewed or superimposed over the 3D CT reconstruction for further validation of the landmark position.

*3.8.5.1 Select Landmark*

For the determination of most landmarks the procedure is:

Open the select landmark form by picking Landmarks in the main Interrogate control form (Fig. 3.5). The select landmark menu is shown in Figure 3.11.

To select the anatomical region for the landmark:

(a) Select the appropriate bone in the Bone browser

The top part of the menu allows the selection of a particular bone with a slide bar on the left hand side to move through the list of available bones. This button of the first bone box allow selection of all bones, or individual bones or bones can be selected by pointing with the cursor on the appropriate lines.

(i) Select the landmark in the Landmark Browser

(ii) Locate the landmark in one image of a 3D CT reconstruction

(iii) Rotate to another image of the 3D CT reconstruction about either of the axes and relocate the same landmark to enable triangulation and thus determination of the landmark position in three dimensions

(iv) Rotate to other images as necessary to refine the landmarks position

(v) Further refine the position if necessary in each of the orthogonal slices (X, Y and Z cut views) to ensure that the landmarks is located appropriately relative to the bone surface.

Save the landmark by pressing the **Save** button.

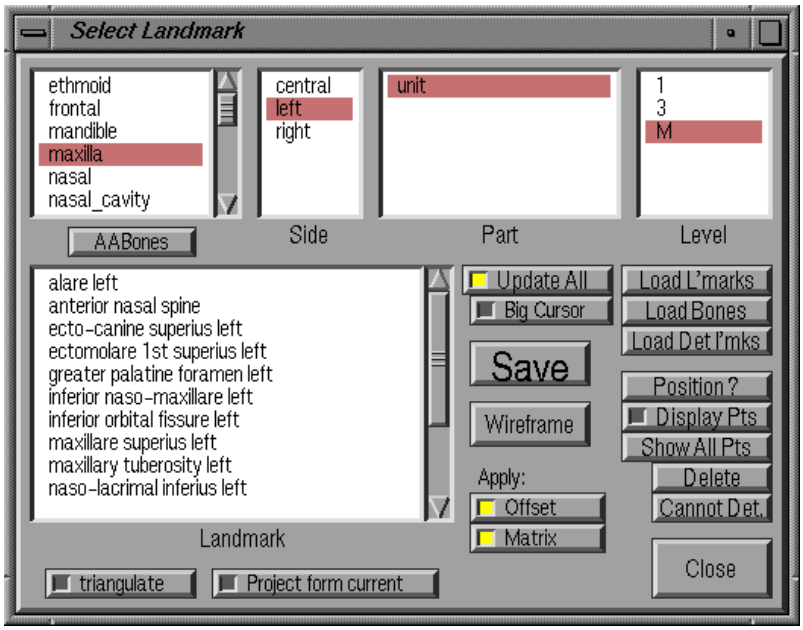


**Figure 3.11** An example of the landmark window showing the bones for landmark determination.

### 3.8.6 Wireframe Display

Wireframe displays are initiated by pressing the Wire-frame button on the Select Landmark form (Figs. 3.12 – 3.13). The Display button toggles the screen display of the wire-frame model without affecting the selections. The Overlay on Cuts buttons toggles on and off to display the wire-frames on the X, Y, or Z cut views.

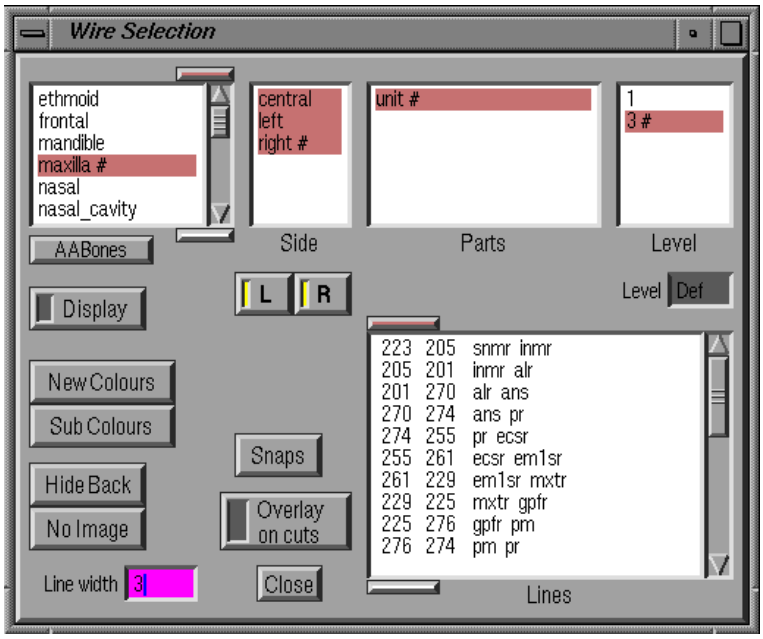


**Figure 3.12**

The wireframe display window.

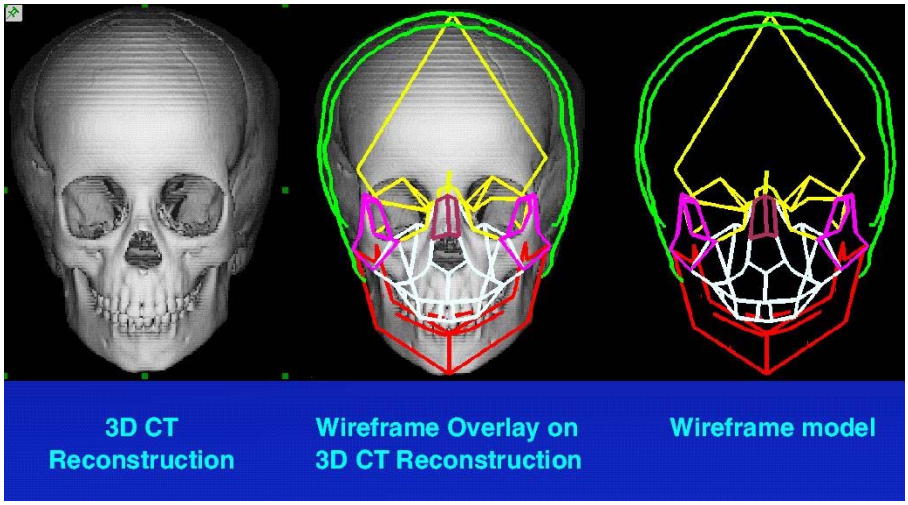


**Figure 3.13** Wire-frame models of identified landmarks can be colour-coded and overlayed on a 3D reconstructions and cuts.

### 3.8.7 Measure

Measurement can be made on any views (Z, Y, X, Oblique, Images 1, Images 2, Magnify) by positioning the active marker within that view.

(i) Select **Measure** on the main control form labelled Interrogate to display the **Measure** menu

Select a measurement type by pressing the long button under the browser:

(a) Distance between two points (1and 2)

(b) Angle between three points (2->1, 2->3)

(c) Angle between two lines defined by four points (2,1) and (3,4)

(d) Ratio of the lengths of two lines (2-1)/(3-4)

(e) Percent ratio of the lengths of two lines (2-1)/(3-4)%

The measurements in the browser can be saved using the save button and previously saved measurements can be loaded using the Load button (Fig. 3.5).

### 3.8.8 Quit

Use the Quit button to leave the Interrogate module. This will close down all the files and views (Fig. 3.5).

## 3.9 *Persona* Software and the Cleft Data

Once the 3D CT scans were loaded into the Persona program, the slice data were rendered to produce 3D volume reconstructions for both the cleft and non-cleft data (Fig 3.14.)

a.

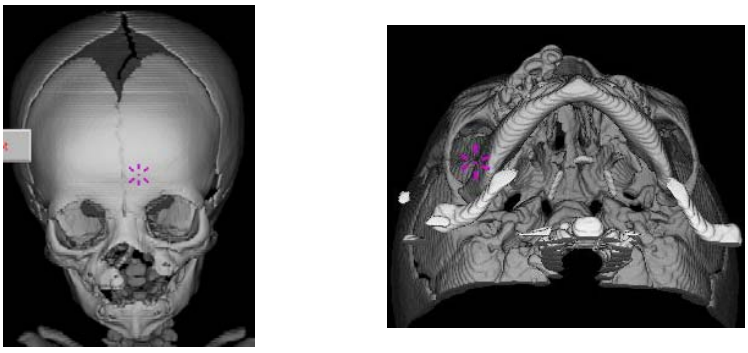

b.

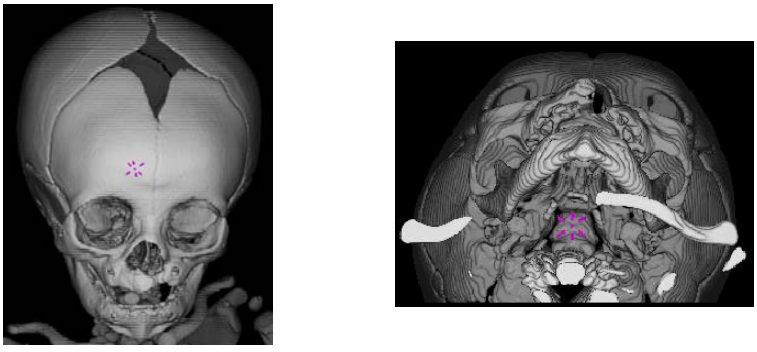

c.

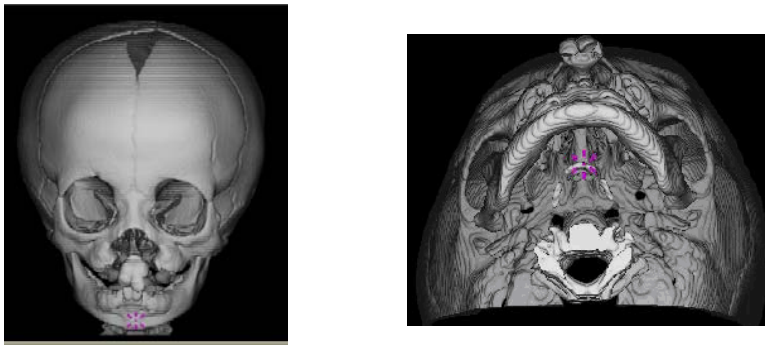

d.

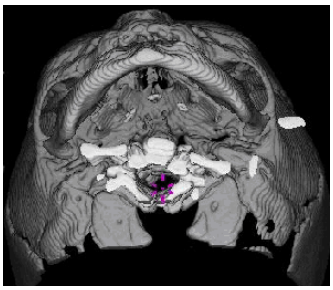

e.

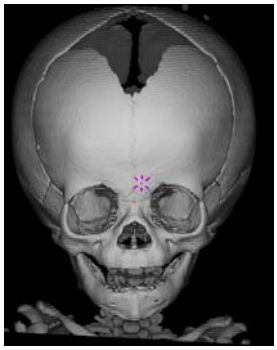

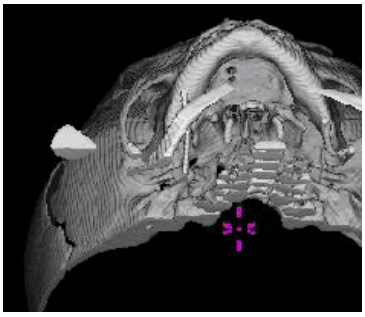

**Figure 3.14** 3D CT reconstructions of: (a) UCLP (b) CL (c) BCLP (d) ICP and (e) NC.

*Persona* was used to produce views of the bony elements or soft tissues (Fig. 3.15). Coronal, axial and sagittal slices through the soft tissue were also created (Fig. 3.16).

a.

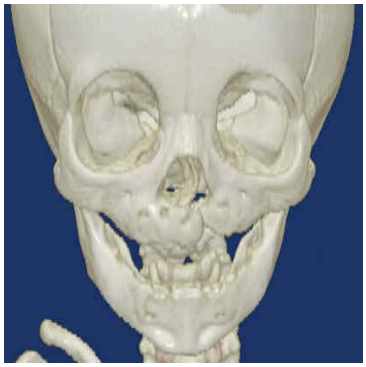

b.

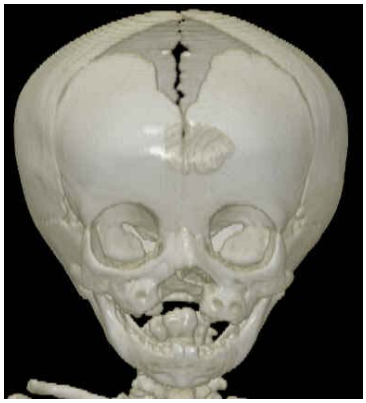

**Figure 3.15** Bony and soft tissue views of (a) CL and (b) UCLP.

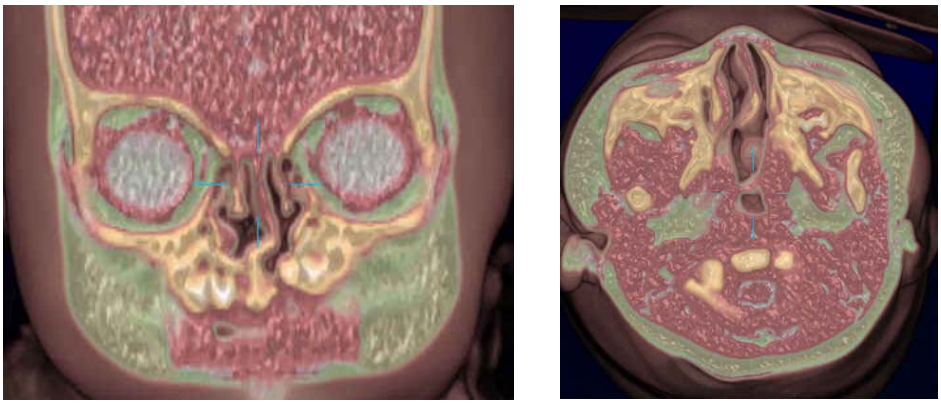

**Figure 3.16** Coronal slice (left) and axial slice (right) through the nasal septum of a UCLP patient showing the nasal turbinates. The deviated nasal septum is also visible.

## 3.10 Measurement of Distances, Dimensions and Angles

The measurements for each anatomical area were divided into 3 groups:

(i) Distances - representing the measurement between adjacent landmarks which specifically form the outline of the cranial bone or anatomical unit.

(ii) Dimensions - representing measurement between landmarks which do not follow the outline of the cranial bone but represent overall bony size (maximum width, length etc.)

(iii) Angles - representing the shape of the anatomical unit. Angles were measured by two methods. The angle between three points was measured or between the projected bisection of two lines (four points).

### 3.10.1 Methods of Measurement of Distances and Angles

As all landmarks were recorded as 3D coordinate data, the measurement of distances and angles was possible. Calculations were made by determining the distance $d_{ij}$, between 2 landmarks whose positions are specified by the vectors $\mathbf{x}_i = (x_i, y_i, z_i)$ and $\mathbf{x}_j = (x_j, y_j, z_j)$. The distance, $d_{ij}$, is the magnitude of the vector difference between the points: $d_{ij} = | \mathbf{x}_i - \mathbf{x}_j |$; that is $d_{ij} = \sqrt{[(x_i - x_j)^2 + (y_i - y_j)^2 + (z_i - z_j)^2]}$

The angle, q, between 2 vectors defined by 3 landmarks $\mathbf{x}_i$, $\mathbf{x}_j$, $\mathbf{x}_k$ is calculated from the dot product of difference vectors (that is, the vectors $(\mathbf{x}_i - \mathbf{x}_j)$ and $(\mathbf{x}_k - \mathbf{x}_j)$):

$$\cos(q) = \frac{(\mathbf{x}_i-\mathbf{x}_j)\ |\mathbf{x}_k-\mathbf{x}_j|}{|\mathbf{x}_i-\mathbf{x}_j|\ |\mathbf{x}_k-\mathbf{x}_j|}$$

Similarly the angle, q, between two vectors, specified by the landmarks $\mathbf{x}_i$, $\mathbf{x}_j$, $\mathbf{x}_k$, and $\mathbf{x}_l$, (that is, the vectors $(\mathbf{x}_j - \mathbf{x}_i)$ and $(\mathbf{x}_l - \mathbf{x}_k)$) is given by

$$\cos(q) = \frac{(\mathbf{x}_j-\mathbf{x}_i)\ (\mathbf{x}_l-\mathbf{x}_k)}{|\mathbf{x}_j-\mathbf{x}_i|\ |\mathbf{x}_l-\mathbf{x}_k|}$$

## 3.11 Statistical Analysis

Basic descriptive statistics, including means (√), standard deviations (SD) and coefficients of variation (CV) were used to summarise the quantitative data. The coefficient of variation, where CV = (SD/√)*100%, provided a measure of relative variations of the study variables. Preliminary assessments of frequency distributions indicated that all the quantitative study variables were approximately normally distributed.

### 3.11.1 Generalized Linear Modeling

The Generalized Linear Model (GLM) (PROC GLM, SAS 2001) is a statistical package that allows data to be decomposed into 3 groups:

1. Effects of interest – variance that explains relevant experimental effects

2. Effects of no interest – variance that can be explained but it not interesting

3. Errors – unexplained variance.

It is a flexible statistical model that incorporates normally distributed dependent variables and categorical and continuous independent variables. Although the CLP and NC groups were matched for age as closely as possible, the use of a covariate model that accounted for possible age effects was preferred, rather than applying simple t-tests.

In this study a linear model incorporating the fixed effects of 'gender' and 'cleft group', and, using 'age' as a covariate, was fitted to all measurements.

The model was as follows:

Variable = Age (14-340 days)

Gender (male, female)

Group (NC, UCLP, BCLP, ICP, CL)

Higher-order interactions were not analysed for this small data set. Linear contrasts were arranged to compare the control group (NC) with all other groups, and to compare the ICP group (a morphologically distinct cleft-type) with other cleft groups.

Within this model there are 3 types of sums of squares (SS) that generate an adjusted mean:

1. Type I sums of squares – calculates the reduction in error sums of squares by adding each effect to the model sequentially.

2. Type II sums of squares – calculates the sums of squares of an effect in the model adjusted for other appropriate effects.

3. Type III sums of squares – calculates the reduction in error sums of squares by adding the effect after all the other effects are adjusted.

In this study the type III sums of squares was used. Both unadjusted and adjusted mean values are reported for the various quantitative study variables. The adjusted statistics take account of the effect of age in the CLP and NC groups.

Chi-square tests (using 2 X 2 tables) were used to test for any associations between qualitative variables in the study groups.

The level of significance was set at 5% for all statistical tests.

## 3.12 Errors of Measurement and their Analysis

### 3.12.1 General Introduction

In areas of research such as morphometrics, it is very important to establish the degree of reliability of the methods employed. Invariably there will be errors of observation arising from the technique applied. Prior to a discussion of error measurement, it is

important to distinguish two basic terms: validity and reproducibility.

Validity refers to the extent to which, in the absence of measurement error, the value obtained represents the object of interest. The term accuracy may also be used. Validity is a term used, therefore, for how well an instrument measures what it is supposed to measure.

Reproducibility or precision refers to the closeness of successive measurements of the same object. Reproducibility of measurements varies depending on the quality of records, the conditions under which they are measured, and the care and skill of the measurer. Assessment by the process of double determination (e.g. Abbott *et al.*, 1990) has indicated that the 3D CT technique used at the ACFU has acceptable validity and reproducibility in its application to both normal and abnormal situations.

#### *3.12.1.1 Types of Errors*

Errors of measurement can be either systematic or random. Systematic errors arise from limitation in the materials or methods used, leading to consistent over- or under-estimation e.g. failure to correct for magnification factors, measuring from copy records where expansion may have occurred, or measurements made by different observers with different concepts of particular landmarks.

Random accidental errors may result from variations in the positioning of patients, or variations in film density and sharpness in cephalometric studies. Perhaps the greatest source of random error in morphometric studies is difficulty in identifying a particular landmark or imprecision in its definition.

The magnitude of errors and the extent to which they may affect results can be assessed by replicability studies. Replicability studies may involve double determinations of variables or repeated measures on more than two occasions.

### *3.12.1.2 Detecting Systematic Errors*

A reasonable method for detecting systematic errors is to use the paired t-test to analyse the differences between two determinations on a paired comparison basis. This is a sensitive test which essentially tests whether the mean difference is significantly different from zero.

### *3.12.1.3 Estimating Random Error*

Random errors are important because they add to the natural variability of the measurements and may therefore obscure real differences between groups. One measure of random error is $S_d$, the standard deviation of the differences between replicates. $S_d^2$ represents the variance of the differences between replicates. The variance of the difference between two measures is double that of a single measurement. The error variance of a single determination, $S_e^2$, can be estimated as half $S_d^2$.

$$\text{i.e. } S_e^2 = S_d^2/2 \quad \text{therefore} \quad S_e = \sqrt{\frac{\sum d^2}{2N}}$$

This is the familiar formula proposed by Dahlberg (1940) to estimate the standard deviation of a single determination. It is also referred to as the technical error of measurement. The term $S_e^2$ is referred to as the error variance.

### 3.12.2 Error Analysis for this Study

In this study, repeat determinations were performed for all infants after a period of one month to assess the reproducibility of landmark determination and the reliability of variables derived from these landmarks. Due to ethical reasons and radiation exposure, it was not possible to rescan the patients. Therefore, the double determinations were based on the same CT scans, with landmarks replotted at least one month apart. This time interval ensured point identification clues for specific individuals would not be recalled and influence relocation.

The anatomical osseous landmarks considered in this investigation are detailed in Appendix II. Fifty-nine osseous landmarks were considered for the study of reproducibility.

The following is essentially a multi-variate description of Dahlberg's method of double determination.

The variable of interest (distance measurement or point location) is determined on *n* individuals on two occasions sufficiently separated in time that non-landmark related cues are forgotten.

Let $\mathbf{d}_1, \mathbf{d}_2, \ldots, \mathbf{d}_n$ be the observed differences for the *n* double determinations of a *p*-dimensional variable (here 1, 2 or 3 dimensions) and each $\mathbf{d}_j$ have a *p*-variate normal distribution with mean $\boldsymbol{\mu}_d$ and variance-covariance matrix $\boldsymbol{\Sigma}_d$. Then the mean difference vector is given by

$$\bar{\mathbf{d}} = \frac{1}{n}\sum_{j=1}^{n}\mathbf{d}_j$$

and the estimated variance-covariance matrix $\mathbf{S}_d$ is given by

$$\mathbf{S}_d = \frac{1}{n-1}\sum_{j=1}^{n}(\mathbf{d}_j - \bar{\mathbf{d}})(\mathbf{d}_j - \bar{\mathbf{d}})'$$

(Johnson and Wichern, 1988). Bold letters indicate vectors of dimension *p* and the prime indicates transpose.

When the null hypothesis of no systematic error holds $\bar{\mathbf{d}} \sim \mathbf{N}_p(0, \Sigma_d / n)$, that is, $\boldsymbol{\mu}_d = \mathbf{0}$.

The test statistic

$$T^2 = n\bar{\mathbf{d}}'\mathbf{S}_d^{-1}\bar{\mathbf{d}}$$

has a Hotelling's $T^2$ distribution and is used to test the null hypothesis. The null hypothesis is rejected at the $\alpha$-level if

$$T^2 > \frac{(n-1)p}{(n-p)}F_{p,n-p}(\alpha)$$

If the null hypothesis is retained then a suitable measure of the variance-covariance matrix of the random error associated with a single determination of a *p*-dimensional variable is

$$\mathbf{S} = \frac{1}{2n}\sum_{j=1}^{n}\mathbf{d}_j\mathbf{d}_j'$$

The factor of two in the denominator arises because the measurement error can be equally ascribed to either determination. The factor n is used rather than the (*n*-1) because the mean error has been taken to be zero.

In this study $p = 3$ dimensions for point measurements. For anthropometric variables such as distances where $p = 1$ the formulae reduces to Dahlberg's original formulation given by

$$s^2 = \frac{1}{2n}\sum_{j=1}^{n} d_j^2$$

In one dimension the $T^2$ test statistic becomes:

$$T^2 = n\bar{\mathrm{d}}^2 / s_{\mathrm{d}}^2 \sim F_{1,n-1}(\alpha) \quad \text{or} \quad t = T = \sqrt{n}(\bar{\mathrm{d}}/s_{\mathrm{d}}) \sim t_{n-1}(\alpha)$$

where $s_d$ is the estimator of the standard deviation of the differences between each determination and $t_{n-1}(\alpha)$ is Student's t-distribution.

*3.12.2.1 Landmark relocation error*

From Table 3.2, the overall or pooled landmark location error taken over 59 landmarks was 0.45mm. For the landmark relocation error (|**xyz**|), the minimum magnitude was 0.16mm for inferior spheno-occipital synchondrosis width left and maximum magnitude was 0.82mm for zygo-maxillare inferius right.

The median error provides an indication of the general osseous landmark relocation error. In this study its value was 0.38 mm. Apart from calculating the landmark relocation error, the two determinations were averaged for each of the landmarks to provide better estimates of the landmark coordinates.

**Table 3.2** Landmark relocation error.

| Landmark No | x | y | z | \|xyz\| | n | Landmark |
|---|---|---|---|---|---|---|
| 270 | 0.21 | 0.23 | 0.2 | 0.37 | 39 | anterior nasal spine |
| 868 | 0.57 | 0.22 | 0.27 | 0.67 | 38 | basi-occipital sychondrosis inferius left |
| 869 | 0.49 | 0.27 | 0.37 | 0.67 | 38 | basi-occipital sychondrosis inferius right |
| 866 | 0.59 | 0.34 | 0.24 | 0.72 | 38 | basi-occipital sychondrosis superius left |
| 867 | 0.51 | 0.29 | 0.16 | 0.19 | 38 | basi-occipital sychondrosis superius right |
| 8680 | 0.18 | 0.07 | 0.19 | 0.27 | 39 | basi-occipital sychondrosis inferius for width left |
| 8681 | 0.24 | 0.1 | 0.3 | 0.37 | 39 | basi-occipital sychondrosis inferius for width right |
| 8682 | 0.11 | 0.1 | 0.13 | 0.20 | 39 | basi-occipital sychondrosis superius for width left |
| 8683 | 0.36 | 0.19 | 0.27 | 0.49 | 39 | basi-occipital sychondrosis superius for width right |
| 870 | 0.22 | 0.28 | 0.12 | 0.38 | 41 | basion |
| 1520 | 0.28 | 0.25 | 0.08 | 0.38 | 18 | 01 c1 anterior superior midline |
| 1521 | 0.26 | 0.45 | 0.08 | 0.53 | 18 | 02 c1 anterior inferior midline |
| 1522 | 0.23 | 0.24 | 0.1 | 0.35 | 40 | 03 c2 anterior superior midline |
| 1523 | 0.34 | 0.41 | 0.16 | 0.55 | 40 | 04 c2 anterior inferior midline |
| 1524 | 0.24 | 0.24 | 0.21 | 0.22 | 40 | 05 c3 anterior superior midline |
| 1525 | 0.26 | 0.23 | 0.12 | 0.37 | 40 | 06 c3 anterior inferior midline |
| 1526 | 0.26 | 0.29 | 0.2 | 0.44 | 40 | 07 c4 anterior superior midline |
| 1527 | 0.32 | 0.3 | 0.13 | 0.46 | 39 | 08 c4 anterior inferior midline |
| 1528 | 0.33 | 0.3 | 0.21 | 0.44 | 39 | 09 c5 anterior superior midline |
| 1529 | 0.4 | 0.39 | 0.13 | 0.57 | 39 | 10 c5 anterior inferior midline |
| 1530 | 0.32 | 0.29 | 0.25 | 0.50 | 38 | 11 c6 anterior superior midline |
| 1531 | 0.37 | 0.43 | 0.21 | 0.60 | 36 | 12 c6 anterior inferior midline |
| 1532 | 0.42 | 0.32 | 0.28 | 0.60 | 31 | 13 c7 anterior superior midline |
| 1533 | 0.47 | 0.47 | 0.24 | 0.71 | 19 | 14 c7 anterior inferior midline |
| 1500 | 0.16 | 0.15 | 0.27 | 0.35 | 39 | greater horn posterior tip left |
| 1501 | 0.22 | 0.15 | 0.29 | 0.39 | 39 | greater horn posterior tip right |
| 1502 | 0.19 | 0.19 | 0.09 | 0.28 | 39 | greater horn anterior-inferior tip left |
| 1503 | 0.27 | 0.34 | 0.15 | 0.46 | 39 | greater horn anterior-inferior tip right |
| 1504 | 0.31 | 0.2 | 0.27 | 0.46 | 39 | greater horn anterior-superior tip left |
| 1505 | 0.24 | 0.2 | 0.28 | 0.42 | 39 | greater horn anterior-superior tip right |
| 202 | 0.23 | 0.23 | 0.14 | 0.35 | 41 | hamular notch left |
| 203 | 0.19 | 0.22 | 0.14 | 0.33 | 41 | hamular notch right |
| 1012 | 0.18 | 0.35 | 0.25 | 0.47 | 41 | hamular process left |
| 1013 | 0.18 | 0.26 | 0.18 | 0.36 | 41 | hamular process right |
| 1070 | 0.18 | 0.2 | 0.38 | 0.47 | 41 | hormion |
| 1510 | 0.29 | 0.23 | 0.36 | 0.51 | 35 | hyoid body inferior tip left |
| 1511 | 0.2 | 0.19 | 0.27 | 0.38 | 35 | hyoid body inferior tip right |
| 1512 | 0.12 | 0.24 | 0.31 | 0.40 | 35 | hyoid body superior tip left |
| 1513 | 0.11 | 0.19 | 0.25 | 0.34 | 35 | hyoid body superior tip right |
| 1514 | 0.29 | 0.3 | 0.1 | 0.43 | 35 | hyoid body inferior midline |
| 1515 | 0.31 | 0.22 | 0.08 | 0.33 | 35 | hyoid body superior midline |
| 1069 | 0.25 | 0.24 | 0.27 | 0.44 | 40 | inf spheno-occipital synchondrosis centrale |
| 1064 | 0.28 | 0.26 | 0.17 | 0.42 | 39 | inf spheno-occipital synchondrosis left |
| 1065 | 0.41 | 0.27 | 0.17 | 0.53 | 39 | inf spheno-occipital synchondrosis right |
| 10640 | 0.12 | 0.08 | 0.08 | 0.16 | 39 | inf spheno-occipital synchondrosis for width left |
| 10641 | 0.2 | 0.14 | 0.17 | 0.30 | 39 | inf spheno-occipital synchondrosis for width right |
| 228 | 0.25 | 0.36 | 0.25 | 0.50 | 41 | maxillary tuberosity left |
| 229 | 0.26 | 0.44 | 0.3 | 0.59 | 41 | maxillary tuberosity right |
| 271 | 0.37 | 0.28 | 0.16 | 0.50 | 38 | nasale |
| 272 | 0.36 | 0.22 | 0.42 | 0.60 | 40 | nasion |
| 1220 | 0.21 | 0.37 | 0.26 | 0.50 | 41 | pterygo-inferius left |
| 1221 | 0.19 | 0.4 | 0.23 | 0.50 | 41 | pterygo-inferius right |
| 1071 | 0.38 | 0.26 | 0.4 | 0.61 | 39 | sella |
| 1062 | 0.3 | 0.12 | 0.28 | 0.43 | 38 | sup spheno-occipital synchondrosis left |
| 1063 | 0.42 | 0.19 | 0.33 | 0.57 | 38 | sup spheno-occipital synchondrosis right |
| 10620 | 0.16 | 0.07 | 0.22 | 0.28 | 39 | sup spheno-occipital synchondrosis for width left |
| 10621 | 0.29 | 0.12 | 0.28 | 0.42 | 39 | sup spheno-occipital synchondrosis for width right |
| 514 | 0.54 | 0.4 | 0.35 | 0.76 | 41 | zygo-maxillare inferius left |
| 515 | 0.6 | 0.44 | 0.33 | 0.82 | 41 | zygo-maxillare inferius right |

### *3.12.2.2 Errors of variables*

A total of 68 comparisons were made for this analysis. Of the 61 distances and seven angles compared, one yielded a significant error at the $p<0.01$ level (marked # in Table 3.3) and nine differed at the $p<0.05$ level (marked with + in Table 3.3).

**Table 3.3** Errors of variables.

| Variable | Unit | Mean diff | Median | SD | D | t | Landmarks | | | | Variables |
|---|---|---|---|---|---|---|---|---|---|---|---|
| CRANIAL BASE | | | | | | | | | | | |
| Height | mm | -0.1 | -0.1 | 0.3 | 0.3 | -1.6 | sssl | issl | | | Height basi-sphenoid left |
| | mm | 0 | 0 | 0.3 | 0.3 | -0.14 | sssr | issr | | | Height basi-sphenoid right |
| | mm | -0.1 | -0.1 | 0.4 | 0.4 | -1.26 | bossl | bosil | | | Height basi-occipital left |
| | mm | 0 | 0 | 0.5 | 0.4 | 1.77 | bossr | bosir | | | Height basi-occipital right |
| SPHENO-OCCIPITAL SYNCHONDROSIS (sos) | | | | | | | | | | | |
| Width | mm | 0.1 | 0 | 0.2 | 0.2 | 1.88 | isswl | bosiwl | | | Width inferior sos left |
| | mm | 0 | 0 | 0.2 | 0.2 | 0.88 | isswr | bosiwr | | | Width inferior sos right |
| | mm | 0 | 0 | 0.2 | 0.2 | 0.93 | ssswl | bosswl | | | Width superior sos left |
| | mm | 0.1 | 0.1 | 0.2 | 0.2 | 2.06 + | ssswr | bosswr | | | Width superior sos right |
| ANGLES | | | | | | | | | | | |
| | deg | -0.1 | 0.2 | 1.9 | 1.9 | -0.33 | ba | s | n | | cranial base angle |
| | deg | 0 | -0.1 | 2.5 | 2.5 | -0.04 | hpl | mxtl | ptil | | Pterygoid hamulus angle l |
| | deg | 0.1 | -0.2 | 2.7 | 2.7 | 0.14 | hpr | mxtr | ptir | | Pterygoid hamulus angle r |
| | deg | 0.2 | 0.2 | 1 | 1 | 0.95 | n | s | ans | | Sphenopalatine angle |
| | deg | -0.2 | -0.2 | 1.3 | 1.3 | -1.03 | s | n | ans | h | Vomerine angle |
| | deg | 0.3 | 0.2 | 1.5 | 1.5 | 1.15 | n | s | hbsm | | Hyoid bone angle |
| | deg | 0.1 | 0.1 | 1.5 | 1.5 | 0.53 | n | s | c3aim | | Craniocervical angle |
| CRANIAL BASE (cb) LENGTH | | | | | | | | | | | |
| | mm | 0 | 0 | 0.5 | 0.5 | -0.1 | ba | n | | | cranial base length |
| | mm | 0.1 | 0.1 | 0.5 | 0.5 | 0.7 | ba | s | | | posterior cb length |
| | mm | 0 | 0 | 0.4 | 0.4 | -0.44 | s | n | | | anterior cb length |
| Sella length | | | | | | | | | | | |
| | mm | 0 | -0.1 | 0.4 | 0.4 | -0.11 | s | sssl | | | L sella sphenoid length |
| | mm | 0 | 0.1 | 0.5 | 0.5 | 0.41 | s | sssr | | | R sella sphenoid length |
| Clivus length | | | | | | | | | | | |
| | mm | 0 | 0 | 0.4 | 0.4 | 0.74 | ba | bossl | | | L sup clivus length |
| | mm | 0 | 0 | 0.2 | 0.2 | -0.93 | ba | bossr | | | R sup clivus length |
| | mm | -0.1 | 0 | 0.4 | 0.4 | -1.15 | ba | bosil | | | L inf clivus length |
| | mm | -0.1 | 0 | 0.5 | 0.5 | -1.07 | ba | bosir | | | R inf clivus length |
| HYOID | | | | | | | | | | | |
| Greater horn (gh) | | | | | | | | | | | |
| | mm | 0.1 | 0.2 | 0.3 | 0.3 | 2.67 + | ghptl | ghaitl | | | length gh left lower |
| | mm | 0.1 | 0 | 0.4 | 0.4 | 1.53 | ghastl | ghptl | | | length gh left upper |
| | mm | -0.1 | -0.1 | 0.4 | 0.4 | -0.83 | ghptr | ghaitr | | | length gh right lower |
| | mm | 0.1 | 0.1 | 0.4 | 0.4 | 2.38 + | ghastr | ghptr | | | length gh right upper |
| | mm | 0 | 0 | 0.3 | 0.3 | -0.33 | ghaitl | ghastl | | | height gh left |
| | mm | 0.1 | 0.1 | 0.4 | 0.4 | 1.27 | ghaitr | ghastr | | | height gh right |

**Table 3.3** (cont.)

| Variable | Unit | Mean diff | Median | SD | D | t | Landmarks | | | Variables |
|---|---|---|---|---|---|---|---|---|---|---|
| Hyoid Body | | | | | | | | | | |
| | mm | -0.1 | -0.1 | 0.8 | 0.7 | -0.42 | hbitl | hbstl | | hyoid body height left |
| | mm | 0.1 | 0 | 0.5 | 0.5 | 0.65 | hbstl | hbsm | | hyoid body length upper l |
| | mm | -0.1 | 0 | 0.7 | 0.6 | -0.78 | hbitl | hbim | | hyoid body length lower l |
| | mm | 0.2 | 0.1 | 0.5 | 0.5 | 2.19 + | hbitr | hbstr | | hyoid body height right |
| | mm | 0 | 0 | 0.4 | 0.4 | 0.2 | hbstr | hbsm | | hyoid body length upper r |
| | mm | 0 | 0.1 | 0.6 | 0.6 | -0.3 | hbitr | hbim | | hyoid body length lower r |
| Inferior Airway | | | | | | | | | | |
| | mm | 0 | 0 | 0.4 | 0.4 | 0.40 | hbsm | c2asm | c4aim | Perpendicular distance superior hyoid body - cervical spine tangent line |
| | mm | -0.1 | 0 | 0.4 | 0.4 | -0.95 | hbim | c2asm | c4aim | Perpendicular distance inferior hyoid body - cervical spine tangent line |
| Hyoid Distance Relative to Cranial Base | | | | | | | | | | |
| | mm | -0.2 | -0.2 | 0.4 | 0.4 | -3.07 # | hbsm | ba | | hyoid - basion |
| | mm | 0.1 | 0.1 | 0.4 | 0.4 | 1.2 | hbsm | isosc | | hyoid - inferior sos |
| CERVICAL SPINE | | | | | | | | | | |
| | mm | 0 | 0 | 0.2 | 0.2 | -0.59 | c1asm | c1aim | | Height C1 |
| | mm | -0.2 | -0.3 | 0.5 | 0.5 | -1.71 | c1aim | c2asm | | C1 - C2 |
| | mm | 0.1 | 0 | 0.2 | 0.2 | 1.41 | c2asm | c2aim | | Height C2 |
| | mm | -0.1 | -0.1 | 0.4 | 0.4 | -1.84 | c2aim | c3asm | | C2 - C3 |
| | mm | 0 | 0.0 | 0.2 | 0.2 | 0.77 | c3asm | c3aim | | Height C3 |
| | mm | 0 | 0 | 0.3 | 0.3 | -0.57 | c3aim | c4asm | | C3 - C4 |
| | mm | 0.1 | 0 | 0.3 | 0.3 | 1.86 | c4asm | c4aim | | Height C4 |
| | mm | -0.1 | -0.1 | 0.4 | 0.4 | -1.99 | c4aim | c5asm | | C4 - C5 |
| | mm | 0.1 | 0.1 | 0.3 | 0.3 | 2.22 + | c5asm | c5aim | | Height C5 |
| | mm | -0.2 | -0.1 | 0.4 | 0.4 | -2.31 + | c5aim | c6asm | | C5 - C6 |
| | mm | 0 | 0.1 | 0.4 | 0.3 | 0 | c6asm | c6aim | | Height C6 |
| | mm | 0 | -0.1 | 0.5 | 0.5 | 0.28 | c6aim | c7asm | | C6 - C7 |
| | mm | 0 | -0.1 | 0.4 | 0.4 | 0.06 | c7asm | c7aim | | Height C7 |
| | mm | 0 | 0 | 0.3 | 0.3 | -0.37 | c2asm | c6aim | | Length C2(s) - C6(i) |
| | mm | -0.1 | -0.1 | 0.3 | 0.3 | -1.04 | c2asm | c7asm | | Length C2(s) - C7(s) |
| | mm | -0.1 | -0.1 | 0.3 | 0.3 | -1.45 | c2asm | c7aim | | Length C2(s) - C7(i) |
| MAXILLA - Posterior width of maxilla | | | | | | | | | | |
| | mm | 0 | -0.1 | 0.5 | 0.5 | 0.22 | mxtl | mxtr | | tuberosity |
| PHARYNX | | | | | | | | | | |
| | mm | -0.2 | -0.2 | 0.4 | 0.4 | -2.40 + | h | hpl | | L sup ant height |
| | mm | -0.2 | -0.2 | 0.4 | 0.4 | -2.59 + | h | hpr | | R sup ant height |
| | mm | -0.1 | 0 | 0.5 | 0.5 | -1.06 | h | ba | | Post height |
| | mm | 0.1 | 0.2 | 0.6 | 0.6 | 0.83 | ba | hpl | | L inf ant depth |
| | mm | 0 | 0 | 0.5 | 0.5 | -0.64 | ba | hpr | | R inf ant depth |
| | mm | 0.1 | 0 | 0.5 | 0.5 | 0.86 | hnl | hnr | | Post width-hamular notch |
| | mm | 0.1 | 0.1 | 0.3 | 0.3 | 1.27 | hpl | hpr | | Pterygoid hamulus width |
| | mm | 0 | 0 | 0.4 | 0.4 | 0.57 | ptil | ptir | | Distance ptil - ptir |
| | mm | -0.1 | -0.1 | 0.6 | 0.6 | -1.09 | hpl | ptil | | Distance hpl - ptil |
| | mm | -0.2 | -0.2 | 0.5 | 0.5 | -2.35 + | hpr | ptir | | Distance hpr - ptir |
| ZYGOMA | | | | | | | | | | |
| | mm | -0.1 | -0.1 | 1.2 | 1.1 | -0.35 | zmil | zmir | | Interzygomatic distance |

The statistically significant systematic error associated with measurement of the distance from hyoid to basion most probably resulted from the rounded structure of the basion and the high variation in its shape, but the mean difference between determinations was only 0.2 mm. This systematic error was smaller than the standard deviation of the differences (0.4mm) and substantially smaller than the observed population standard deviation of approximately 2.4mm. The average differences that were found to be statistically significant at the $p<0.05$ level were in the range 0.1mm to 0.2mm. This reflects the extent of differences in landmark location by the author on two separate occasions.

The average differences that were found to be non-significant between the first and second determinations were all in the range 0mm to 0.2mm.

The random measurement errors (Table 3.3) were found to lie in the range 0.2mm for the width of the synchondrosis to 1.1mm for the interzygomatic distances. Random errors for angular variables ranged from 1.0° for the sphenopalatine angle to 2.7° for the pterygoid hamulus angle (right).

### 3.12.3 Conclusion

The method used for three-dimensional data acquisition enabled positions and relocation errors of a large number of osseous landmarks to be determined for patients with CLP and NC. The reliability of these three-dimensional coordinate positions facilitated the description of the craniofacial complex and provided the key to proceed with the analysis and quantification of craniofacial morphology in three dimensions.

The conclusion derived from the reliability studies was that most landmarks could be located and variables derived from three-dimensional CT reconstruction with good reliability.

The errors of the method need to be taken in account when analysing the results of the studies reported in subsequent chapters but generally they were small in magnitude and unlikely to bias the results.

The clarity of the 3D CT reconstructions facilitated the confident identification of many more landmarks than would be possible from 2D radiographs, even in the presence of pathological conditions.

## References

Abbott AH, Netherway DJ, David DJ, Brown T. (1990) Application and comparison of techniques for 3D analysis of craniofacial anomalies. *J Craniofac Surg* 1:119-134.

Abbott AH, Netherway DJ, Niemann DB, Clark B, Yamamoto M, Cole J, Hanieh A, Moore MH, David DJ (2000). CT-determined intracranial volume for a normal population. J Craniofac Surg 11:211-223.

Dahlberg G (1940). Statistical methods for medical and biological students. London: George Allen and Unwin Ltd.

Johnson RA, Wichern DW. (1988). Applied Multivariate Statistical Analysis. London: Prentice-Hall International.

Netherway DJ, Abbott AH, Abbott JR, David DJ (1999). Techniques for characterisation of the human craniofacial skeleton using computer tomography data. Perspectives in Human Biology: Dento-Facial Variation in Perspective. CE Oxnard, GC Townsend, J Kieser (Eds.). 4:155-165.

Netherway DJ, Abbott AH, Yamamoto M (1997). Intracranial volume measurement for craniofacial surgery. *Asian J Surg* 20:68-78.

PROC SAS (2001). SAS/STAT User Guide, Version 8, SAS Inst. Inc., Cary, N.C.

Robb RA (1995). Three-Dimensional Biomedical Imaging. Principles and Practice. Chapter 3: The Image Computer VCH Publisher, Inc.

Yusof A, Netherway DJ, Townsend GC, Abbott AH, Shuaib I, David DJ. (2003). 3D-CT analysis of craniofacial growth changes in Malaysians. *J Den Res* 82;C8:108.

# CHAPTER 4

# THE HYOID BONE IN INFANTS WITH CLEFT LIP AND PALATE

## 4.1 Introduction

The hyoid bone is a unique structure in humans as it has no bony articulation. The floor of the mouth and the tongue lie superiorly, the larynx below, and the epiglottis and pharynx are located behind it. Several important muscles are attached to it, and it has a range of functions including maintenance of the airway, swallowing and the prevention of regurgitation. Problems with these vital functions may be associated with the anatomical position of the hyoid bone in relation to the craniofacial structures and head posture (Tallgren and Solow, 1987; Athanasiou *et al.,* 1991).

The hyoid bone develops from the cartilage of the second and third branchial arches – lesser horn from the second branchial arches; greater horn from the third branchial arches; body from both second and third branchial arches (Koebke , 1978). It ossifies from six centres – a pair for the body and one on each horn. Ossification commences in the greater horn at the end of intrauterine life, followed by the body at birth and the lesser horn at puberty.

The morphology and position of hyoid bone is not well described in the literature on orofacial clefts. This paucity of data relates to a large extent with difficulty in visualizing the hyoid bone using conventional radiographic techniques. Only one study (Kaduk *et al.,* 2003) has compared the position of the hyoid bone in patients

with orofacial clefts to non-cleft subjects using a lateral cephalometric technique. However, lateral cephalometry has significant limitations, such as superimposition of structures, difficulty identifying landmarks and poor visualization of 3D structures (Maue-Dickson, 1979; Moyers and Bookstein, 1979; Cohen, 1984; Richstmeier and Cheverud, 1986; Fisher *et al.,* 1999; Singh *et al.*, 2004).

Alteration in the position of the hyoid presents significant potential problems in terms of breathing, swallowing and head posture, because of alterations in attachments of the muscles responsible for these functions. It is unclear also whether anatomical variations in hyoid position and/or morphology are associated with in utero disturbances or due to surgical corrections. Nevertheless, as four out of 29 subjects in the present study (three with BCLP and one with ICP) were admitted to hospital with significant respiratory problems, the role of the hyoid in protecting the airway in patients with cleft lip and palate needs to be further investigated. For these reasons, the author has carried out the first detailed 3D CT study of this vital bone in unoperated CLP infants compared with an aged-matched NC group.

The specific objectives of this study are:

- To compare the anatomical length and height of the hyoid bone between unoperated infants with CLP and NC infants.
- To compare the position of the hyoid bone and epiglottis in relation to the cervical vertebrae and cranial base
- To quantify any anatomical variation
- To relate the findings to any clinical problems, such as aspiration pneumonia
- To see if differences exist between males and females.

## 4.2 Materials and Methods

The methods of data collection and statistical analysis have already been outlined in Chapter 3.

### 4.2.1 Data Collection

The sources of patients selected for this study, the breakdown by age, gender and cleft (CLP) or non-cleft (NC) group, and the problems encountered in collecting this information are detailed in Section 3.5.

### 4.2.2 CT Protocol

Axial scans were obtained with a GE Lightspeed Plus CT Scanner System at the Department of Radiology, Hospital Universiti Sains Malaysia. The protocol used is detailed in Section 3.6. Infants are imaged in a resting state, sedated and not intubated. Thus there are no muscle movements or extrinsic deforming factors and the change from supine to upright posture does not affect the hyoid bone location.

### 4.2.3 Hyoid Variables

Measurements of the hyoid bone were obtained as follows:

i. Length and height of the greater horn of the hyoid bone (greater horn left and right).

   The length of the greater horn was measured from the greater horn's posterior tip to the greater horn's anterior inferior tip, on the right and left, representing the lower length of the hyoid bone. Similarly the upper length of the hyoid bone was measured from the greater horn's posterior tip to the greater horn's

anterior superior tip on the right and left. The height of the greater horn was measured from the greater horn's anterior inferior tip to the greater horn's anterior superior tip on the right and left (Fig. 4.1).

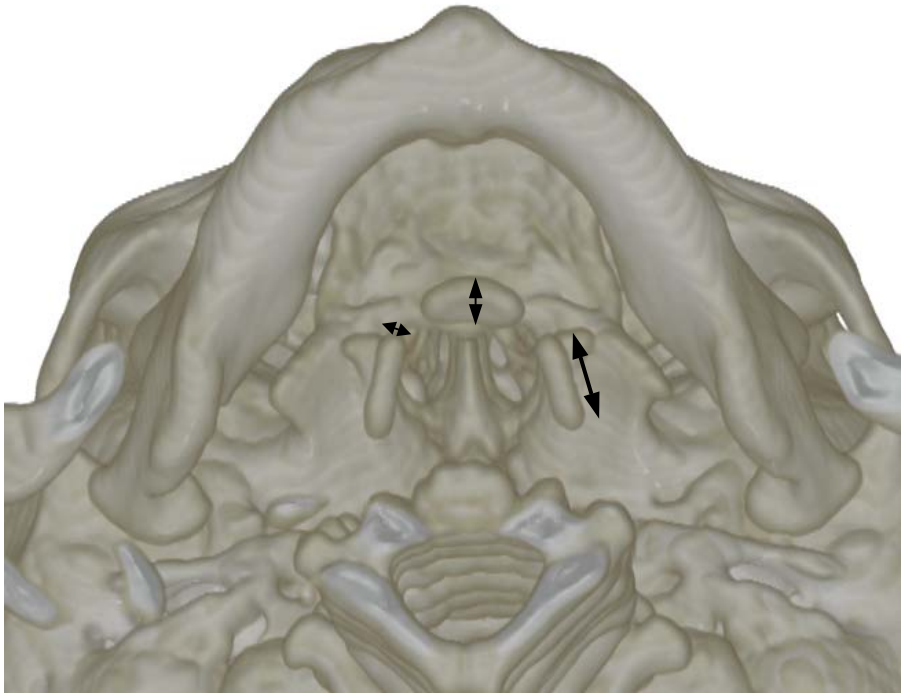

**Figure 4.1** Measuring the length and height of the greater horn (greater horn left and right) and the height of the body of hyoid bone at the anterior part.

ii. Height and length of the body of the hyoid bone

The height of the hyoid bone from the most anterior-superior point to the most anterior inferior point on the surface of the body of the hyoid bone, was measured on both sides. The length from the upper and lower parts of the hyoid body to medial upper and lower points were also measured on both sides (Fig. 4.1).

iii. Level of the hyoid bone in relation to the cranial base

The most inferior point of the anterior aspect of the foramen magnum in the mid-sagittal plane (basion) and the most inferior point of the spheno-occipital

synchondrosis (SOS) on the sphenoid bone were located. Two lines were constructed from these landmarks to the anterior-superior medial surface of the body of the hyoid bone (Fig. 4.2).

**Figure 4.2** Sagittal view showing the level of the hyoid bone in relation to the cranial base (measured from basion and inferior spheno-occipital synchondrosis).

iv. Distances of the hyoid bone to the cervical spine

Cervical tangent: A reference line was dropped from C2 to C5, touching the most anterior point on the surface of the bodies of C2 and C5 in mid-sagittal plane.

The distances from the superior and inferior aspects of the hyoid body to the cervical tangent line were then measured (Fig. 4.3).

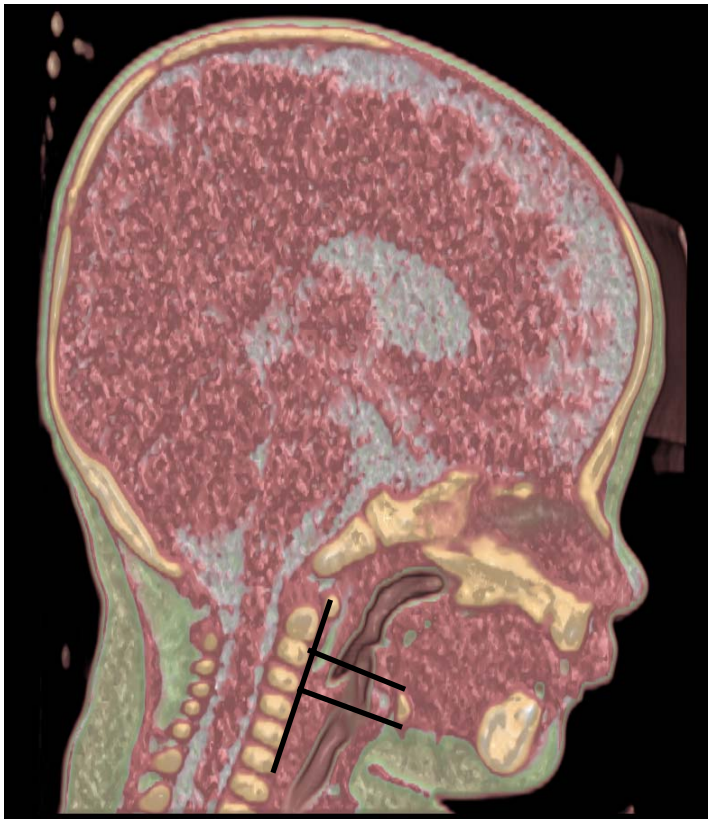

**Figure 4.3** The distance from the hyoid bone to the cervical spine (sagittal view).

v. Level of the hyoid bone and tip of the epiglottis in relation to the cervical vertebrae

A perpendicular line was drawn from the most anterior point on the surface of the body of the hyoid bone to the cervical tangent (as above) to determine the position of the hyoid bone in relation to the cervical vertebrae.

A similar line was also drawn from the tip of the epiglottis to the cervical tangent line to determine the position of the epiglottis in relation to the cervical vertebrae (Fig. 4.4).

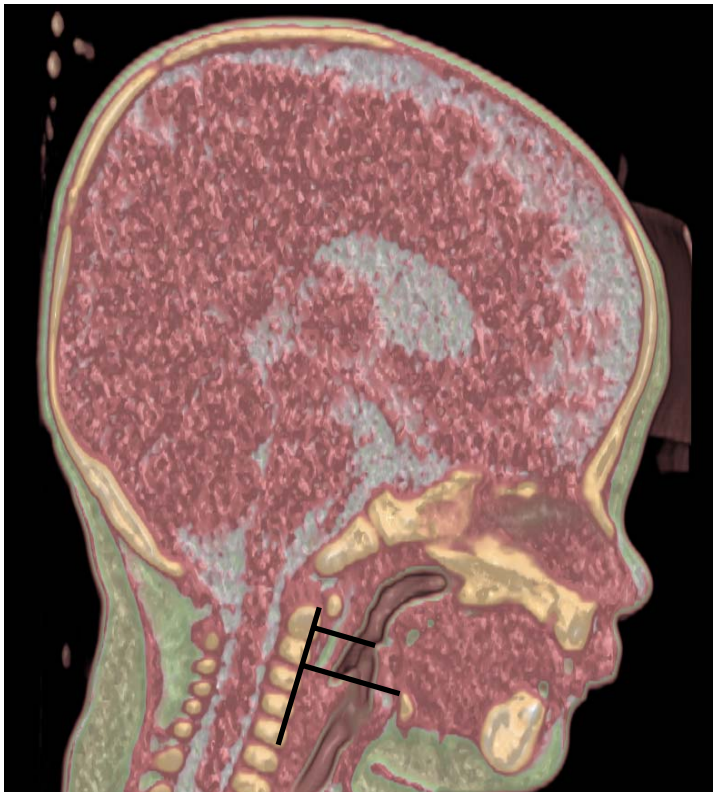

**Figure 4.4** Level of the hyoid bone and tip of the epiglottis in relation to the cervical vertebrae (sagittal view).

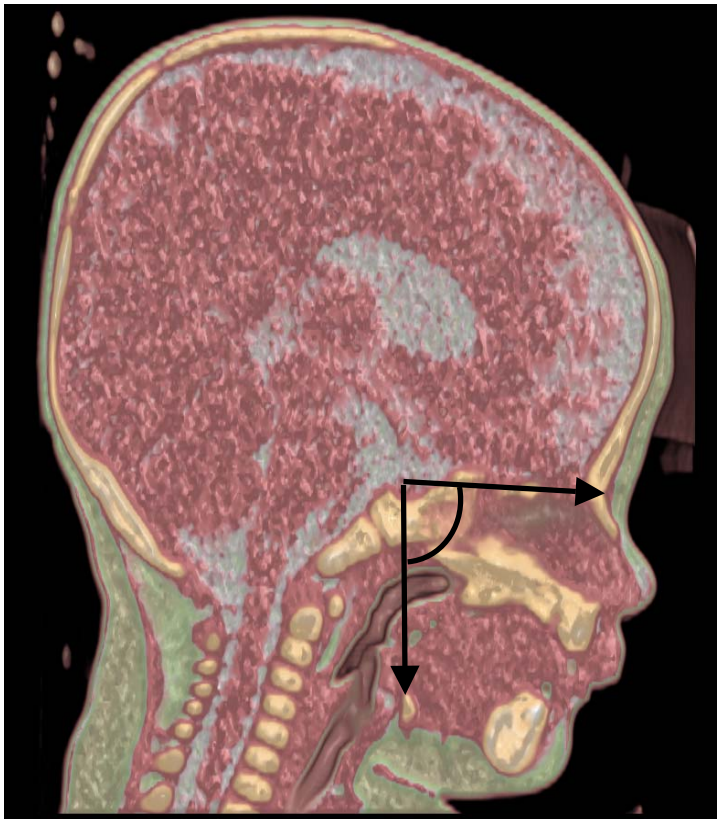

**Figure 4.5** Hyoid bone angle was measured from the most superior medial point on the surface of the body of the hyoid to sella and nasion (sagittal view).

v. Hyoid Bone Angle

This angle was measured from the most superior medial point on the surface of the body of the hyoid to sella and nasion (hbsm-s-n) (Fig. 4.5).

### 4.2.4 Statistical Analysis

The statistical model used to analyse the hyoid bone data has already been described in Section 3.11.

### 4.2.5 Errors of the Method

The methods for determining errors in the landmark determination and anthropometric variables derived from these landmarks by the use of repeated determinations are outlined in Section 3.12. Systematic errors in landmark location were tested using Hotelling's $T^2$ statistic. For anthropometric variables Student's paired t-tests were used to detect systematic errors (i.e. to ascertain whether the mean difference between repeated measures deviated significantly from zero) and Dahlberg's (1940) method of double determination was used to quantify the magnitude of random errors.

## 4.3 Results

The relocation errors for individual landmarks ranged from 0.3mm for the greater horn anterior inferior tip left to 0.5mm for the hyoid body inferior tip left. The pooled landmark relocation error was 0.4mm. The paired t-tests between repeat determinations of anthropometric variables indicated that there were systematic errors

at $p<0.01$ for hyoid to basion distance and $p<0.05$ for left lower length of greater horn, right upper length greater horn and right height hyoid body. The statistically significant systematic error associated with measurement of the distance from hyoid to basion was explained in Chapter 3. Those mean differences that were found to be statistically significant at the $p<0.05$ level were all in the range from 0.1mm to 0.2mm and the random errors, quantified using the Dahlberg statistic, ranged from 0.3 to 0.5 mm. Random errors for other hyoid bone variables, ranged from 0.3mm for height of the greater horn left to 0.7mm for height left hyoid body and the error for the hyoid bone angle was 1.2 degrees. The mean measurement error was 0.5mm. These measurement errors are approximately one pixel in size (0.488mm) and indicate that errors in the method were acceptable for this study and unlikely to bias the results.

Table 4.1 gives descriptive statistics including unadjusted means, standard deviations (SD) and coefficients of variation of all hyoid bone variables. None of the variables displayed significant differences in values between males and females in either CLP or NC groups.

**Table 4.1** Unadjusted means ($\bar{x}$), standard deviations (SD) and coefficients of variation (CV) of the hyoid bone variables (in mm or degrees).

| **Variable** | **Groups** | | | | | | | | | | | | | | |
|---|---|---|---|---|---|---|---|---|---|---|---|---|---|---|---|
| **Hyoid** | **NC (n=12)** | | | **UCLP (n=10)** | | | **BCLP (n=4)** | | | **CL (n=7)** | | | **ICP (n=8)** | | |
| | $\bar{x}$ | **SD** | **CV** | $\bar{x}$ | **SD** | **CV** | $\bar{x}$ | **SD** | **CV** | $\bar{x}$ | **SD** | **CV** | $\bar{x}$ | **SD** | **CV** |
| Lwr length lt GH | 9.3 | 1.63 | 17.5 | 8.3 | 2.54 | 30.7 | 9.4 | 1.41 | 15.0 | 7.3 | 2.70 | 36.7 | 7.3 | 3.22 | 44.1 |
| Lwr length rt GH | 9.2 | 2.54 | 27.8 | 9.3 | 1.83 | 19.6 | 7.5 | 2.87 | 37.2 | 7.1 | 2.78 | 38.9 | 8.1 | 3.03 | 37.2 |
| Upr length lt GH | 9.2 | 1.59 | 17.3 | 8.4 | 2.49 | 29.7 | 9.2 | 0.90 | 9.9 | 7.1 | 2.80 | 39.5 | 7.1 | 3.44 | 48.6 |
| Upr length rt GH | 9.0 | 2.66 | 29.6 | 9.0 | 1.70 | 18.9 | 7.5 | 2.64 | 35.2 | 7.2 | 2.94 | 40.9 | 7.7 | 3.11 | 40.6 |
| Height lt GH | 2.9 | 0.28 | 9.8 | 2.5 | 0.70 | 28.7 | 2.3 | 0.26 | 14.2 | 2.7 | 0.20 | 7.4 | 2.3 | 0.52 | 22.6 |
| Height rt GH | 2.8 | 0.63 | 22.8 | 2.4 | 0.37 | 15.0 | 2.1 | 0.50 | 25.9 | 2.7 | 0.16 | 6.0 | 2.5 | 0.69 | 27.5 |
| HB height lt | 2.5 | 0.87 | 35.4 | 2.3 | 0.74 | 33.0 | 2.4 | 0.71 | 30.0 | 2.4 | 0.79 | 32.3 | 2.3 | 0.59 | 25.1 |
| HB height rt | 2.3 | 0.76 | 33.5 | 2.1 | 0.62 | 29.6 | 2.6 | 0.90 | 34.2 | 2.3 | 0.69 | 30.6 | 2.3 | 0.57 | 24.4 |
| HB upr length lt | 4.6 | 0.97 | 21.2 | 3.8 | 0.80 | 21.3 | 4.2 | 1.21 | 28.6 | 4.9 | 1.52 | 30.9 | 4.1 | 0.77 | 18.5 |
| HB upr length rt | 4.6 | 0.54 | 11.9 | 3.6 | 0.91 | 25.1 | 3.8 | 1.31 | 34.5 | 4.7 | 1.19 | 25.1 | 4.2 | 0.69 | 16.4 |
| HB lwr length lt | 4.3 | 1.15 | 26.5 | 3.4 | 0.54 | 15.8 | 4.0 | 1.50 | 37.9 | 4.2 | 1.27 | 30.2 | 4.0 | 0.94 | 23.6 |
| HB lwr length rt | 4.2 | 0.88 | 20.9 | 3.4 | 1.06 | 31.0 | 3.5 | 0.78 | 22.0 | 4.0 | 1.08 | 27.2 | 3.3 | 0.88 | 26.2 |
| Hyoid - upr cervical | 22.7 | 2.97 | 13.1 | 20.4 | 2.23 | 10.9 | 20.9 | 1.68 | 8.0 | 21.1 | 2.36 | 11.2 | 19.4 | 2.66 | 13.8 |
| Hyoid - lwr cervical | 23.0 | 2.73 | 11.9 | 21.5 | 2.54 | 11.8 | 21.5 | 2.18 | 10.2 | 21.9 | 1.36 | 6.2 | 20.2 | 2.62 | 13.0 |
| Hyoid - basion | 28.3 | 3.77 | 13.4 | 31.7 | 2.84 | 9.1 | 32.0 | 2.34 | 7.3 | 28.9 | 4.24 | 14.7 | 30.2 | 3.46 | 9.9 |
| Hyoid-inf SOS | 31.4 | 3.57 | 11.3 | 31.7 | 2.88 | 9.1 | 33.6 | 3.75 | 11.2 | 30.2 | 4.15 | 13.8 | 32.3 | 4.36 | 13.3 |
| Hyoid angle (deg) | 92.9 | 5.82 | 6.3 | 86.2 | 6.21 | 7.2 | 86.5 | 4.91 | 5.7 | 88.8 | 6.04 | 6.8 | 86.5 | 4.23 | 4.9 |

GH = Greater Horn HB = Hyoid Body lwr = lower upr = upper lt = left rt = right

**Table 4.2** Adjusted means and standard errors of the hyoid bone variables (in mm or degrees).

| Variables | Groups | | | | | | | | | |
|---|---|---|---|---|---|---|---|---|---|---|
| **Hyoid** | **NC (n=12)** | | **UCLP (n=10)** | | **BCLP (n=4)** | | **CL (n=7)** | | **ICP (n=8)** | |
| | $\bar{x}$ | **SE** | $\bar{x}$ | **SE** | $\bar{x}$ | **SE** | $\bar{x}$ | **SE** | $\bar{x}$ | **SE** |
| Lwr length lt GH | 8.5 | 0.62 | 8.8 | 0.62 | 10.2 | 0.96 | 7.6 | 0.71 | 7.0+ | 0.67 |
| Lwr length rt GH | 8.5 | 0.56 | 10.0 | 0.58 | 8.3 | 0.90 | 7.4 | 0.67 | 7.7 | 0.63 |
| Upr length lt GH | 8.3 | 0.62 | 9.0 | 0.61 | 9.9 | 0.95 | 7.3 | 0.70 | 6.8+ | 0.66 |
| Upr length rt GH | 8.3 | 0.56 | 9.7 | 0.58 | 8.4 | 0.91 | 7.4 | 0.67 | 7.2 | 0.63 |
| Height lt GH | 2.8 | 0.16 | 2.5 | 0.15 | 2.4 | 0.24 | 2.7 | 0.18 | 2.3 | 0.17 |
| Height rt GH | 2.7 | 0.16 | 2.5 | 0.16 | 2.2 | 0.25 | 2.7 | 0.18 | 2.5 | 0.18 |
| HB height lt | 2.4 | 0.23 | 2.2 | 0.28 | 2.3 | 0.45 | 2.4 | 0.32 | 2.4 | 0.30 |
| HB height rt | 2.2 | 0.21 | 2.1 | 0.25 | 2.6 | 0.40 | 2.3 | 0.28 | 2.4 | 0.27 |
| HB upr length lt | 4.4 | 0.27 | 3.9 | 0.32 | 4.3 | 0.52 | 5.0 | 0.36 | 4.1 | 0.35 |
| HB upr length rt | 4.4 | 0.24 | 3.6 | 0.29 | 3.8 | 0.46 | 4.7 | 0.32 | 4.2 | 0.31 |
| HB lwr length lt | 4.1 | 0.29 | 3.5 | 0.35 | 4.0 | 0.56 | 4.2 | 0.40 | 4.0 | 0.38 |
| HB lwr length rt | 4.1 | 0.29 | 3.5 | 0.34 | 3.5 | 0.55 | 4.0 | 0.39 | 3.4 | 0.37 |
| Hyoid - upr cervical | 22.1 | 0.63 | 20.8 | 0.72 | 21.1 | 1.16 | 21.3 | 0.81 | 19.2 | 0.77 |
| Hyoid - lwr cervical | 22.5 | 0.64 | 21.9 | 0.73 | 21.6 | 1.18 | 22.1 | 0.83 | 20.0 | 0.79 |
| Hyoid - basion* | 27.5 | 0.72 | 32.3 | 0.86 | 32.2 | 1.38 | 29.1 | 0.97 | 29.9 | 0.92 |
| Hyoid - inf SOS | 30.7 | 0.86 | 32.3 | 1.04 | 33.9 | 1.68 | 30.4 | 1.18 | 31.9 | 1.12 |
| Hyoid angle (deg) * | 92.9 | 1.76 | 85.8 | 2.10 | 86.2 | 3.37 | 88.7 | 2.37 | 87.1 | 2.46 |

GH = Greater Horn HB = Hyoid Body lwr = lower upr = upper lt = left rt = right

*Significant difference at $p<0.05$ between all cleft groups and non-cleft

+ Significant difference at $p<0.05$ between ICP and other cleft groups combined

Table 4.2 shows adjusted means and their standard errors for the four cleft groups and NC group. Using Generalized Linear Modeling analysis (PROC SAS, 2001), no significant difference in the overall left and right length of the greater horn was found between CLP and NC groups (Table 4.2). However, the lower and upper length of the left greater horn was significantly smaller in the ICP group compared to other affected groups ($p<0.05$) (Figs. 4.6 - 4.9).

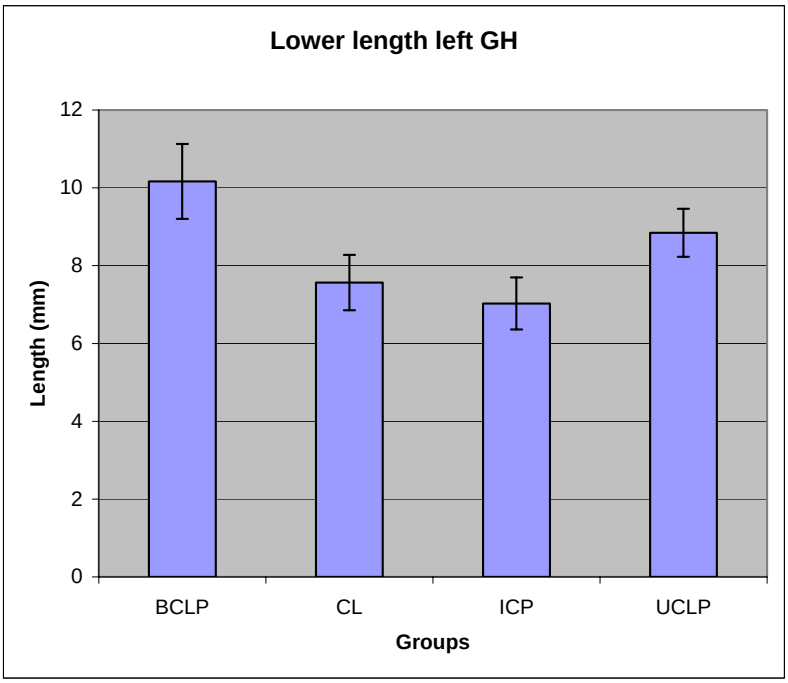


**Figure 4.6** Adjusted means and standard errors for the lower length of the left greater horn of the hyoid bone. The ICP group was significantly smaller than the other cleft groups.

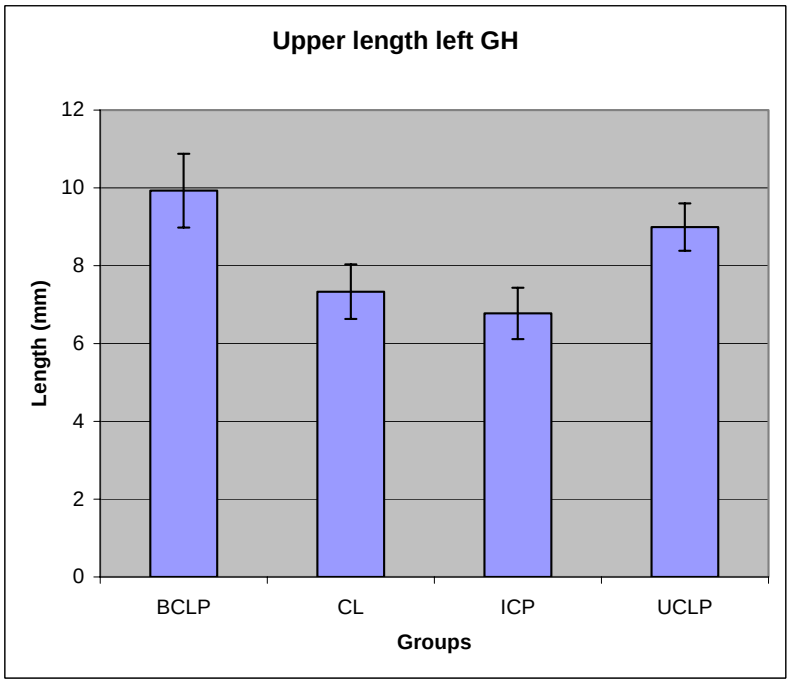


**Figure 4.7** Adjusted means and standard errors for the upper length of the left greater horn of the hyoid bone. The ICP group was significantly smaller than the other cleft groups.

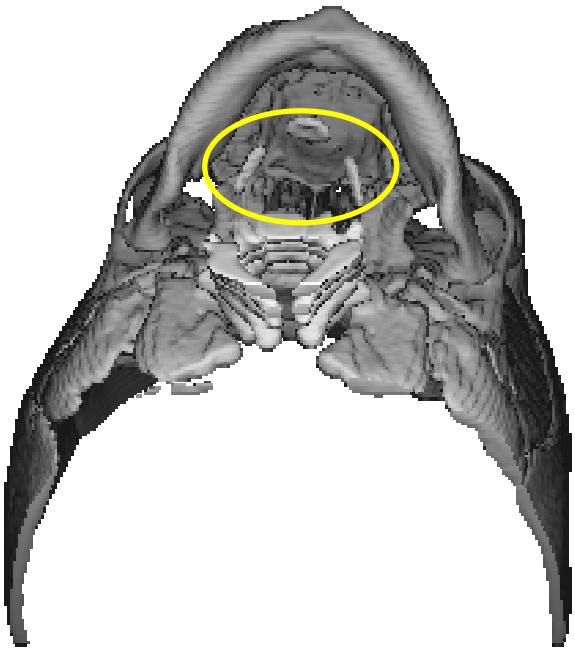

**Figure 4.8** Illustrating the normal shape of the hyoid bone in NC patients (inferior view).

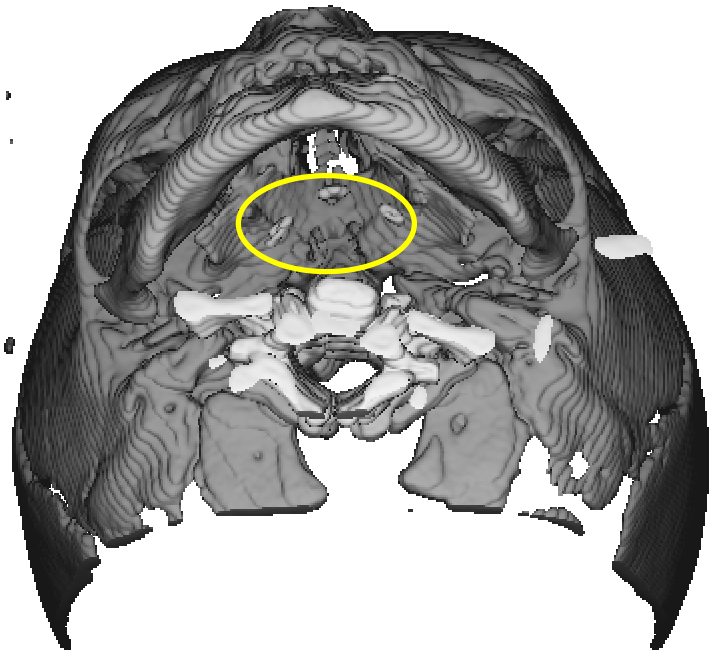

**Figure 4.9** Illustrating the smaller size of the hyoid bone in patients with ICP (inferior view).

Comparison of the height of the left greater horn of the hyoid bone between CLP infants and the NC group yielded a p value of 0.059.

The height of the right greater horn did not differ significantly between the CLP and NC groups. No differences in the overall size of the body of the hyoid were found. There was a tendency for smaller airway distances from the superior and inferior aspect of the hyoid body to the cervical vertebrae in the cleft group (p=0.06). The distance of the hyoid bone to the cranial base (basion) was significantly lower in the neck relative to cranial base ($p<0.05$) (Fig. 4.10) but the distance to the inferior sphenoid at spheno-occipital synchondrosis (SOS) was not statistically significant.

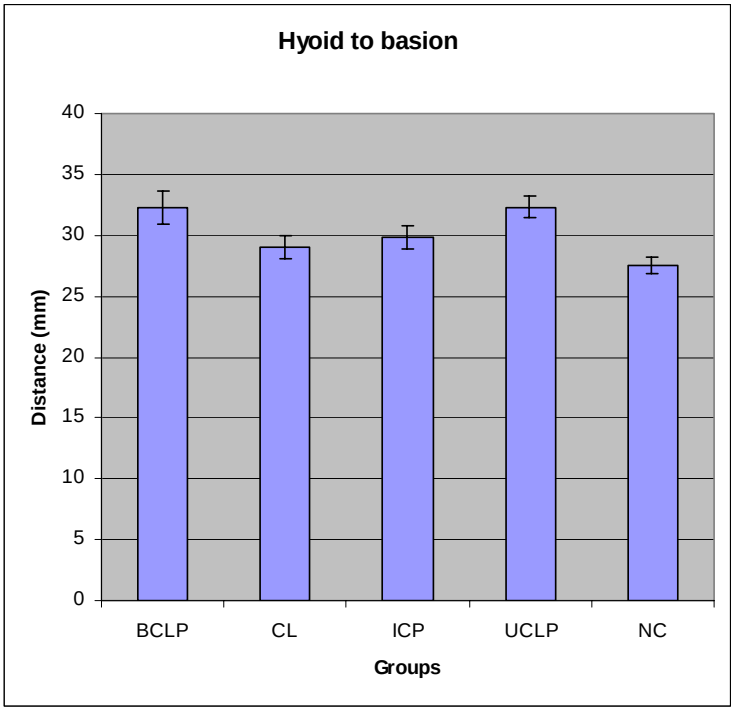


**Figure 4.10** Adjusted means and standard errors for the distance from the hyoid bone to the basion. The CLP groups were significantly larger than the NC group.

The angulation of the hyoid bone was significantly reduced in children with CLP compared to the non-CLP group ($p<0.05$) (Fig. 4.11).

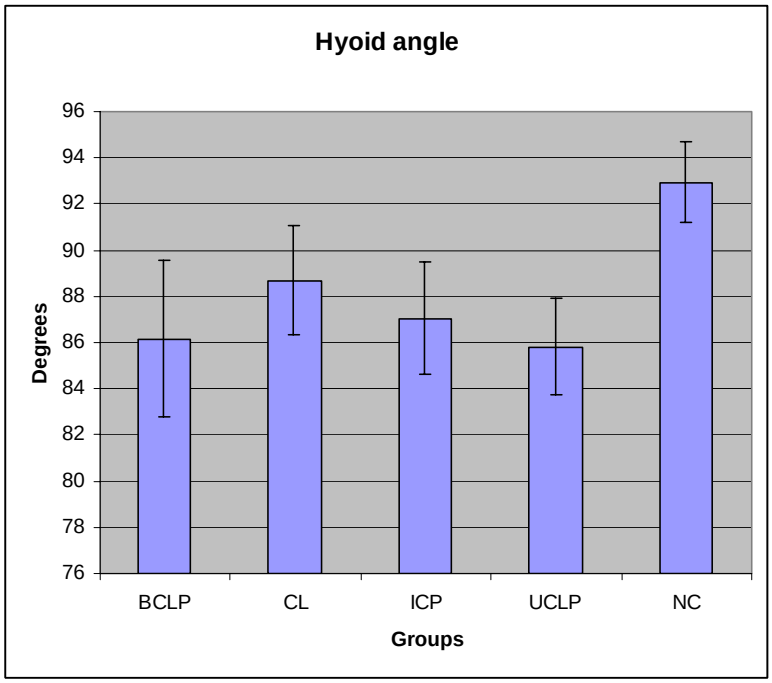


**Figure 4.11** Adjusted means and standard errors for the angle of the hyoid bone. The CLP groups were significantly smaller than the NC group.

Furthermore, chi-square analyses (Tables 4.3a-c and 4.4a-b) showed a significant association between the level of the hyoid in relation to the cervical vertebrae ($X^2$=8.80, df=1, $p<0.05$) and occurrence of aspiration pneumonia ($X^2$=4.97, df=1, $p<0.05$) (Fig. 4.12 and 4.13).

**Figure 4.12** Low level of the hyoid bone in relation to cervical vertebrae (at C4) (sagittal view).

**Figure 4.13** Showing the high level of the hyoid bone in relation to cervical vertebrae in an NC patient (at C2) (sagittal view).

There was also a significant association between the level of the epiglottis with aspiration pneumonia ($X^2$=5.16, df=1; p<0.05) (Fig. 4.14).

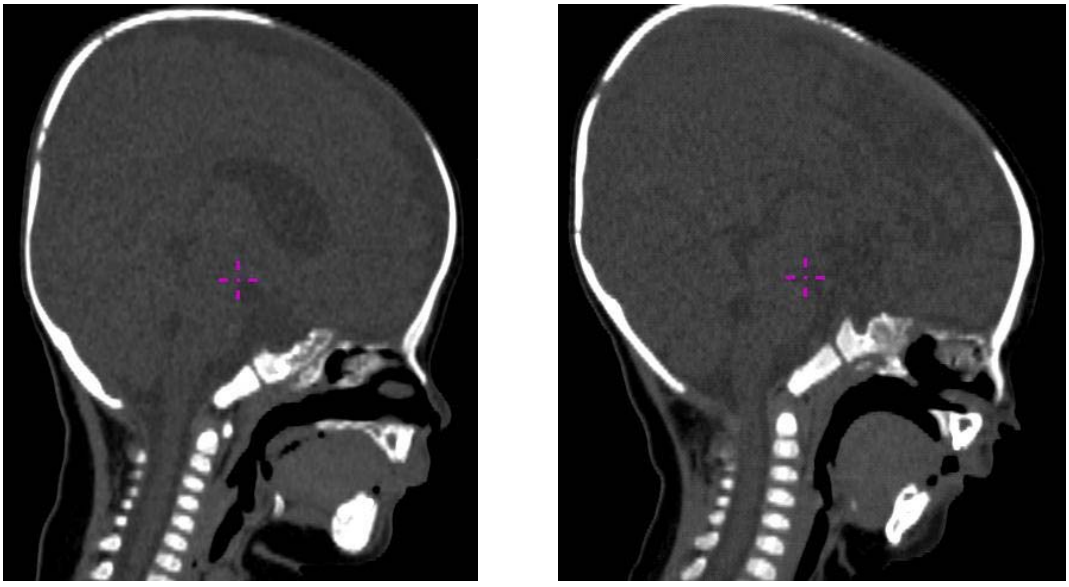

**Figure 4.14** Sagittal views showing the position of the hyoid bone and the epiglottis. The tip of epiglottis of NC (left) is at C2, however, for the CLP it is at a lower position (between C2 and C3).

In the CLP group, 17% of the children showed no ossification of body of the hyoid bone (5/29) (Figs. 4.15 and 4.16).

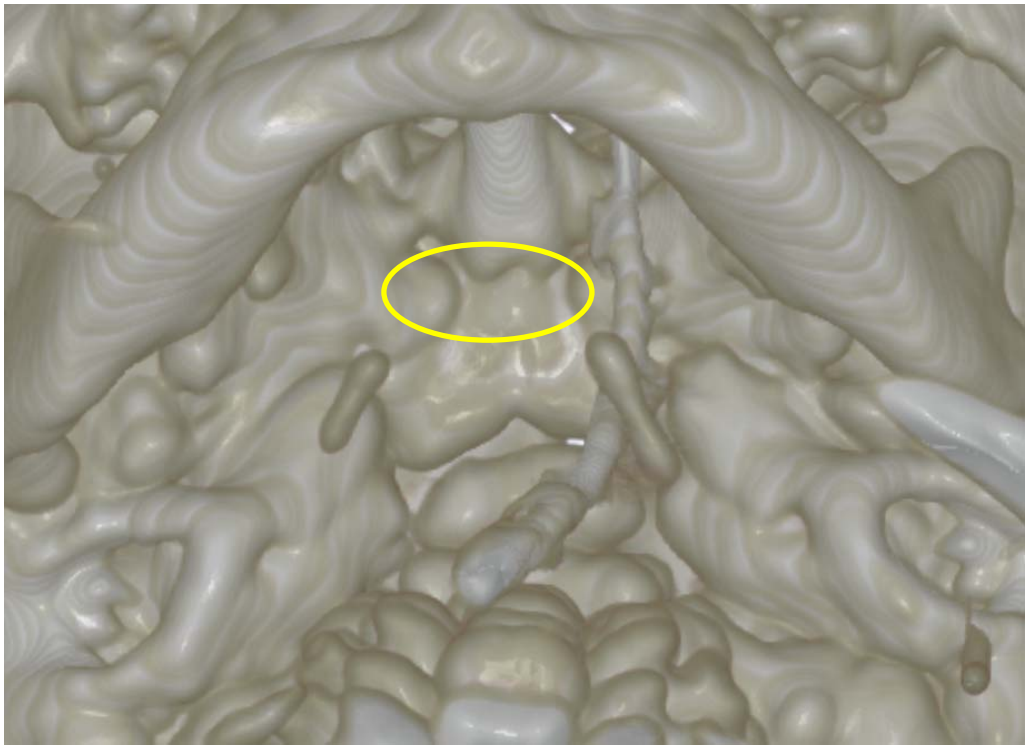

**Figure 4.15** Showing an absence of ossification of the body of the hyoid bone in CLP patients (inferior view).

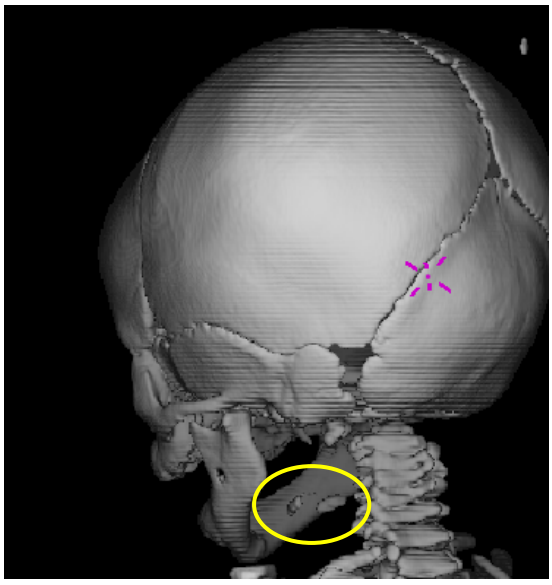

**Figure 4.16** A CT scan showing the absence of ossification of the body of the hyoid bone in CLP patients (posterior view).

**Table 4.3a** The level of the hyoid in relation to the cervical vertebrae and occurrence of aspiration pneumonia.

| Group | No. of patients | Cervical spine level | Absence of ossification | Aspiration pneumonia |
|---|---|---|---|---|
| UCLP (10) | 3<br>3 | C4<br>C3 | 2 | nil |
| BCLP (4) | 3 | C3 | 1 | 3 |
| ICP (8) | 1<br>2 | C4<br>C3 | 1 | 1 |
| CL (7) | 1 | C4 | 1 | nil |
| **Total CLP (29)** | **5**<br>**9** | **C4**<br>**C3** | **5** | **4** |
| **Total NC (12)** | **12** | **C2-C3** | **nil** | **nil** |

**Table 4.3b** Chi-square analysis for the level of the hyoid bone relative to C3.

| | CLP | NC | Total |
|---|---|---|---|
| **C3 and above** | 14 | 0 | **14** |
| **C3 and below** | 15 | 12 | **27** |
| **Total** | **29** | **12** | **41** |

Hyoid level ($X^2$=8.80, df=1; p<0.05)

**Table 4.3c** Chi-square analysis for the level of the hyoid bone and aspiration pneumonia.

| | Aspiration Pneumonia | None | Total |
|---|---|---|---|
| **C3 and above** | 0 | 15 | **15** |
| **C3 and below** | 4 | 10 | **14** |
| **Total** | **4** | **25** | **29** |

Aspiration pneumonia ($X^2$=4.97, df=1; p<0.05)

**Table 4.4a** Level of the tip of the epiglottis in relation to aspiration pneumonia.

| Groups | No. of patients | Level of the tip of the epiglottis | Aspiration Pneumonia |
|---|---|---|---|
| UCLP (10) | 4<br>4<br>2 | mid C2<br>lower C2<br>at C3 | nil |
| BCLP (4) | 1<br>1<br>2 | mid C2<br>lower C2<br>at C3 | <br>1<br>2 |
| ICP (8) | 4<br>4 | mid C2<br>C2-C3 | <br>1 |
| CL (7) | 4<br>2<br>1 | mid C2<br>lower C2<br>at C3 | nil |
| NC | 12 | mid C2 | nil |

**Table 4.4b** Chi-square analysis for the level of the epiglottis and aspiration pneumonia.

| | **Aspiration Pneumonia** | **None** | **Total** |
|---|---|---|---|
| **Mid C2** | 0 | 13 | **13** |
| **Below C2** | 4 | 8 | **12** |
| **Total** | **4** | **21** | **25** |

Aspiration pneumonia ($X^2$=5.16, df=1, $p<0.05$)

## 4.4 Discussion

This is the first 3D CT study, as far as the author is aware, on the size, location and morphology of the hyoid bone in unoperated infants with cleft lip and palate. At 23-25 weeks in utero, the foetal hyoid and larynx are situated high relative to the cervical vertebrae, extending from the basiocciput to the level of C3 or C4 (Lieberman *et al.*, 2001). The larynx is higher in children than in adults, with the hyoid bone found at the level of C2 and C3 from birth to 2 years and at the C3 level in older children (Hudgins *et al.*, 1997). The latter findings obtained with CT and MRI are consistent with those of an earlier study (Roche and Barkla., 1965) using conventional radiography.

The overall length of the greater horn was not significantly different when compared between CLP and NC groups. However, the overall length of the left greater horn was significantly smaller in the ICP group compared to other affected groups. It was found that the height of the left greater horn of the hyoid bone was reduced in CLP when compared to the NC group. However, the height of the right greater horn did not differ significantly between the CLP and NC groups. The fact that the ICP group was significantly smaller compared to other affected groups may relate to its different aetiology than the other affected groups. (Figures 4.8 and 4.9 show a smaller hyoid bone in a patient with ICP compared to NC). No differences in the overall size of the body of the hyoid were found.

The position of the hyoid bone in the CLP groups was investigated in relation to the cranial base. In infants with CLP, the hyoid bone was found to be significantly lower or inferior compared to the NC group. Only one study (Kaduk *et al.*, 2003) has

compared the position of the hyoid bone in patients with CLP to NC individuals. This study showed that the hyoid bone in cleft patients was located more caudally (inferiorly) and anteriorly than in non-cleft subjects. However, Kaduk *et al.* (2003) relied on lateral cephalometric technique and different landmarks were applied.

The patients with CLP differed significantly from the NC group with regard to the hyoid bone angle (nasion-sella to superior medial part of hyoid body). This indicates that the hyoid is located anteriorly in the neck compared to the NC group.

In the present study, 17% (5/29) of the CLP infants showed no ossification of the body of the hyoid bone (2 for UCLP; 1 for BCLP; 1 for ICP; 1 for CL**)** (Figures 4.15 and 4.16). This finding suggests a high prevalence of hyoid bone non-ossification in patients with CLP compared with unaffected individuals. The author did not find any hyoid bone anomalies in the non-CLP group, although the sample size was small. In terms of embryology, this finding indicates that the underlying factors associated with clefting not only affect the labiomaxillary and palatine structures of the first arch, but also influence the development of structures derived from the second and third branchial arches.

While this finding might suggest differences in the ossification pattern or skeletal maturation of the hyoid bone in CLP, the decrease in size of the hyoid bone may reflect the systemic condition, as it is known that children with CLP are often smaller than their non-cleft counterparts (Bowers *et al.,* 1987; Seth and McWilliams, 1988; Harris and Hullings, 1990; Lilius and Nordstrom, 1992; Neiman and Savage, 1997; Grippaudo and Kennedy, 1999; Spyropoulos and Burdi, 2001).

The significant deformities of the hyoid bone noted in this study, together with its reduced size, are consistent with an alteration in the ossification pattern or skeletal development. It is unknown whether these findings merely represent a developmental delay in hyoid bone development in CLP compared with NC infants. The hypothesis remains as the premise for further studies on hyoid bone development in children with CLP.

Anomalies of the hyoid bone may also contribute to abnormal breathing patterns in some infants. Previous studies have shown that infants need to exert additional force to open a closed pharyngeal airway compared with that required to maintain its patency, presumably because of airway wall adhesion (Wilson *et al.*, 1980, 1981). In patients with CLP and abnormal ossification of the hyoid bone, the absence of muscle attachments to the body of the hyoid, which are important for its stabilization, may compromise the function of swallowing and breathing. Consequentially, an incomplete epiglottal seal could lead to laryngeal penetration by aspiration. This situation represents inefficiency in the proper coordination of swallowing and breathing and could predispose certain infants to the aspiration of pharyngeal contents.

Ingram (1962) concluded from his study that between the ages of 6 and 12 weeks most babies change their pattern of suckling and swallowing. The tongue no longer comes forward as the jaw is opened and there is more jaw movement than previously. This change in the pattern of suckling and swallowing is an indication that the child is learning to breathe through the mouth. It is also an indication that the child is ready for semi-solid food as more definite movements of the mandible occur. However, not all children will change their pattern of suckling and swallowing, some continuing in

a similar fashion to that of the newborn. The presence of abnormalities of the hyoid bone, as described in this study, may compromise swallowing pattern development in infants with CLP and may be implicated in the sequelae of aspiration pneumonia and failure to thrive. Frequent and persistent nasal regurgitation in the absence of vomiting is common in cleft palate infants and has generally been attributed to inadequate separation of the nasal and pharyngeal cavities (Logan and Bosma 1967).

In this study, the lowered position of the hyoid bone was associated with a lower epiglottic position (Fig.4.14). Sasaki *et al.* (1977) reported on post-natal descent of the epiglottis, concluding that the age interval from 4 to 6 months seems to represent a transitional period from obligatory nasal breathing to potential oral respiration. The age of infants in the current study falls within this apparently critical time period. Sasaki *et al.* (1977) also reported that the larynx and nasal cavities remained interlocked during respiration but separated during the act of crying and subsequent respiratory efforts. This finding may be important clinically because it appears to reflect a period of potential respiratory instability coinciding with the peak incidence of sudden infant death syndrome (SIDS). Sasaki *et al.* (1977) reflect the views of Mossey *et al.* (1999) that further research of the airway is required for the understanding of SIDS. Moreover, the observations of abnormal ossification of the hyoid, coinciding with premature descent of the hyoid bone and epiglottis suggest that these developmental anomalies may also be associated with breathing disorders in CLP infants.

The position of the hyoid bone in the CLP groups was also investigated in relation to cervical vertebrae. In children with CLP it was found to be significantly lower, at the level of C3 and C4 compared to NC infants in whom it was at the level between of C2

and C3. This finding is consistent with previous studies in NC children of similar ages that have indicated the hyoid bone is situated at a higher level, at the junction of C2 and C3 (Roche and Barkla, 1965; Hudgins *et al.*, 1997; Lieberman *et al.*, 2001).

It is possible that an association may exist between these hyoid abnormalities and the problems that CLP infants have with suckling, swallowing and the propensity for chest infection. Bamford *et al.* (1992) showed that normal newborn infants have a stable and uniform swallow rate within 48 hours of birth, but their breathing is not coordinated with swallowing, with ventilation being reduced during feeding. From that study, it appears that mild and transient oxygen desaturation (hypoventilation) is well tolerated by newborns, but the same may not be true for older infants with an increasing metabolic demand, a decreased tolerance for hypoxia, and an increased respiratory drive. This study indicates that patients with cleft lip and palate suffer aspiration pneumonia quite commonly (14%) in the newborn to 6 months age range. This respiratory illness was particularly associated with BCLP (3 patients out of 4) and ICP (1 patient out of 8) around 4 months of age.

Azmi *et al.* (1983) found an association between the occurrence of cleft lip and palate, esophageal atresia and tracheo-esophageal fistula. They suggested that this association could cause clinical problems, such as difficulties in swallowing and recurrent chest infections. In addition, Azmi *et al.* (1983) recommended that the possible presence of second and further hidden anomalies should be fully investigated in a newborn with obvious craniofacial malformations, and that delays in diagnosis should be minimized. In this study, there was clinical suspicion that two of the infants may have tracheo-esophageal fistulae, requiring further special investigation.

Thus, CT scans of these infants may well be justified on the basis of identifying or excluding other related anomalies of the upper aerodigestive tract.

Several avenues of future research have been opened up by the findings reported here. It is possible that the smaller size of the hyoid bone in infants with CLP may be associated with lower general body weight. If so, the application of geometric morphometric analyses to the landmark data would enable a more detailed assessment of whether the hyoid in disproportionately smaller in affected infants. A more extensive study based on larger numbers also seems justified to determine the prevalence of aspiration pneumonia and tracheo-esophageal fistula in CLP infants. More reliable records of the incidence of aspiration pneumonia would also be desirable so that the suggestion of a relationship between anatomical variations of the hyoid bone and functional problems relating to breathing and swallowing could be confirmed. Finally, as this study was conducted in Malays subjects, future studies are required to ascertain whether similar variations in the size, location and morphology of the hyoid bone in CLP also occur in other ethnic groups.

Although the sample sizes were relatively small and the reproducibility of some of the landmarks involving the hyoid bone was low, the present 3D CT study has shown for the first time significant abnormalities in the size, location and morphology of the hyoid bone in children with CLP. The hyoid bone descent may be disadvantageous in cleft infants because the low position of the hyoid causes the epiglottis to lose its ability to protect the airway, increasing the risk of aspirating food and developing dysphagia.

## References

Athanasiou ES, Toutountzakis N, Mavreas D, Ritzau M, Wenzel N (1991). Alteration of hyoid bone position and pharyngeal depth and their relationship after surgical correction of mandibular prognathism. *Am J Orthod Dentofac Orthop* 100:259-265.

Azmi AF, Raine PAM, Young DG (1983). Orofacial clefts and oesophageal atresia. *Arch Dis Child* 58:639-640.

Bamford O, Taciak V, Gewolb IH (1992). The relationship between rhythmic swallowing and breathing during suckle feeding in term neonates. Pediatr Res 31:619-624

Bowers EJ, Mayro RF, Whitaker LA, Pasquariello PS, LaRossa D, Randall P (1987). General body growth in children with clefts of the lip, palate, and craniofacial structure. *Scand J Plast Reconstr Surg* 21:7-14.

Cohen AM (1984). Uncertainty in cephalometrics. *Br J Orthod* 11:44-48.

Dahlberg G (1940). Statistical methods for medical and biological students. London: George Allen and Unwin Ltd.

Fisher DM, Lo JL, Chen YR, Noordhoff MS (1999). Three-dimensional computed tomography analysis of the primary nasal deformity in 3-month-old-infants with complete unilateral cleft lip and palate. *Plast Reconstr Surg* 103:1826-1834.

Grippaudo FR, Kennedy DC (1999). General body growth in children with cleft lip and palate in a developing country. *Br J Plast Surg* 52:672-673.

Harris EF, Hullings JG (1990). Delayed dental development in children with isolated cleft lip and palate. *Arch Oral Biol* 35:469-473.

Hudgins PA, Siegel J, Jacobs I, Abramowsky CR (1997). The normal pediatric larynx on CT and MR. *Am J Neuroradiol* 18:239-245.

Ingram TTS (1962). Clinical significance of the infantile feeding reflexes. *Dev Med Child Neurology* 4:159-169.

Kaduk WMH, Grabowski, Gundlach KKH (2003). Position of the hyoid bone in cleft lip, alveolus, and palate: Variation of normal anatomy or sign accompanying the malformation? *Cleft Palate Craniofac J* 40:1-5.

Koebke J (1978). Some observations on the development of the human hyoid bone. *Anat Embryol* 153:279-286.

Lieberman DE, McCarty RC, Hiiemae KM, Palmer JB (2001). Ontogeny of postnatal hyoid and larynx descent in humans. *Arch Oral Biol* 46:117-128.

Lilius GP, Nordstrom RE (1992). Birth weight and placental weight in cleft probands. *Scand J Plast Reconstr Hand Surg* 26:51-54.

Logan WJ, Bosma JF (1967). Oral and pharyngeal dysphagia in infancy. *Pediatr Clin North Am* 14:47-61

Maue-Dickson W (1979). The craniofacial complex in cleft lip and palate: an update review of anatomy and function. *Cleft Palate J* 16:291-317.

Mossey P, Singh GD, Smith ME (1999). More extensive analysis is needed when assessing facial structure in SIDS. *Br Med J* 318:396-397.

Moyers RE, Bookstein FL (1979). The inappropriateness of conventional cephalometrics. *Am J Orthod* 75:599-617.

Neiman GS, Savage HE (1997). Development of infants and toddlers with clefts from birth to three years of age. *Cleft Palate Craniofac J* 34:218-225.

PROC SAS (2001). SAS/STAT User Guide, Version 8, SAS Inst. Inc., Cary, N.C.

Richtsmeier JT and Cheverud JM (1986). Finite element scaling analysis of normal growth of the human craniofacial complex. *J Craniofac Genet Dev Biol* 6: 289-323

Roche AF, Barkla DH (1965). The level of the larynx during childhood. *Ann Otol Rhinol Laryngol* 74:645-654.

Sasaki CT, Levine PA, Laitman JT, Crelin ES (1977). Postnatal descent of the epiglottis in man. *Arch Otolaryngol* 103:169-171.

Seth AK, McWilliams BJ (1988). Weight gain in children with cleft palate from birth to two years. *Cleft Palate J* 25:146-150

Singh GD, Rivera-Robles J, Jesus-Vinas J (2004). Longitudinal craniofacial growth patterns in patients with orofacial clefts: geometric morphometrics. *Cleft Palate Craniofac J* 41:136-143.

Spyropoulos 2001, Spyropoulos MN and Burdi AR (2001). Pattern of body and visceral growth in human prenates with clefts of the lip and palate. *Cleft Palate Craniofac J* 38:341-345

Tallgren A, Solow B (1987). Hyoid bone position, facial morphology and head posture in adults. *Eur J Orthod* 9:1-8.

Wilson SL, Thach TT, Brouillette RT, Abu-Osba YK (1980). Upper airway patency in human infant: influence of airway pressure and posture. *J Appl Physiol* 48:500-504.

Wilson SL, Thach TT, Brouillette RT, Abu-Osba YK (1981). Coordination of breathing and swallowing in human infants. *J Appl Physiol* 50:851-858.